

**A Thesis Submitted for the Degree of PhD at the University of Warwick**

**Permanent WRAP URL:**

<http://wrap.warwick.ac.uk/178856>

**Copyright and reuse:**

This thesis is made available online and is protected by original copyright.

Please scroll down to view the document itself.

Please refer to the repository record for this item for information to help you to cite it.

Our policy information is available from the repository home page.

For more information, please contact the WRAP Team at: [wrap@warwick.ac.uk](mailto:wrap@warwick.ac.uk)



# A New Kind of Microplasma for Nitrogen-Fixation Multifunctional Nanoparticle Synthesis Towards Selected Applications

by

**Hue Quoc Pho**

*M. Sc. (Biomedical Engineering),*

*Chung Yuan Christian University - Taiwan, 2017*

Dissertation submitted in fulfilment of the requirements for

**Jointly Awarded Doctor of Philosophy**

in

School of Chemical Engineering and Advanced Materials  
The University of Adelaide

&

School of Engineering  
The University of Warwick

09 February 2023

**Supervisors from home institution, The University of Adelaide:**

**Professor Volker Hessel,**  
*School of Chemical Engineering and Advanced Materials,*  
*The University of Adelaide*

**Professor Dusan Losic,**  
*School of Chemical Engineering and Advanced Materials,*  
*The University of Adelaide*

**Supervisors from host institution, The University of Warwick:**

**Professor Evgeny V. Rebrov,**  
*School of Engineering,*  
*The University of Warwick*

**Associate Professor Petr Denissenko,**  
*School of Engineering,*  
*The University of Warwick*

# Table of Contents

Table of Contents .....	iii
Summary .....	v
State of Originality .....	viii
Acknowledgements.....	x
Preface .....	xii
<b>Chapter 1. Introduction .....</b>	<b>1</b>
1.1. Abstract.....	2
1.2. Introduction .....	3
1.3. Research Background.....	6
1.3.1. Nitrogen-fixation plasma.....	6
1.3.2. N-doped carbon quantum dots as an emerging advanced nanomaterial.....	8
1.3.3. Properties of N-doped carbon quantum dots .....	11
1.3.3.1. Adsorption .....	11
1.3.3.2. Fluorescence property .....	12
1.3.3.3. Phosphorescence .....	13
1.3.3.4. Chemiluminescence .....	14
1.3.3.5. Photoluminescence .....	14
1.3.3.6. Optoelectronic properties .....	14
1.3.3.7. Quantum Yield .....	15
1.3.4. Various synthesis methodologies of N-doped carbon dots.....	15
1.3.4.1. Top-down approaches .....	17
1.3.4.2. Bottom-up approaches.....	19
1.3.5. Characterisation methods of N-doped carbon quantum dots .....	21
1.3.6. Microplasma-assisted synthesis of N-doped carbon quantum dots .....	22
1.3.7. kINPen®IND microplasma jet .....	24
1.3.8. Potential applications of N-doped carbon quantum dots.....	25
1.3.8.1. N-doped carbon quantum dots as potential nanopesticides .....	25
1.3.8.2. N-doped carbon quantum dots as photocatalysts for wastewater treatment.....	26
1.3.8.3. N-doped carbon quantum dots as theranostic agents in biomedical applications.....	27

1.4. Research aims and objectives .....	29
1.5. Thesis outline.....	32
1.6. Budget and Research Funding.....	35
1.7. Thesis Editing & Format .....	35
1.8. References .....	35
<b>Chapter 2. Literature review .....</b>	<b>47</b>
<b>Chapter 3. Sustainability assessment of various large-scale synthesis processes of NCQDs .....</b>	<b>74</b>
<b>Chapter 4. Process intensification for gram scale synthesis of NCQDs .....</b>	<b>94</b>
<b>Chapter 5. Rationally designed microplasma synthesis of NCQDs for targeted applications.....</b>	<b>108</b>
<b>Chapter 6. Insight into plasma-catalysis in triphasic microplasma synthesis for NCQDs.....</b>	<b>124</b>
<b>Chapter 7. Stagnant Liquid Layer as “Microreaction System” in Submerged Plasma Micro-Jet.....</b>	<b>157</b>
<b>Chapter 8. Conclusions &amp; Perspectives.....</b>	<b>188</b>

# Summary

N-doped carbon quantum dot (NCQDs) is an emerging material in the carbon family, which possess many advantageous qualities such as low toxicity, good compatibility with living cells, stability in chemical reactions, strong photoluminescence, photocatalysis, and efficient transfer of electrons when exposed to light. These properties make CDs a highly promising material to mitigate the current challenges in pest control, environmental treatment and theranostic medicine. This thesis study carried out a comprehensive literature review on the potential applications of these materials in pest control. Although a tremendous benefit from NCQDs has been revealed, generating these materials in large-scale production in a green and sustainable manner is still challenging. Therefore, a comprehensive assessment of all available large-scale production of NCQDs in terms of sustainability is significant. It has been revealed that non-thermal nitrogen fixation microplasma is a potential large-scale synthesis method in terms of sustainability while lacking mass efficiency. Therefore, it is crucial to overcome the improvement of mass efficiency of the non-thermal nitrogen fixation microplasma method. In addition, most of these CD synthesis strategies are classified as the trial-and-error approach. It is a time-consuming journey with cost- and process inefficiency to create CDs with a suitable structure and properties available for a specific application.

For this reason, it is also urgent to develop a rational design strategy for synthesising NCQDs towards selected applications (pest control, environmental treatment and theranostic medicine), which are emerging issues mentioned above. It has been revealed that the photoluminescence of the as-prepared NCQD increases by 18.4% in the presence of metal flakes as catalysts. However, the role of plasma-liquid-catalyst interaction in the production of NCQDs is still unclear. Therefore, it is also significant to have a deep understanding of the plasma-liquid-catalyst mechanism in the reaction to control the large-scale production of NCQDs better. Finally, it has also been important to have an insight into the reaction rate in the production of NCQDs and to determine factors (viscosity and liquid surface area) that affect the reaction rate.

The primary aim of this thesis is to develop a new kind of microplasma to address the challenges associated with the large-scale production of N-fixation multifunctional N-doped carbon quantum dots (NCQD) for selected applications. The objectives of this thesis are

organised into 8 chapters that will be presented in the form of a collection of published and submitted papers, which are the research outcomes. In addition, a literature review has been provided to establish the background of microplasma-assisted synthesis of NCQDs and highlight the potential applications of this material in agriculture. Overall, this thesis's main contributions to developing a new kind of microplasma-assisted synthesis process are discovering, investigating, understanding, designing, fabricating, and improving the concept of using the non-thermal nitrogen fixation microplasma process to generate high-quality NCQDs for selected applications. The main contributions are summarised in the following chapters:

- **Chapter 2.** Literature review: Perspectives on the plasma-assisted synthesis of N-doped nanoparticles as nanopesticides for crop pest control (Published paper 1).
- **Chapter 3.** Sustainability assessment of large-scale synthesis processes of NCQDs (Published paper 2).
- **Chapter 4.** Process intensification for gram-scale synthesis of NCQDs (Published Paper 3).
- **Chapter 5.** Rationally designed microplasma synthesis of NCQDs for targeted applications (Published paper 4).
- **Chapter 6.** Insight into plasma-catalysis in triphasic microplasma synthesis for NCQDs (Ready manuscript 5).
- **Chapter 7.** Stagnant Liquid Layer as “Microreaction System” in Submerged Plasma Micro-Jet for Formation of Carbon Quantum Dots (Submitted).

**BLANK PAGE**



# State of Originality

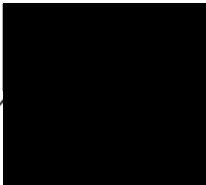
I certify that this work contains no materials which have been accepted for the award of any other degree or diploma in my name, in any university or tertiary institution and, to the best of my knowledge and belief, contains no material previously published or written by another person, except where due reference has been made in the text. In addition, I certify that no part of this work will, in the future, be used in a submission in my name for any other degree or diploma in any university or other tertiary institution without the prior approval of the University of Adelaide and where applicable, any partner institution responsible for the joint-award of this degree.

I acknowledge that the copyright of published works contained within the thesis besides with the copyright holder(s) of those works.

I also give permission for the digital version of my thesis to be made available on the web via the University's digital research repository, the Library Search and also through web search engines unless permission has been granted by the University to restrict access for a period of time.

Hue Quoc Pho

Adelaide, 09 February 2023.



**BLANK PAGE**

# Acknowledgements

First of all, I would like to express “thank you” to **Dr Triet Friedhoff** – a friend and talented mentor. Your precious advice and experience in preparing for the graduate school applications you shared with me have always been helpful until now.

I am honoured to thank everyone who accompanied me during this incredible journey to “make my own history” at the University of Adelaide. Especially from the bottom of my heart, I would like to express my sincerest appreciation to my principal supervisor, **Prof Volker Hessel**, for offering me “unique” opportunities to conduct interdisciplinary research with international collaborations in “SCOPE project” funded by European Commission. Without his enthusiasm, tremendous guidance, and inspiration to supervise me, I could not go this far in accomplishing this journey. I also would like to thank **Prof Evgeny V. Rebrov** and **Associate Prof Petr Denissenko** for their full support and supervision in the joint PhD program between Adelaide-Warwick University.

I would like to thank my co-supervisor at the Adelaide University, **Prof Dusan Losic**, who gave me full access to laboratory equipment and materials necessary for my study. I also would like to extend my gratitude to **Dr Nam Nghiep Tran** and **Dr Tung Tran** two big brothers in my academia and life, for sharing their priceless advice, scientific insights, and knowledge in this journey.

My study in this beautiful city of Adelaide would not be exciting without my research colleagues' companionship, assistance, and encouragement. **Dr Mohsen Sarafraz**, **Dr Van Long Nguyen**, **Don Tran**, **Svenja Schmidt**, **Chang Ping Zhuang**, **Tu Le**, and other friends in Adelaide are very supportive. In addition, I would like to thank all of the awesome administrative, academic, and workshop staff at The School of Chemical Engineering for their very kind support related to my PhD study.

Last but not least, my journey would have never been completed without my loved family and friends in Vietnam. My special thanks go to my dear parents - **Tua Chau** and **Ngoan Pho**, to my brother – **Vinh Pho** and my sister – **Yen Pho**, for their love and support.

*“All challenges in life are catalysts to make you more mature. Be calm and confident towards challenges! You will seek light at the end of your journey” – Hue Pho (Bill Fu).*

**BLANK PAGE**

# Preface

This thesis is submitted as a “thesis by publication” in accordance with the “Specifications for Thesis 2023” of The University of Adelaide. This thesis contains the following list of publications over a span of three and a half years of my PhD candidature. The outcomes generated during my PhD candidature include **14 published-or-under-reviewed journal articles and book chapters** (7 first-authored, 7 co-authored), **7 conference presentations**, and **8 awards & achievements**, as well as involving **various administration and leadership positions** at school and university levels.

## First-authored Journal Articles & Book Chapter

[7]. **Pho, Q.H.**, Lin, L., Rebrov, E.V., Sarafraz, M.M., Tran, T.T., Tran, N.N., Losic, D. and Hessel, V., 2023. Process intensification for gram-scale synthesis of N-doped carbon quantum dots immersing a microplasma jet in a gas-liquid reactor. *Chemical Engineering Journal*, 452, p.139164. (Q1, IF = 16.744) <Link>

[6]. **Pho, Q.H.**, Lin, L., Tran, N.N., Tran, T.T., Nguyen, A.H., Losic, D., Rebrov, E.V. and Hessel, V., 2022. Rational design for the microplasma synthesis from vitamin B9 to N-doped carbon quantum dots towards selected applications. *Carbon*, 198, pp.22-33. (Q1, IF = 11.307) <Link>

[5]. **Pho, Q.H.**, Escriba-Gelonch, M., Losic, D., Rebrov, E.V., Tran, N.N. and Hessel, V., 2021. Survey of synthesis processes for N-doped carbon dots assessed by green chemistry and circular and EcoScale metrics. *ACS Sustainable Chemistry & Engineering*, 9(13), pp.4755-4770. (Q1, IF = 9.224) <Link>

[4]. **Pho, Q.H.**, Losic, D., Ostrikov, K.K., Tran, N.N. and Hessel, V., 2020. Perspectives on plasma-assisted synthesis of N-doped nanoparticles as nanopesticides for pest control in crops. *Reaction Chemistry & Engineering*, 5(8), pp.1374-1396. (Q1, IF = 5.2) <Link>

[3]. **Pho, Q.H.**, Jiao, Y. R., Jiao Y., Sun, W., Tansu, N., Wojnicki, M., Shabbir, H., Rogoz, K., Tran, N. N., Lewis, D., and Hessel, V., 2023. *Quantum Materials*, Ullmann's Encyclopedia of Industrial Chemistry, Wiley, Germany. (Book Chapter, Accepted)

[2]. **Pho, Q.H.**, Tran, H.Q., Zhuang C.P., Nguyen, V.L., Tran, N.N., Rebrov, E.V., Losic, D., and Hessel, V., 2023. Deciphering Plasma-Catalysis in Triphasic Microplasma for N-doped Carbon Quantum Dots from Vitamin B9 via Optical Emission Spectroscopy. *Chemical Engineering Journal*. (Ready manuscript)

[1]. **Pho, Q.H.**, Hessel, V., Rebrov, E.V., Lamichhane, P., Tran, N.N., and Losic, D., 2023. Stagnant Liquid Layer as “Microreaction System” in Submerged Plasma Micro-Jet for Formation of Carbon Quantum Dots. *Chemical Engineering Journal*. (Submitted)

## Co-authored Journal Articles & Book Chapters

- [7]. Tran, T. T., Pereira, A. L. C, Poloni, E., Dang, N. M., Wang, J., Dinh, T. S., Kim, Y., **Pho, Q. H.**, J., Nine, Md J., Hessel, V., and Losic, D., 2023, Irradiation Methods for Graphene-based Materials Production, Applied Physics Review.(**Q1, IF = 19.527, Accepted**)
- [6]. Tran, N.N, Escriba-Gelonch, M., Sarafraz, M.M., **Pho, Q.H.**, Sagadevan, S., and Hessel, V., 2023. Process Technology and Sustainability Assessment of Wastewater Treatment. Industrial & Engineering Chemistry Research. (**Q1, IF = 4.326**) [<Link>](#)
- [5]. Sang, N.X., Na, T.T.L., Anh, L.T.L., Thuy, P.T., Tuan, N.T., Tung, T.T., Tran, A.T.T., **Pho, Q.H.**, Shearer, C.J. and Losic, D., 2022. Engineering of ZnO/graphene nanocomposite for enhancing visible photocatalytic ability. Physica status solidi (a), p.2200172. (**IF = 3.277**) [<Link>](#)
- [4]. Tran, N.N., Le, T.N.Q., **Pho, Q.H.**, Tran, T.T. and Hessel, V., 2022. Nanofertilizers and Nanopesticides for Crop Growth. In Plant and Nanoparticles (pp. 367-394). Springer, Singapore. (**Book Chapter**) [<Link>](#)
- [3]. Lin, L., **Pho, Q.H.**, Zong, L., Li, S., Pourali, N., Rebrov, E., Tran, N.N., Ostrikov, K.K. and Hessel, V., 2021. Microfluidic plasmas: Novel technique for chemistry and chemical engineering. Chemical Engineering Journal, 417, p.129355. (**Q1, IF = 16.744**) [<Link>](#)
- [2]. Warne, G.R., Williams, P.M., **Pho, Q. H.**, Tran, N.N., Hessel, V. and Fisk, I.D., 2021. Impact of cold plasma on the biomolecules and organoleptic properties of foods: A review. Journal of Food Science, 86(9), pp.3762-3777. (**IF = 3.693**) [<Link>](#)
- [1]. Anh, N.T.H., Phuc, T.T., An, T.N.M., **Pho, Q.H.** and Van Cuong, N., 2020. Microwave-assisted preparation of magnetic citric acid-sugarcane bagasse for removal of textile dyes. Indonesian Journal of Chemistry, 20(5), pp.1101-1109. [<Link>](#)

## Conferences

- [7]. **Pho, Q.H.**, Lin, L., Tran, N.N., Tran, T.T., Nguyen, A.H., Losic, D., Rebrov, E.V. and Hessel, V., 2022. Rational design for the microplasma synthesis from vitamin B9 to N-doped carbon quantum dots towards selected applications, the first 2022 CEAM HDR Conference, The University of Adelaide, Australia, 7 December, 2022. (**Oral Presentation**)
- [6]. **Pho, Q.H.**, Lin, L., Rebrov, E.V., Sarafraz, M.M., Tran, T.T., Tran, N.N., Losic, D. and Hessel, V., 2022. Process intensification for gram-scale synthesis of N-doped carbon quantum dots immersing a microplasma jet in a gas-liquid reactor. Second International Conference on Unconventional Catalysis, Reactors and Applications, Warwickshire, United Kingdom, 21-23 September, 2022. (**Oral Presentation**)

[5]. **Pho, Q.H.**, Lin, L., Tran, N.N., Tran, T.T., Nguyen, A.H., Losic, D., Rebrov, E.V. and Hessel, V., 2022. Rational design for the microplasma synthesis from vitamin B9 to N-doped carbon quantum dots towards selected applications, Seventh International Conference on Multifunctional, Hybrid and Nanomaterials, Genova, Italy, 19 – 22 October 2022. **(Oral presentation)**

[4]. **Pho, Q.H.**, Tran, N. N., Losic, D., Hessel, V., Gram-scale process of n-doped of carbon dots using microplasma: Recycling and purification, Chemeca 2021: Advance, Disrupt and Sustain: Advance, Disrupt and Sustain, Engineers Australia Barton, ACT2021, pp. 311-312. **(Oral Presentation)**

[3]. Fisk, I., Tran, N.N., Hessel, V., Warne, G., Williams, P., Schmidt, S. **Pho, Q.H.**, Development of a novel processing system for food personalisation during space travel, 43<sup>rd</sup> COSPAR Scientific Assembly. Held 28 January-4 February 43 (2021) 2058. **(Poster presentation)**

[2]. **Pho, Q.H.**, Tran, N. N., Losic, D., Rebrov, E, Hessel, V., Gram-scale process of n-doped of carbon dots using microplasma: Recycling and purification, The Warwick Engineering PGR Symposium, The University of Warwick, Coventry, United Kingdom, 12-17 July 2021. **(Poster presentation)**

[1]. **Pho, Q.H.**, Lin, L., Tran, N.N., Tran, T.T., Nguyen, A.H., Losic, D., Rebrov, E.V. and Hessel, V., Rational design for the microplasma synthesis from vitamin B9 to N-doped carbon quantum dots towards selected applications, Advanced Materials Workshop and Networking Event 2022: Research and Applications of Nanomaterials of Chemical Engineering Processes, National Wine Center, Adelaide, Australia, 2022. **(Poster Presentation)**

## Awards & Acheivements

[8]. **CEAM HDR Travel Grant**, School of Chemical Engineering and Advanced Materials, The Univerisity of Adelaide, 2022.

[7]. **DAAD Scholarship** for Research Exchange in Germany, 2022.

[6]. **Adelaide -Warwick University joint PhD award**, 2019-2023.

[5]. **“SCOPE” project travel grant** from European Comission, 2022.

[4]. **Excellence in Research Award (Poster Presentation)**, Advanced Materials Workshop and Networking Event 2022: Research and Applications of Nanomaterials of Chemical Engineering Processes, National Wine Center, Adelaide, SA, Australia, 2022.

[3]. **The ECMS Faculty People’s Choice Prize in 3-Minute-Thesis Competition**, Faculty of Engineering, Computer, and Maths Science, The University of Adelaide, SA, Australia, 2021.

[2]. Faculty of Engineering, Computer & Mathematical Sciences **(ECMS) Divisional Scholarship**, The University of Adelaide, SA, Australia, 2019.

[1]. **Full fee Scholarship**, The University of Adelaide, SA, Australia, 2019.

## Administration and leadership

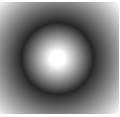
- [1]. **Chair of CEAM HDR Comittitee** at School of Chemical Engineering and Advanced Materials, 2021-2022.
- [2]. **Key board member** of Adelaide University Postgraduate Society, 2020-2021.
- [3]. **CEAM HDR comittitee leader** of organizing members of the 1<sup>st</sup> CEAM HDR Conference, 7 December, 2022.



**BLANK PAGE**

# Chapter 1

## Introduction



---

**T**his introductory chapter describes the motivation for considering the problems that this dissertation addresses and discusses the challenging nature of those problems. The chapter also summarizes the contributions made in the following chapters and provides an overview of the dissertation's structure.

---

### 1.1. Abstract

The increasing world population and its demands for food, agriculture-based products, industrial activities, environmental degradation, and health care system are major challenges that government bodies will have to address in the future. Industrial production of fertilizers has become essential for agricultural crop productivity. Nitrogen-fixation process is key to overcoming the challenges of food demand and can generate new types of nitrogen-containing multifunctional materials for use in environmental treatment and health care. Non-thermal microplasma technology, which utilizes high-energy positively and negatively charged gases, has become an emerging material in nitrogen fixation processes because of its ability to break the triple bonds of dinitrogenous molecules in the air into active free nitrogen, which can react with water or hydrogen to form  $\text{NH}_3$  or other related compounds and perform nitrogen doping on the surface of materials. Non-thermal microplasma technology can generate high-quality nitrogen-doped carbon quantum dots (NCQDs). NCQDs have shown promising potential in various applications, particularly in photocatalysis due to their ultrasmall size, water solubility and excellent optical properties, and their ability to strongly decompose pollutants in wastewater under solar irradiation can be enhanced by doping nitrogen on the surface of CDs, making them suitable for multifunctional uses in health care, pest control, and environmental treatment. The outstanding properties of NCQDs make them suitable for various applications, but fabricating these advanced materials using traditional synthesis techniques can be time-consuming and inefficient. Non-thermal microplasma technology is a key solution to overcome these challenges in creating CDs with suitable structures and properties for targeted applications. This study proposes to innovate a new kind of microplasma for synthesising N-doped carbon quantum dots using a microplasma jet-based reactor and aims to benefit from a commercial design with intended industrial use. The research aims to develop a new type of microplasma reactor that can rationally design N-doped carbon quantum dots from folic acid (vitamin B9) for selected applications while also exploring the massive synthesis and process intensification, and gaining deep insights into plasma catalysis in production processes.

### 1.2. Introduction

With an alarming rate of population escalation, a census has been reached that the world's population has currently passed 7.7 billion in 2019, and is predicted to increase by more than 9.7 billion in 2050, according to “the World Population Prospects 2019: Highlights” from United Nations Organization. Therefore, an increase by 50 – 80 % in crop production is estimated to high demand for food and agriculture-based products by 2050 [1]. This also means an emerging demand for an extremely large number of fertilisers and nanopesticides to facilitate the agricultural sector to adequately provide food for people worldwide. In addition, along with population growth, industrial activities, especially textile and food industries, have also been triggered to improve human life [2]. As a result, this will lead to environmental degradation due to contaminated wastewater leakage into surrounding groundwater from industrial zones [3]. According to a United Nations report on the state of the world's water, more than 5 billion people could suffer inadequate water supplies by 2050 because of several reasons related to global climate warming and contaminated soil, air and water resources [4]. In addition, with an increasing rate of population, it is estimated that the world's burden of health care is put on the government bodies. Therefore, health care, food demand and environmental deterioration are three foreseen challenges that all government bodies need to adequately control in the forthcoming future.

From the aspect of food supplies, agricultural production is still predicted to be a primary source of food demand by 2050. However, agricultural production has always confronted many unforeseen factors, such as global warming, degraded cultivating land, and pesticide-resisted phytopathogen that adversely affect crop productivity leading to approximately 40% of crop loss [5-7]. Consequently, this will result in a remarkable decrease in biodiversity and impairment of ecosystem functions needed for a green agroecosystem. Based on the emerging need for agricultural crop productivity, industrial production of fertilisers has become indispensable. Although nitrogen sources are abundant on earth, nitrogen provision as nutrients for plants is always challenging. It is a motivation to discover an alternative nitrogen fixation that converts nitrogen molecules in the air into nitrogen-containing compounds, that can be efficiently used as pesticides and/or fertilisers.

As far as environmental degradation is concerned, contaminated water with heavy metals [10] and dye wastewater [11] are always classified as one of the most problematic pollution groups due to their severe toxicity to human well-beings and natural habitats. With a remarkable growth in industrial activities due to the escalation of the world's population, a tremendous amount of wastewater must be under the pre-treatment process before releasing into the natural environment. This is predicted to be challenging in the next few decades. Therefore, seeking an optimal solution to this environmental issue is essential for protecting our way of life. Among several wastewater treatment methods, photocatalysis degradation, also

known as an advanced oxidation process, is one of the most effective and practical approaches in terms of energy-efficiency [12] and eco-friendliness [13, 14] due to their capacity to lessen undesirable effects on the environment. In advanced oxidation processes, highly reactive oxygen species, such as hydroxyl radicals ( $\bullet\text{OH}$ ), can decompose complex organic compounds into carbon dioxide, inorganic ions, and more simple structured compounds [15]. It has been recently noticed that introducing nitrogen into the surface of photocatalysts can enhance photocatalysis degradation in wastewater treatment [16]. Therefore, it is also a driving force to look for a nitrogen fixation process that can convert nitrogen from the air into nitrogen-containing compounds, that can be efficiently used as strong photocatalysts.

Regarding health care, breast cancer is a disease caused by the uncontrolled growth of cells that develop and form a tumour [17]. This tumour becomes oncogenic if cancer cells invade nor metastasize the blood or the network of lymphatic vessels. The limitations of current clinical imaging systems for diagnosis and conventional chemotherapy strategies for breast cancer treatment, such as the undesirable side effects to patients and the high-cost of treatment, bring about this phenomenon. Hence, a great effort has been made recently to develop new theranostic or multifunctional nanoparticles (NPs) to combat cancer disease more effectively. It also has been noticed that introducing nitrogen can enhance the intensity of photoluminescence of multifunctional nanoparticles [18], thus improving theranostic applications in cancer treatment. For this reason, nitrogen fixation also plays an important role in generating nitrogen-containing multifunctional nanoparticles for theranostic applications.

Mitigating issues in food demand, environmental degradation, and health care have become more and more challenging in the next decades. As discussed above, an alternative nitrogen-fixation is the key to overcoming these challenges. In other words, this nitrogen fixation process can generate a new type of nitrogen-containing multifunctional materials that can be used as fertilisers and/or nanopesticides, photocatalysts, and theranostic medicine.

In spite of being newly discovered in the last decade, carbon dots (CDs) have shown their more prominent potential in comparison with semiconductor quantum dots in many applications, especially in photocatalysis due to their high-quality ultrasmall size [19-21], water solubility [22, 23] and excellent optical properties [24, 25]. CDs are able to strongly decompose pollutants in wastewater under solar irradiation [26-28]. In addition, it has been recently reported that the photocatalytic properties of CDs can be enhanced by doping nitrogen on the surface of CDs [29]. It is because the nitrogen atoms in CDs can provide excess electrons and inject them into CDs, thus increasing significant optical properties, especially fluorescence quantum yields. Therefore, it is strongly believed that this type of material can meet the requirement of new multifunctional materials as theranostic medicine in health care as fertilisers and/or nanopesticides in pest control and photocatalysts in environmental treatment.

Because of the outstanding properties of CDs for various applications, fabricating these advanced materials has become urgent. Various synthesis techniques have been used to fabricate CDs, such as laser ablation, arc discharge, hydrothermal, pyrolysis, solvothermal, ultrasonic, etc. Most of these CD synthesis strategies can be classified as the trial-and-error approach in searching for suitable applications. It is a time-consuming journey with cost- and process inefficiency to create CDs with suitable structures and properties available for a targeted application. Among these synthesis technologies, non-thermal microplasma technology is the key to overcoming these synthesis challenges.

Non-thermal microplasma technology with major components of high-energy positively and negatively charged gases has become emerging in nitrogen fixation processes because of several atmospheric pressure operations, non-equilibrium chemistry, important specific power densities, microscale geometries, and self-assembly phenomena. These properties make them particularly suitable for the cost-effective and highly efficient production of high-quality nanomaterials [30]. Firstly, it has been assumed that these charged gases and free radicals can break the triple bonds of dinitrogenous molecules in the air into active free nitrogen, which is ready to react with water or hydrogen to form  $\text{NH}_3$  or other related compounds [31]. In addition, it is also proven that non-thermal microplasma can cause a chemistry reaction, which performs nitrogen doping on the surface of materials [32]. Secondly, non-thermal microplasma technology, previously much too energy-intensive, is slowly closing its energy- efficiency gap to industrial needs. It can be operated with high safety control because it is operated under atmospheric pressure and low temperature [33]. Therefore, it becomes more attractive for ammonia synthesis and, as a more disruptive industrial scenario, for nanofabrication [34-40]. There have been increasing findings showing that confining plasma to a smaller size will result in new physical properties that conventional plasma could not possess. The electric field distributions are changed [41]. Plasma, which is confined to a millimetre size, is called microplasma. It is explained because of the increased ratio of surface to volume and the significantly decreased size and space; these are the winning points of microreactors, which are applied on an industrial scale these days. For this reason, in order to maintain the plasma at non-equilibrium state at atmospheric pressure and temperature, the operation parameters such as pressure, gas composition, input power and electrodes distance must be controlled.

As for such beneficial reasons of microplasma, in this study, it is proposed to innovate a new kind of microplasma for synthesising N-doped carbon quantum dots. This innovative idea is based on a microplasma jet-based reactor. We aim to profit from a commercial design with intended industrial use, developed by our plasma technology collaboration partner Ronny Brandenburg (Uni Greifswald, Germany) [42]. Microplasma jet (kINPen®IND) provides microplasma over the surface of the liquid. This research work generally attempted to develop a microplasma jet (kINPen®IND)-based reactor that could rationally

design N-doped carbon quantum dots from folic acid (vitamin B9) for selected applications (nanopesticides and nanofertilizers). Mass synthesis of NCQDs has also been explored by means of process intensification. Also affected were the deep insights into plasma catalysis in production processes. It is characterized by emission spectroscopy.

### 1.3. Research Background

#### 1.3.1. Nitrogen-fixation plasma

Nitrogen fixation process is defined as a nitrogen transformation in the atmospheric air into ammonia, nitrates, and other valuable nitrogen-containing substances (Figure 1) [43-45]. However, it is believed that most biological processes in nature cannot undergo the metabolization of these di-nitrogenous molecules because it is not easy to break their triple bonds and very stable electronic configuration [45]. In the 21<sup>st</sup> century, nitrogen fixation has become one of the most essential processes in the chemical industry due to outstanding applications of their nitrogen- fixed products, e.g. ammonia  $\text{NH}_3$ , in many industrial sectors. In terms of the history of nitrogen fixation, Joseph Priestley dating back in 1774, first discovered ammonia [46]. Over a decade later, William Austin attempted to synthesize ammonia for the first time, which is known as a chemical nitrogen fixation. Until 1880, Herman Hellriegel and Hermann Wilfarth first confirmed that living organisms could biologically transform nitrogen in the air into nitrogenous compounds known as biological nitrogen fixation. In 1903, Kristian Birkeland and Samuel Eyde introduced a new nitrogen fixation process by passing air through an electric arc to produce nitrogen oxides. In 1909, Fritz Haber first tried synthesising ammonia from nitrogen and hydrogen gas. This process was scaled up to massive production by Carl Bosch, known as Haber-Bosch process, making it one of the most important processes in the 20th century. In 2014, the power consumption in the ammonia synthesis process was estimated from 33 to 36 GJ/ton N [44]. The Haber-Bosch process consumes 1-2% of all energy in this planet.

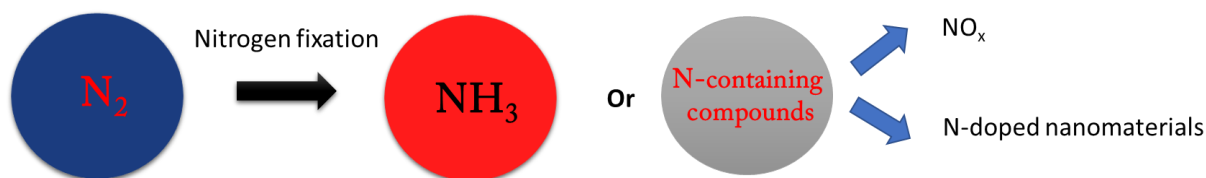


**Figure 1.** Nitrogen fixation process to convert nitrogen gas into other nitrogen-containing compounds

Recently, various types of plasma have received immense attention in the nitrogen fixation process, including thermal and non-thermal plasma nitrogen fixation [47]. Concerning the former, an illustrative

example is the Birkland-Eyde process for nitrogen oxide synthesis, which utilizes an electrical arc discharge to form a high-temperature thermal plasma. However, the low energy efficiency of this process is challenging, leading to less progression in recent years. The key to any industrial application is to bring the energy efficiency of non-thermal plasma nitrogen fixation down to an industrially acceptable range, and the non-thermal plasma foreseen is on its way, allowing to keep reaction temperature and energy consumption relatively low [48]. Microplasma refers to a type of plasma that is smaller in scale than traditional plasmas, often on the order of micrometres or millimetres. In the context of nonthermal nitrogen fixation, microplasma may be used to create the high-energy conditions necessary to convert  $N_2$  to a usable form without the need for high temperatures (Figure 2). Research in this area is still in its early stages, but it has the potential to be a sustainable and energy-efficient method for producing fertilizer.

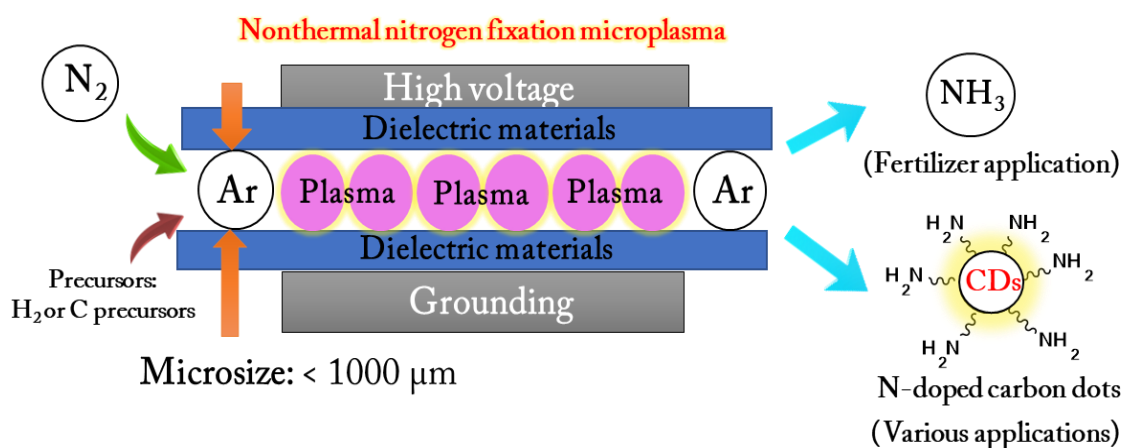


**Figure 2.** Nonthermal nitrogen fixation microplasma process

Nonthermal nitrogen fixation microplasma is a promising new approach to producing nitrogen-containing compounds. The process utilizes a microplasma to ionize the atmospheric nitrogen ( $N_2$ ) to form reactive nitrogen species (RNS), which can then react with other molecules. The high energy conditions created by the microplasma can facilitate these reactions without the need for high temperatures traditionally required for nitrogen fixation.

One of the advantages of this approach is that it does not require the use of high-pressure vessels or catalysts, which can make the process more cost-effective and sustainable. Additionally, since it uses atmospheric nitrogen as the starting material, it does not rely on finite resources such as natural gas or coal. Currently, research on nonthermal nitrogen fixation using microplasma mainly focuses on laboratory-scale experiments, but there are ongoing efforts to develop a commercial-scale technology. It should be noted that this technology is still in the early stages of development and is not yet commercially available.



In practice, nitrogen fixation and oxidation should both occur. This means that the surface of NCQDs is functionalised with  $\text{NH}_2$  (nitrogen fixation) and  $-\text{OH}$  (oxidation). However, in order to improve the quantum yield and fluorescence intensity, nitrogen doping on the surface by nitrogen fixation plays a key role. Therefore, the author emphasises nitrogen fixation's importance in this study, as described in the thesis's title.

### 1.3.2. N-doped carbon quantum dots as an emerging advanced nanomaterial

Carbon-based materials are important in the field of materials science and have a wide range of applications. From traditional industrial carbon materials like activated carbon and carbon black, to newer industrial carbon materials like carbon fibres and graphite, to newer carbon nanomaterials like graphene and carbon nanotubes (CNTs), research and applications of carbon-based materials have been popular due to their environmentally friendly properties. However, macroscopic carbon materials typically lack an appropriate band gap, making them poor candidates for use as fluorescent materials.

Carbon dots, or CDs, are an emerging material in the carbon family, which is zero-dimension carbon-based nanomaterials that measure less than 10 nanometres in size. They are a newly developed carbon nanomaterial made up of small, spherical particles. CDs were first found in 2004 during the purification process of single-walled carbon nanotubes [49] and were later named "carbon quantum dots" by Sun et al. in 2006 [50]. They are being considered for various applications [51-58] due to their unique structure and properties, such as simple synthesis methods and enhancement of fluorescence emission through surface passivation and chemical modification [59]. After their discovery, CDs gained a lot of interest due to their unique structure and properties. As a new form of carbon, they possess many advantageous qualities such as low toxicity [60], good compatibility with living cells [61], stability in chemical reactions [62], ability to efficiently absorb light [62], and efficient transfer of electrons when exposed to light [63]. These properties make CDs a highly promising material for a wide range of applications, including biosensors [64], bioimaging [65], optoelectronic devices [66], and solar cells [67].

Carbon dots, also known as small carbon nanoparticles that can be found in aqueous or other suspensions, are typically divided into three categories (Figure 3): graphene quantum dots (GQDs), carbon nanodots (CNDs), and carbonized polymeric dots (CPDs). The classification is not fixed; one type can be transformed into another by adjusting the graphene layers and carbonization degree. They are often composed of a hybridized  $\text{sp}^2/\text{sp}^3$  carbon core with surface functional groups. For example, GQDs are composed of single or multiple layers of nanosized graphite, with functional groups or defects on the surface or at the edges. They have an anisotropic shape with larger lateral dimensions than height [68, 69]. The

optical properties of GQDs mainly depend on the size of the  $\pi$ -conjugated domains and surface/edge structures [70].

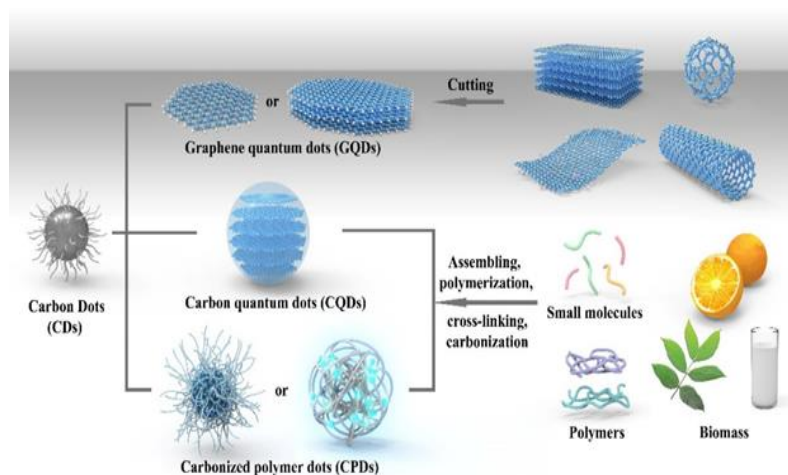


**Figure 3.** Classification of carbon dots based on their formation mechanism, micro- and nanostructures, and properties (This figure is adapted from [71], Copyright 2020, American Chemical Society)

In contrast to GQDs, CQDs and CPDs typically have a spherical core connected to surface groups. The spherical core of CQDs is composed of multiple layers of graphite. Their ability to emit light (photoluminescence) is primarily determined by the intrinsic state of luminescence and the quantum confinement effect of size [72]. CPDs combine aggregated/cross-linked carbon cores and polymer chain shells. The optical properties of CPDs are mainly influenced by the molecular state and cross-link structure [73].

The various structures of CDs are influenced by different synthesis methods, which can be broadly categorized into "bottom-up" and "top-down" strategies [71, 74-79]. CQDs and CPDs are often produced from small molecules, polymers, or biomass by assembling, polymerization, crosslinking, and carbonization via "bottom-up" methods (e.g., combustion, thermal treatment) [52, 80-82], while GQDs are typically obtained through "top-down" methods, such as cutting larger graphitized carbon materials into small pieces [83]. The surface functional groups of CDs can be altered by using different synthesis methods, allowing for tunable light emission. Additionally, the modified surface moieties of CDs allow for expansion of the light utilization range from different states of emissive trap due to their efficient up-converted photoluminescence behaviour [84], meaning that efficient visible-light-responsive CDs can be designed to utilize the full spectrum of sunlight. Furthermore, the ability of CDs-based composites to absorb light improves photocatalytic efficiency through photoexcited electron transfer [85].

Non-doped or pristine carbon dots (CDs) and N-doped CDs have some key differences in their properties due to the presence of nitrogen atoms in the latter. Here are some comparative differences between non-doped and N-doped CDs:

- **Optical Properties:** N-doped CDs have red-shifted absorption and emission spectra compared to non-doped CDs. This is due to the incorporation of nitrogen atoms into the carbon matrix, which creates new energy levels in the electronic band structure of the CDs. The presence of nitrogen also enhances the quantum yield and stability of the CDs.
- **Chemical Properties:** The introduction of nitrogen atoms in CDs changes their chemical properties, such as surface charge, hydrophilicity, and chemical reactivity. N-doped CDs tend to have a more hydrophilic surface due to the presence of polar nitrogen atoms, making them more biocompatible and suitable for biological applications.
- **Electronic Properties:** N-doped CDs have a higher electron density and electrical conductivity than non-doped CDs due to the doping of nitrogen atoms. Nitrogen also enhances the CDs' electron transfer properties, making them useful for applications in electrochemistry and energy storage.
- **Morphology:** N-doped CDs tend to have larger particle sizes and a more spherical morphology than non-doped CDs. This can be attributed to the introduction of nitrogen atoms, which can influence the growth and morphology of the CDs during synthesis.

Defects in the carbon dot (CD) structure (i.e. N-doped carbon dots) can have an impact on their optical, electronic, and chemical properties. However, the synthesis of CDs is a relatively new field, and there is still ongoing research into the factors that influence the formation of defects in CDs. Here are some strategies that have been proposed to reduce or control crystal defects in CDs:

- **Precursor and Synthesis Conditions:** The choice of precursor and synthesis conditions can have a significant impact on the formation of defects in CDs. Careful selection of the carbon source and the reaction conditions, such as temperature, time, and pH, can reduce the formation of defects. For example, using a carbon source with a high degree of purity and controlling the reaction temperature can help minimize the formation of defects.
- **Post-Synthesis Purification:** Purification of CDs after synthesis can help eliminate or reduce the number of defects. Purification methods such as dialysis or centrifugation can help remove impurities and stabilize the CDs, improving crystal quality.
- **Doping:** Doping of CDs with heteroatoms, such as nitrogen, can modify the electronic properties of the CDs and reduce the formation of defects. Nitrogen-doped CDs have been shown to have improved optical and electronic properties compared to non-doped CDs, which can be attributed to the reduced number of defects.

- Surface Passivation: Surface passivation can be used to reduce the formation of surface defects in CDs. Coating the surface of CDs with a layer of a passivating material, such as silica or polymers, can protect the CDs from oxidation and reduce the formation of surface defects.

### 1.3.3. Properties of N-doped carbon quantum dots

CQDs are commonly classified into three types: GQDs, CQDs, and CPDs. These types are defined in terms of their "core-shell" nanostructure, which consists of a nanoscale carbon core and surface functional groups. The optical properties, electronic properties, and catalytic properties of CQDs are determined by their different structures. GQDs have high quantum yield and strong fluorescence, CQDs have good biocompatibility and stability, and CPDs have high surface area and catalytic activity (Figure 4).

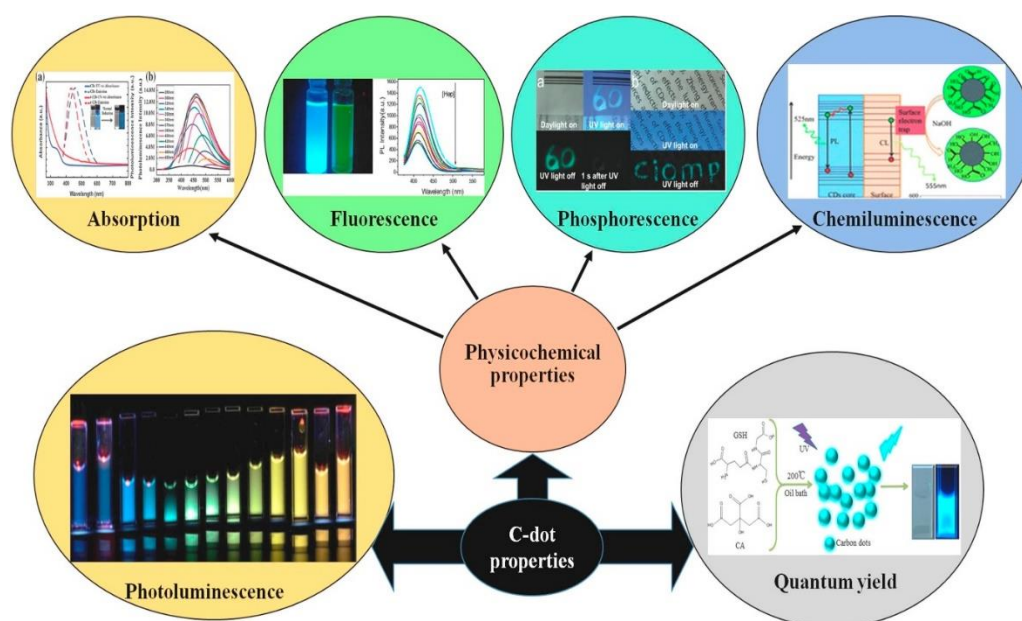


**Figure 4.** Outstanding properties of carbon dots based on their surface and core structure (this figure is adapted from the original work [86], copyright 2018, Elsevier)

#### 1.3.3.1. Adsorption

CDs have strong optical absorption in the ultraviolet (UV) region (mainly 280–360 nm). Surface modifications can regulate the absorption band of CDs, and the emission properties of CDs generally depend on the level of excitation [87]. Surface functional moieties play an important role in determining the absorption ranges of CDs. Passivating CDs with polyethyleneimine (PEI) can produce red (330–355 nm), blue (460–495 nm) or green (530–550 nm) luminescence. However, the nonuniformity of PEI passivation on CDs can disrupt the photoluminescence and cause excitation at longer wavelengths [88].

CDs show optical absorption in the UV region and some traces of absorption in the visible region. Top-down fabricated CDs show size-dependent absorption from 200 to 252 nm (6.20–4.92 eV) with an increase in diameter from 12 to 22 nm. However, CDs fabricated from the same material but using different fabrication techniques, such as microwave, ultrasonic, and hydrothermal approaches, show different absorption bands within the 250–300 nm range [89].

### 1.3.3.2. Fluorescence property

The fluorescence emission of CQDs is one of their most attractive features and has been used in various fields. CQDs have properties such as excitation wavelength-dependent PL emission, tunable PL emission, extraordinary up-converted PL, good fluorescence stability and efficient photobleaching resistance. The PL emissions of CQDs are dependent on their structural characteristics. They can be divided into two categories: one is due to electron transitions corresponding to internal factors dominated emission, which includes the conjugation effect, the surface state and the synergistic effect [90]. This model is suitable for explaining the PL of GQDs with lattice structures or a high degree of graphitization. GQDs have a certain degree of crystallinity and an average lattice parameter of 0.24 nm. The PL emission of CQDs can be tuned by adjusting the size of the conjugated  $\pi$ -domains rather than the actual particle size, as their sizes are smaller than their exciton Bohr radius [91]. The quantum confinement effect of GQDs was supported by theoretical calculations method, as reported by Sk et al., who studied the PL emission of pristine zigzag-edged GQDs with different diameters using Gaussian and time-dependent density-function theory (DFT) [91]. The wavelength of photoluminescence (PL) emissions of graphene quantum dots (GQDs) can vary depending on their diameter. The smallest GQDs with a diameter of 0.5 nm have a wavelength of 235.2 nm, while GQDs with a diameter of 2.31 nm has a wavelength of 999.5 nm. The PL emission of GQDs is observed in the entire visible region (400–770 nm), with the different diameters of GQDs increasing from 0.89 to 1.80 nm, which is attributed to the quantum confinement effect. This particle size dependence is consistent with the quantum confinement effect. The intrinsic state of GQDs also determines their PL emission behaviour due to the quantum confinement effect. The conjugated  $\pi$ -domains are regarded as intrinsic PL centre. The band gaps of GQDs decrease as aromatic rings increase, indicating that PL emissions of GQDs can be adjusted by tuning the size of the conjugated  $\pi$ -domains. By changing the size or shape of GQDs, the electronic transitions can be tuned in nanometer-sized GQDs [92, 93].

In addition to the quantum confinement effect, the surface configurations or surface/edge state of GQDs can also play a key role in the photoluminescence (PL) emission of GQDs [94]. Surface defects, triple carbene at the zigzag edges, and oxygen-containing/other functional groups can induce PL emission

with different characteristics. Heteroatom doping is also used to alter the electronic structures of GQDs and is also attributed to the surface state effect [95]. The PL emission of GQDs can also be pH dependent. It can be affected under a strongly acidic atmosphere due to protonation or deprotonation of functional moieties on the surface of the carbon core-edge state. Different types of organic solvents can also lead to different surface passivation, resulting in different PL emission characteristics [96]. Ding and co-workers proposed a hydrothermal method to prepare a series of GQDs with similar size distributions [61]. These GQDs show surface oxidation-dependent PL emission in the 440-625 nm wavelength range and have potential applications in different fields. The independent PL emission of GQDs is attributed to the presence of a self-passivated layer. Lin et al. discovered that GQDs with zigzag edges have smaller energy gaps than those with armchair edges. PL emission likely originated from triple carbene states instead of quantum confinement effects, which can be quenched and recovered under acidic or alkaline conditions [97].

In addition to the previously mentioned properties of GQDs, it has also been discovered that the hybridization of amine moieties and the carbon core can tune the PL emission [98]. This is due to the modified electronic structure of GQDs through the effective orbital resonance effect. Density functional theory calculations have shown that this method can also decrease the band gap of GQDs. Jin et al. also found that GQDs have two independent molecule-like states attributed to the surface moieties' structure, further emphasizing the impact of the surface state on PL emission. It is important to note that an individual effect cannot fully explain PL emission in GQDs and that synergistic effect models have been proposed to interpret the PL emission mechanism of CDs.

The PL emission mechanisms of CQDs (carbon quantum dots) have been found to include various factors, such as the carbon core and surface state, the conjugation effect and surface functional groups, and the conjugation effect and defects. These mechanisms are thought to originate from the surface/edge state and conjugated  $\pi$ -domains. However, Wang et al. proposed that the PL behaviours of GQDs are likely associated with oxygen-containing functional moieties on the surface of the carbon core, as determined by single-particle spectroscopic measurements [99]. The photoexcited electrons relax from  $\pi^*$  orbit to  $sp^2$  intrinsic and defect states, resulting in blue and green PL emissions, respectively.

### 1.3.3.3. Phosphorescence

CDs have been shown to have phosphorescence properties when used as a water-soluble material. When mixed with a matrix of polyvinyl alcohol (PVA), CDs exhibit clear phosphorescence under UV light. The phosphorescence is believed to be caused by the presence of aromatic carbonyl groups on the surface of the CDs, which provide a triplet excited state [79]. In other words, the phosphorescence observed in

CDs is primarily caused by the radiation transition of the triplet excited state ( $T_n$ ). As shown in Fig. 1, initially, electrons in the ground state ( $S_0$ ) are excited and transferred to the singlet excited state ( $S_n$ ). Then, the electrons relax to the lowest singlet excited state ( $S_1$ ), where they reach  $T_n$  through an intersystem crossing (ISC) process. Finally, the electrons fly back from  $T_1$  to  $S_0$  and generate phosphorescence. Deng et al. also reported on the phosphorescence properties of a CD-based water-soluble phosphorescent material, and found that clear phosphorescence is detected at room temperature.

### 1.3.3.4. Chemiluminescence

The chemiluminescence of CDs is used for the determination of radioactive substances. The intensity of the chemiluminescence depends solely on the concentration of CDs within a certain absorption range. For example, Lin et al. mixed CDs with oxidants, including cerium and potassium permanganate ( $KMnO_4$ ), resulting in the chemiluminescence of the CDs [100]. Reversely, Zhao et al. reported that CDs have excellent electron-donating properties towards dissolved oxygen to generate reactive oxygen species ( $O_2^-$ ) in strong alkali solutions, such as NaOH or KOH, which results in chemiluminescence.

### 1.3.3.5. Photoluminescence

Photoluminescence (PL) is one of the most outstanding features of CDs. While there is an ongoing debate about the source of PL in CDs, it is known that a key aspect is a diameter of less than 10 nm and a zero-dimensional structure. CDs' morphology, composition, size, and crystalline nature also affect their PL properties, which are determined by the initial precursors and fabrication techniques used to form the CDs [101]. Researchers have reported enhanced PL properties in CDs through surface modulation. New fabrication strategies, such as exposure to a single UV light, have been developed to produce CDs that emit blue, green, and red light. Nitrogen-doped CDs have been fabricated using a one-step hydrothermal treatment with *m*-aminobenzoic acid as a precursor for the detection of iron ions. They have been found to have a charge density that changes according to their electron richness, leading to higher QY (quantum yield) and a stronger peak of PL at 415 nm [102].

### 1.3.3.6. Optoelectronic properties

The optoelectronic properties of carbon dots are highly dependent on their surface chemistry. The surface chemistry of CDs can be modified by various chemical functionalization strategies such as surface oxidation, surface passivation, and surface doping. These modifications can alter CDs' chemical composition, surface charge, and surface energy, leading to changes in their optoelectronic properties. One of the key optoelectronic properties of CDs that is affected by surface chemistry is their fluorescence

emission. The fluorescence emission of CDs is highly dependent on the surface functional groups present on their surface. For example, CDs functionalized with carboxylic acid groups exhibit a blue-shifted emission spectrum compared to CDs functionalized with amine groups, which exhibit a red-shifted emission spectrum. This difference in emission wavelength can be attributed to the variation in the surface energy of CDs with different surface functional groups.

Another optoelectronic property that can be affected by surface chemistry is the absorption spectrum of CDs. CDs with different surface chemistries exhibit different absorption spectra due to the variation in the electronic band structure of the CDs. For example, CDs functionalized with nitrogen-doped groups exhibit a red-shifted absorption spectrum compared to undoped CDs, which can be attributed to the introduction of new energy levels in the electronic band structure of the CDs.

### 1.3.3.7. Quantum Yield

Carbon dots (CDs) have been found to exhibit high fluorescence quantum yields (QYs) in the range of 50-90%, depending on the synthesis method and surface chemistry of the CDs. These high QYs are due to the presence of quantum dots (QDs) within the CDs, which act as efficient light-emitting centres. Several factors can affect the quantum yield of CDs, including the size and shape of the QDs, the surface chemistry of the CDs, and the environment in which they are used. For example, the surface modification of CDs can greatly enhance the fluorescence quantum yield by reducing the nonradiative relaxation pathways. Moreover, it was reported that the QY of CDs could be increased by controlling the size and shape of the CDs and by functionalizing their surfaces with molecules that can improve their stability and biocompatibility. Overall, carbon dots (CDs) have been found to exhibit high fluorescence quantum yields (QYs), which make them useful for a wide range of applications in fields such as imaging, sensing, and biotechnology. However, it's important to note that the QY of CDs may vary depending on the synthesis method, surface chemistry, and the environment in which they are used.

### 1.3.4. Various synthesis methodologies of N-doped carbon dots

Various methods have been proposed in recent years to create CDs with specific properties for different applications. These methods can be broadly categorized into two types: "top-down" and "bottom-up" (Figure 5).

Top-down methods involve techniques such as ultrasonic synthesis, chemical exfoliation, electrochemical oxidation, arc-discharge, and laser ablation, to exfoliate and cut macroscopic carbon structures, like graphite powder, carbon black, activated carbon, carbon nanotubes, carbon soot, and carbon fibres, to produce GQDs, which are 2D nanoparticles [103]. In contrast to top-down methods, bottom-up



methods typically involve the polymerization of molecular precursors, such as glucose, sucrose, and citric acid, through techniques like microwave pyrolysis, solvothermal reactions, plasma treatment, and chemical vapour deposition to produce CQDs and CPDs, which are 3D nanoparticles with spherical cores [103]. These methods are generally faster, more controllable, and less expensive than top-down methods.

Additionally, bottom-up methods often produce fewer defects and have high controllability. Here, we will delve into the primary methods for synthesizing CDs, controlling their size, and modifying their surface properties through confined pyrolysis and modification techniques. The surface properties of CDs can also be optimized during preparation or through further treatment for specific applications.

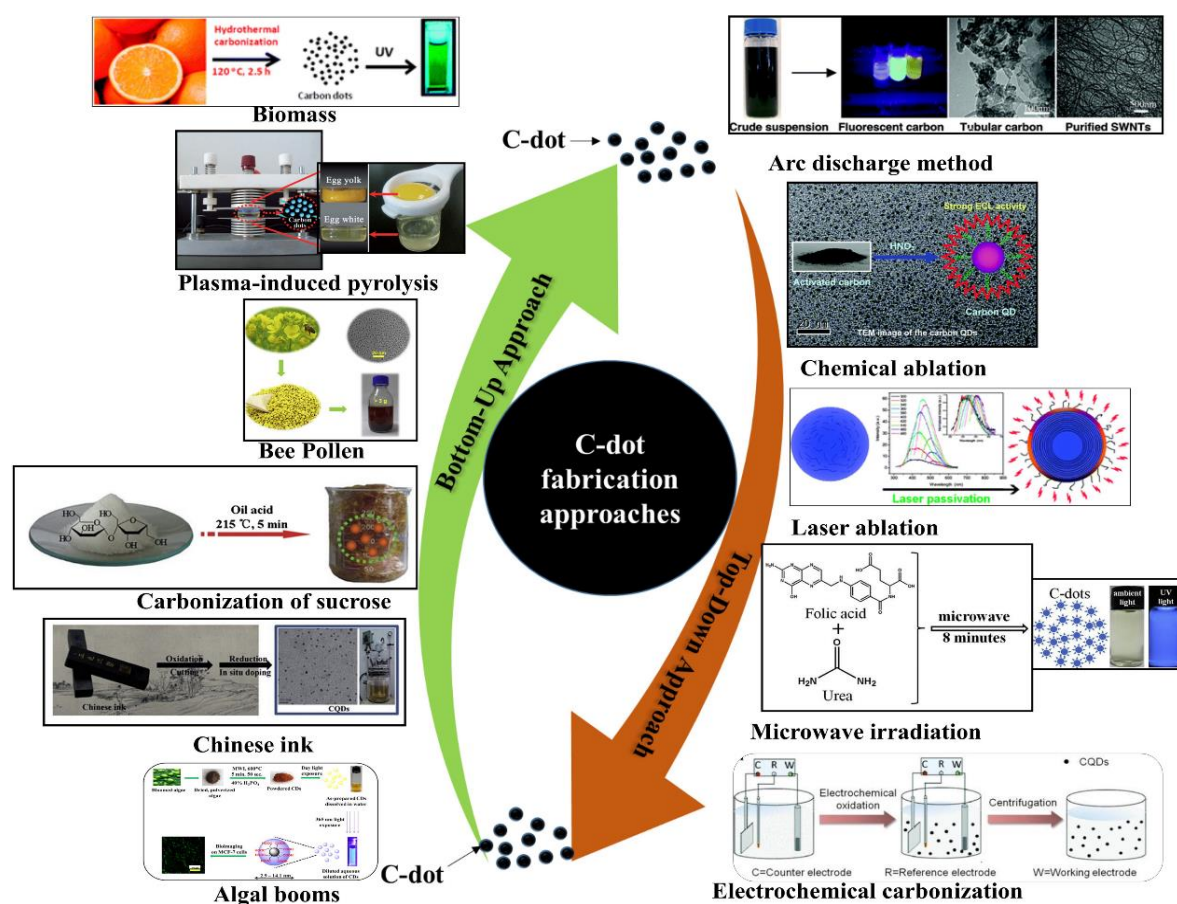


**Figure 5.** Various synthesis approaches of carbon dots (This figure is adapted from the original work [86], copyright 2018, Elsevier)

Based on the literature review, all of the reported large-scale microplasma syntheses of NCQDs are batch-type reactor configurations. Therefore, the flow-type reactor was not discussed and assessed in this study. However, the authors also found that a flow-type reactor or microplasma microfluidic device is an advanced

and scalable technology. Therefore, the authors also discussed this novel technology in another topic “Microfluidic plasmas: Novel technique for chemistry and chemical engineering” by Lin et al. 2021.

Controlling the reaction time, heat, and mass transport in a static batch-type reactor require careful monitoring and management of the operating conditions, mixing system, and heating or cooling system. By optimizing these factors, you can improve the efficiency and effectiveness of the reaction. The following steps are suggested to control reaction time and heat and mass transport in a static batch-type reactor:

- Set the operating conditions: Before starting the reaction, set the desired temperature, pressure, and concentration of reactants. These operating conditions will play a critical role in determining the reaction time, heat, and mass transport.
- Monitor the temperature: Use a thermometer to monitor the temperature inside the reactor. If the temperature deviates from the desired set point, adjust the heating or cooling system accordingly to maintain the temperature.
- Control the reaction time: The reaction time can be controlled by monitoring the progress of the reaction. You can use techniques such as sampling, pH monitoring, or turbidity to determine the completion of the reaction. Adjust the reaction time by extending or reducing the time allowed for the reaction to take place.
- Manage mass transport: The mixing system plays a critical role in managing mass transport. Ensure that the reactor is properly mixed to prevent concentration gradients from forming. If concentration gradients do form, adjust the mixing speed or add baffles to the reactor to help promote mixing.
- Manage heat transport: The reactor's design and heating or cooling system will affect heat transport. Ensure that the reactor is designed to promote efficient heat transfer. If heat is not being transferred effectively, adjust the reactor's design or heating/cooling system accordingly.
- Optimize the reaction conditions: Adjust the operating conditions to optimize the reaction. This may include changing the concentration of reactants, adjusting the temperature or pressure, or modifying the mixing system.
- Control byproduct formation: Monitor the reaction for the formation of byproducts. Byproducts can affect the reaction time, heat, and mass transport. Adjust the reaction conditions or use a catalyst to prevent byproduct formation

### 1.3.4.1. Top-down approaches

**Chemical exfoliation.** It is a simple and efficient method for the mass production of high-quality CDs without complex equipment. This method clears precursor carbon materials such as carbon fibres, graphene

oxide, and carbon nanotubes by strong acids or oxidizing agents. Mao and co-workers were the first to create fluorescent GQDs with different sizes from candle soot using  $\text{HNO}_3$  at a relatively high temperature in 2007 [104]. Later, Peng et al. used  $\text{H}_2\text{SO}_4$  and  $\text{HNO}_3$  to prepare GQDs through the chemical exfoliation of carbon fibres [105]. The resulting GQDs with different size ranges showed yellow, green, and blue PL emissions under different stirring temperatures, indicating that chemically cleaving carbon fibres can successfully prepare GQDs. Researchers have also used low-cost materials as precursors to prepare GQDs under strong acid conditions. For example, Ye and his team used coal to prepare hexagonal GQDs with a size range of 3-6 nm. Zhao et al. also used asphaltene to fabricate GQDs with excitation-dependent PL emission. However, it is tedious to further purify the product by removing excess  $\text{H}_2\text{SO}_4$ , which increases the overall synthesis cost [106].

**Laser ablation.** It is a unique and promising synthesis method for CDs due to its short period and simple operation. Sun et al. were the first to use laser ablation to synthesize GQDs from graphite [59]. Li et al. used rapid laser passivation of carbon particles to prepare GQDs with visible, stable, and tunable PL performance [107]. They also showed that passivation by laser irradiation significantly impacts the origin of PL. Similarly, Hu et al. proposed a simple method to synthesize fluorescent carbon nanoparticles by laser ablation of carbon powder suspensions in organic solvents [108]. The surface of the resulting GQDs can be modified by choosing appropriate solvents, which allows for tuning the PL emission of the GQDs by changing their surface functional groups. Kang proposed a rapid method to synthesize GQDs from multi-wall carbon nanotubes with excellent optoelectronic properties [109]. The synthesized GQDs show stable blue PL emission and a PL quantum yield of 12%, making them suitable for optoelectronic applications. Ren et al. used laser ablation of carbonized *Platanus* biomass in a formamide solution to prepare NM-CQDs, which showed dual-wavelength PL emission [110]. They also proposed an ultrafast method to fabricate homogeneous CQDs through dual-beam pulsed laser ablation, which improves preparation efficiency. A schematic diagram of the synthesis of CQDs from carbon fibre is also presented.

**Ultrasonic-assisted method.** It is a low-cost and simple method for preparing CDs. Alternate high-pressure waves and low-pressure are generated in the ultrasound process, which results in the formation and collapse of small bubbles in the liquid. These bubbles produce strong hydrodynamic shear forces that cut macroscopic carbon materials into nanoscale CDs. Researchers can prepare CDs with different properties by adjusting the ultrasonic power, reaction time, and the ratio of carbon sources and solvents. Zhuo et al. first reported the preparation of GQDs through ultrasonic exfoliation of graphene [111]. Since then, many researchers have used ultrasonic-assisted treatment to prepare GQDs from carbon materials such as graphite, MWCNTs, GO, and carbon fibre in either aqueous or organic solvents. Song and his team prepared GQDs from the aqueous dispersion of graphite and potassium sodium tartrate by ultrasonic-

assisted treatment, which showed blue luminescent emission [112]. The ultrasonic approach also fabricated heteroatom-doped GQDs. Zhao et al. synthesized chlorine-doped GQDs from chlorinated CF precursors through direct ultrasonic exfoliation [113]. Carbon-containing waste materials, such as food waste, have also been used to prepare CQDs through ultrasonic irradiation treatment. Park et al. synthesized water-soluble CQDs from food waste-derived carbon sources and found that about 120g of CDs with an average diameter of 2-4 nm could be produced from a 100 kg mixture of ethanol and food waste [114]. These CDs have good PL properties, low cytotoxicity and high photostability for in vitro bioimaging.

### 1.3.4.2. Bottom-up approaches

**Microwave-assisted synthesis.** It is a cost-effective and efficient method for synthesizing CDs. Using microwaves can provide uniform heat for the formation of CDs. Li et al. were the first to use this method to synthesize green fluorescent GQDs using microwave-assisted chemical cleavage of GO sheets under acidic conditions [115]. The obtained GQDs with a single-layer have an average diameter of 4.5 nm, and can be further designed to have blue fluorescent properties by reducing surface radical moieties. Wang and co-workers reported a simple one-pot microwave-assisted approach to fabricate water-soluble CDs from protein-rich eggshell membranes [116]. The resulting CQDs show excellent fluorescence emission with a quantum yield of about 14% and can simultaneously detect  $\text{Cu}^{2+}$  and glutathione. Yao et al. proposed a new route to produce novel fluorescent CQDs from transition-metal ions and crab shells using microwave-assisted hydrothermal [117]. The resulting Gd@CQDs display high stability against pH and NaCl concentration, indicating potential application in drug delivery. CDs were also obtained from *Mangifera indica* leaves by a simple microwave-assisted hydrothermal, which possess good biocompatibility and high photostability and can be used as an intracellular temperature sensor. Wang et al. proposed a two-step microwave heating process to produce CDs from raw cashew gum, which have good biocompatibility and low cytotoxicity and can be used in live-cell imaging [118].

**Hydrothermal synthesis.** It is a cost-effective and non-toxic method for preparing CDs. It is a simple approach to synthesize CQDs where a mixture of water solution is enclosed in Teflon and heated at high pressure and high temperature [119]. Pan et al. were the first to use this method to prepare blue fluorescence CQDs [95]. Epoxy moieties on the surface of GO sheets were completely broken down into CQDs during hydrothermal treatment. Subsequently, Zhao's group reported a simple and highly efficient route to prepare CQDs by hydrothermal treatment [120]. Some researchers also utilized oxidants to accelerate the hydrothermal reaction. For example, Halder et al. reported a simple hydrothermal method to prepare GQDs by adding  $\text{H}_2\text{O}_2$  to accelerate GO sheets' exfoliation, indicating effective scissors of the GO sheets by  $\text{H}_2\text{O}_2$  during hydrothermal reaction [121]. Mehta et al. used a plant-based hydrothermal route to

synthesize water-soluble fluorescent CQDs from *Saccharum officinarum* juice, which were used to detect  $\text{Cu}^{2+}$  [122]. Lu et al. proposed a hydrothermal route to produce CQDs from pomelo peel, which was used to detect  $\text{Hg}^{2+}$  in lake water samples [123].

**Solvothermal synthesis.** This preparation method of CDs has the advantages of low-cost and simple equipment compared to the hydrothermal method [124]. This method replaces water solution with one or several solvents sealed with Teflon equipped with a steel autoclave. Zhu et al. used this method to prepare green fluorescent GQDs with a PL quantum yield of 11% [125]. Shin and co-workers chemically oxidized natural carbon precursors by using ozone as a non-acid mild oxidant, resulting in GQDs with a high quantum yield and blue PL emission [125]. Tian et al. synthesized blue fluorescent GQDs by solvothermal exfoliation of graphite with the help of mild  $\text{H}_2\text{O}_2$ , which showed a high quantum yield of 15% and good photoluminescence stability in different pH conditions [126]. Liu and his co-workers established a green one-step solvothermal route to fabricate CQDs from L-ascorbic acid and glycol solution in an autoclave at 160 °C for 4 h, which exhibited a strong green fluorescent emission for cell labelling [127].

**Pyrolysis.** It is a powerful technique for fabricating fluorescent CDs using macroscopic carbon structures as precursors. This method offers the advantages of short reaction time, low cost, easy operation, solvent-free approaches and scalable production. The four main processes, heating, dehydration, degradation and carbonization, are critical for converting organic carbon-containing substances into CQDs under high temperatures. Carbon precursors are cleaved into carbon nanoparticles using high-concentration alkali or acid in the pyrolysis process. Ma et al. fabricated N-GQDs by the direct carbonization of ethylene diaminetetra acetic acid at 260–280 °C and proposed a growth mechanism for GQDs [128]. Various types of CQDs were reported by ion doping; for example, Li and co-workers fabricated Cl-GQDs by introducing HCl through the dehydration and formation of GQD nuclei under hydrothermal treatment [129].

**Chemical vapour deposition (CVD) method.** It is used to fabricate CQDs, which has recently been widely explored. The size of the ultimate product can be determined by tuning parameters, including the carbon source, growth time, the flow rate of hydrogen ( $\text{H}_2$ ) and temperature of the substrate. Fan et al. proposed the CVD method to prepare CQDs using methane as a carbon source [130]. Specifically, oxidation groups on the surface of a copper foil were cleaned using alcohol and HCl. Then, the substrate was heated to 1000 °C in  $\text{H}_2$  and Ar ambient conditions.  $\text{H}_2$  supply was turned off, and Ar was continuously supplied to remove  $\text{H}_2$  residues. Afterwards, methane gas ( $\text{CH}_4$ ) was pumped in the furnace at a flow rate of 2 mL/min for only 3 s in an Ar environment. The size of the as-synthesized CQDs was distributed in the range of 5–15 nm, and the height profile thereof was 1–3 nm, indicating the successful preparation of few-layer-thick CQDs.

1.3.5. Characterisation methods of N-doped carbon quantum dots

CQDs, or colloidal quantum dots, are semiconductor nanomaterials with different structures depending on the precursor used to produce them. The size of CQDs can also be adjusted by using different nanocomposites. There are several analytical techniques (Figure 6) that can be used to characterize CQDs, including UV-vis spectroscopy, fluorescence spectroscopy, transmission electron microscopy (TEM), x-ray diffraction (XRD), Fourier transform infrared spectroscopy (FTIR), dynamic light scattering (DLS), atomic force microscopy (AFM), and x-ray photoelectron spectroscopy (XPS) [130]. These techniques can be used to study various properties of CQDs, such as size, composition, crystal structure, and surface chemistry.

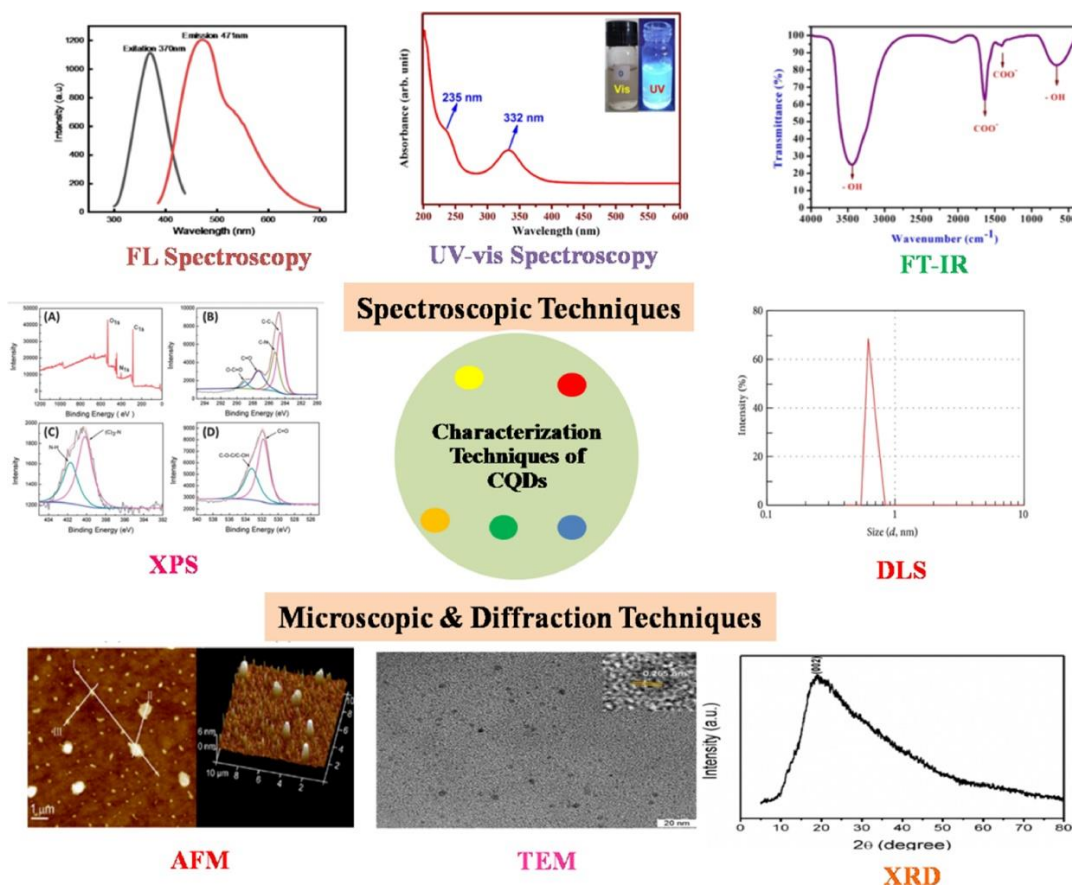


Figure 6. Characterisation technique for analysing the properties of NCQDs (This figure is adapted from the original work [131], Copyright 2022, Elsevier Publishing)

CQDs are typically small particles between 1 and 10 nm in size and are composed of elements such as C, H, O, and N. TEM and AFM are commonly used to analyse the size distribution of CQDs. XPS and EDX are used to confirm the composition of CQDs, while XRD patterns reveal the amorphous or crystalline structure of the particles. FTIR is used to identify the functional groups present in CQDs, such as C-O-C, COOH, C-OH, C-H, and C-C. UV-vis and fluorescence spectroscopy are used to study the

optical properties of CQDs, such as absorption, emission, and excitation peak, typically observed at 280–451 nm, 340 nm, and 480 nm.

### 1.3.6. Microplasma-assisted synthesis of N-doped carbon quantum dots

Despite being discovered in the last decades, NCQDs have become one of the most advanced materials, which can be used for various applications. For this reason, many different fabrication methods have been attempted to produce high-quality N-doped carbon quantum dots. Microplasma synthesis is a method for producing carbon quantum dots (CQDs) using a low-temperature plasma. Recently, the microplasma system has shown its significant advantages in producing N-doped carbon quantum dots. Microplasma synthesis is a relatively simple and low-cost method for producing CQDs and can be easily scaled up for large-scale production. The method involves using a low-temperature plasma, typically generated by a radio frequency (RF) or microwave discharge, to vaporize a carbon-containing precursor. The resulting carbon atoms then condense to form CQDs. N-doping, or the introduction of nitrogen atoms into the CQDs, can be achieved by using a nitrogen-containing precursor such as urea or melamine in the synthesis process. The amount of nitrogen doping can be controlled by adjusting the ratio of the carbon and nitrogen precursors. The nitrogen atoms can be distributed throughout the CQDs in different forms (pyridinic, pyrrolic or graphitic). N-doped CQDs have been shown to have improved optical and electronic properties compared to non-doped CQDs, making them useful in various applications such as bioimaging and solar cells.

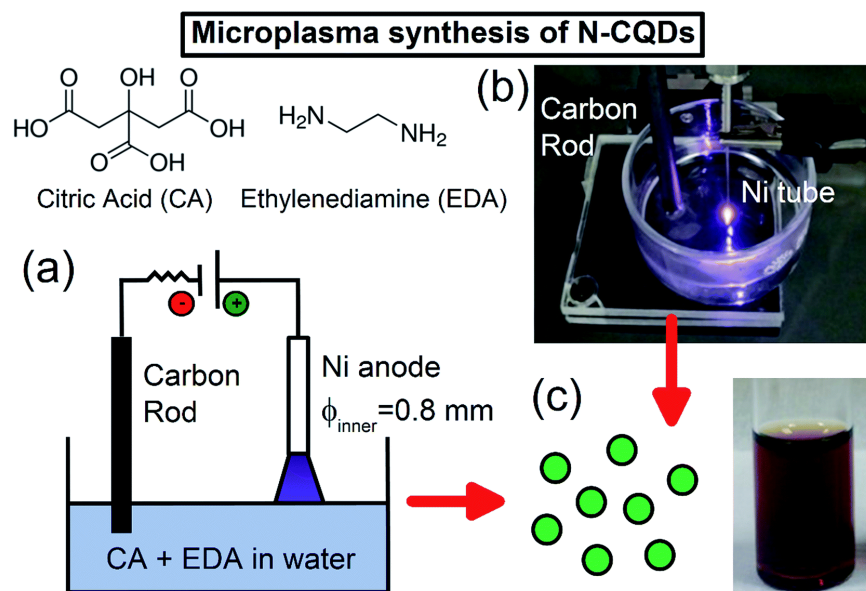


**Figure 7.** Microplasma synthesis of nitrogen-doped carbon dots (NCQDs) from molecular precursors, (a) schematic of the setup used, (b) digital photograph of the microplasma–liquid interaction and (c) the

NCQDs produced from this setup with 1.05 g citric acid and 556  $\mu\text{L}$  ethylenediamine dissolved in 10 mL water. (This figure is adapted from the original work [132], Copyright 2017, RSC Publishing)

Plasma-assisted microplasma synthesis of N-doped carbon quantum dots can either carry out in the form of an indirect or direct plasma-liquid interaction system. Indirect plasma-liquid interaction indicates a system with a plasma generation above the electrolyte solution's surface. In contrast, direct plasma-liquid interaction is described as a setting where plasma is formed within the liquid. In a study, microplasma under atmospheric pressure generated from indirect plasma-liquid interaction produces N-doped CD (Figure 7) [132]. Citric acid (CA) and ethylenediamine (EDA) as starting materials. Typically, a given amount of citric acid (CA) and ethylenediamine (EDA) is used to dissolve in deionized water. Later, a microplasma produced by a DC power under atmospheric pressure is set above the solution's surface.

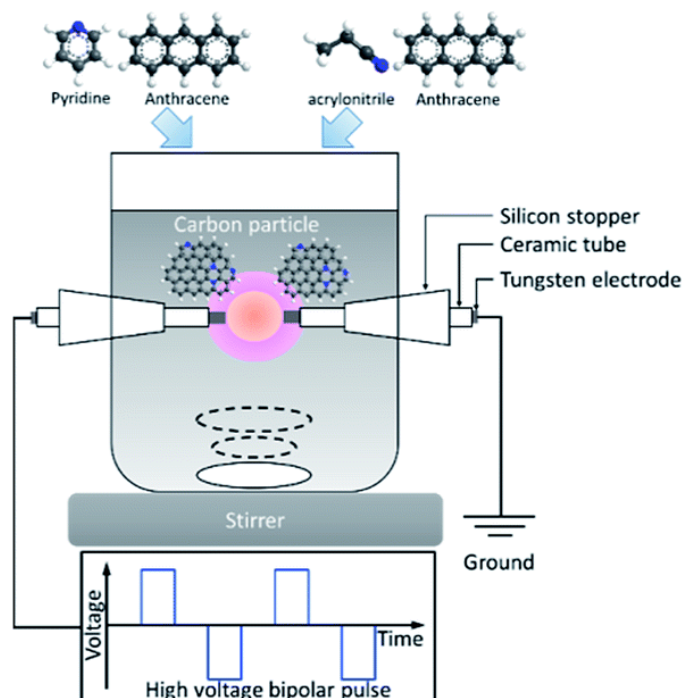


**Figure 8.** Schematic image of the experimental setup of direct plasma-liquid interaction with various types of precursors. (This figure is adapted from the original work [133], Copyright 2017 RSC Publishing)

Regarding direct plasma-liquid interaction, the use of plasma gas is indispensable. Two types of the most well-known electrodes are pin-to-pin and pin-to-plate geometries. A solution plasma process is introduced to produce N-doped carbon quantum dots using acrylonitrile and pyrazine as precursor sources. Microplasma treatment time is about 20 min under stirring [19]. Similarly, another study has also been conducted to fabricate N-doped carbon quantum dots, but the precursor sources for the synthesis are



benzene and pyrazine (Figure 8) [133]. In particular, a tungsten wire with a diameter of 1 mm is designed as electrodes and shielded by a ceramic tube. The starting materials to synthesize N-doped carbon quantum dots are benzene and pyrazine. Microplasma is introduced into the mixed starting materials under vigorous stirring for 20 min. When the microplasma is produced between the electrodes, N-doped carbon quantum dots are formed. The aforementioned evidence demonstrated that microplasma can be used to synthesize N-doped carbon quantum dots from various starting materials. Therefore, it is hypothesised that the two new designs of microplasma reactors are able to generate high-quality N-doped carbon quantum dots.

### 1.3.7. kINPen<sup>®</sup>IND microplasma jet

kINPen<sup>®</sup>IND is a handheld plasma jet device used for various applications such as wound healing, sterilization, and tissue ablation (Figure 9) [42, 134]. The device uses a low-temperature plasma to generate reactive species such as ions, electrons, and radicals that can interact with biological materials. The plasma jet is generated by passing a gas mixture through a high-voltage electric field, which ionizes the gas and creates the plasma. The device is portable, easy to use, and is said to be effective in promoting wound healing and reducing bacterial load. It is designed for use in various settings, including hospitals, clinics, and remote locations.

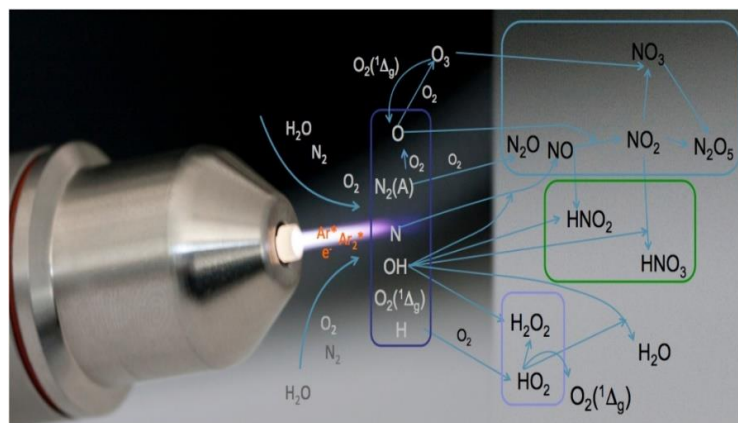


**Figure 9.** Atmospheric pressure plasma jet kINPen initiates strongly non-equilibrium chemical processes (This figure is adapted from the original work [42], Copyright 2018 OP Publishing)

The kINPen<sup>®</sup>IND plasma jet device uses a mixture of gases, typically argon and oxygen, to generate the plasma. The device has a nozzle through which the plasma is emitted, and the plasma jet can be directed onto the target area. The plasma jet is said to have a temperature of around 5,000 K, which is relatively low compared to other plasma-based devices. This low temperature is believed to reduce the risk of thermal

damage to the surrounding tissue. The device is designed to be used in various settings, including hospitals, clinics, and remote locations. It has been used for various applications, such as wound healing, sterilization, and tissue ablation. In wound healing, the plasma jet promotes the formation of new blood vessels, which can help speed up the healing process. The plasma jet kills bacteria, viruses, and other microorganisms in sterilisation. In tissue ablation, the plasma jet removes unwanted tissue, such as tumours or warts. The device is considered safe and has been cleared by the FDA for use in the United States and CE mark in European Union. It is important to note that the device is still considered as an experimental device, and more research is needed to confirm its effectiveness and safety.

### 1.3.8. Potential applications of N-doped carbon quantum dots

#### 1.3.8.1. N-doped carbon quantum dots as potential nanopesticides

N-doped carbon quantum dots (NCQDs) have been studied as potential nanopesticides due to their unique properties, such as high biocompatibility, low toxicity, and strong fluorescence. These properties make NCQDs suitable for the targeted delivery of pesticides to pests and for detecting pests in agricultural settings.

Several studies have investigated the use of NCQDs as nanopesticides [135]. For example, NCQDs are effective against various plant pests, such as cotton bollworm and rice stem borer. The NCQDs have also been found to be toxic to various fungal pathogens, such as *Fusarium oxysporum* and *Botrytis cinerea*. Additionally, NCQDs have been explored for their ability to enhance the efficacy of traditional pesticides. For example, NCQDs have been found to increase the effectiveness of carbendazim, a fungicide commonly used in agriculture, against *Fusarium oxysporum*.

Although CDs can express antifungal and bactericidal activity, these properties are not strong enough under visible light, which limits their potential for pest control. Therefore, nanotechnologists thought of a novel solution to enhance this characteristic under visible light. One of the most efficient methods is to modify the surface of CDs by doping with nitrogen atoms to form N-doped carbon quantum dots since the nitrogen atoms in CDs can provide access electrons and inject into carbon dots, thus changing their photocatalytic and optical properties. As a result, the light absorption of N-doped carbon quantum dots can extend from UV to visible light. Therefore, N-doped carbon quantum dots are more dominant than CDs in antibacterial and antifungal activity under visible light. It is shown that 25 and 75  $\mu\text{L.mL}^{-1}$  of N-doped carbon quantum dots could induce 100% antibacterial activity in the case of *E. Coli* and *S. Aureus*, respectively [136]. It is concluded that nitrogen-containing groups such as amides and amines are of utmost importance in improving antibacterial activity [137]. It is also believed that the death cause of bacteria is involved electrostatic force between protonated forms in nitrogen-containing groups and lipids in the

cellular membrane of bacteria. Another explanation for bacterial and fungal death is that CDs can produce active oxygen species to damage the cellular components of bacteria and fungi. Though there are a few studies of N-doped carbon quantum dots, the evidence above strongly showed that this type of material could be very promising candidate in inhibiting the growth of fungi-and bacteria-caused pathogens throughout photocatalysis under visible light in crops.

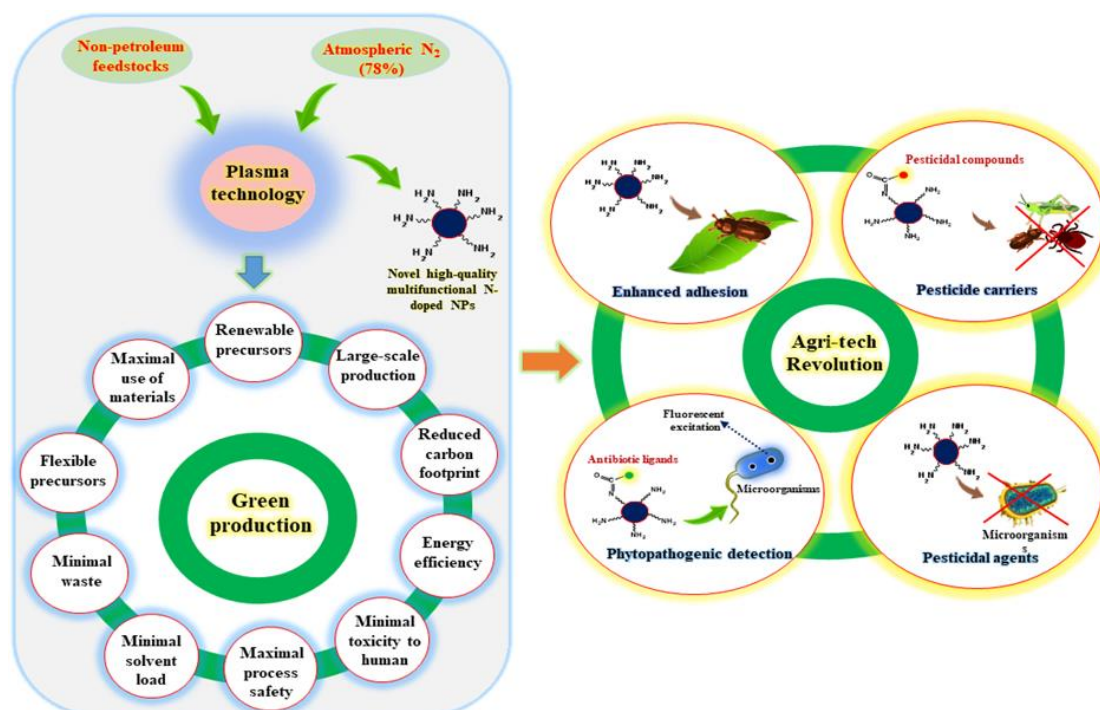


**Figure 10.** Potential applications of plasma technology-assisted N-doped CDs in the new agritech revolution (This figure is adapted from the original work [135], Copyright 2020RSC Publishing)

Overall, NCQDs have shown great potential as nanopesticides due to their unique properties and potential to enhance the efficacy of traditional pesticides. However, more research is needed to fully understand the mechanism of action of NCQDs as nanopesticides and to optimize their performance in agricultural applications.

### 1.3.8.2. N-doped carbon quantum dots as photocatalysts for wastewater treatment

N-doped carbon quantum dots (NCQDs) have been studied as photocatalysts in wastewater treatment due to their unique properties, such as high conductivity, high surface area, and strong fluorescence. These properties make NCQDs suitable for photocatalytic reactions to degrade pollutants in wastewater.

Research has shown that NCQDs have high photocatalytic activity under visible light irradiation due to the presence of nitrogen dopants, which can act as electron acceptors, enhancing the separation of

photogenerated electron-hole pairs. NCQDs is effective in degrading various pollutants, such as dyes, phenols, and organic pollutants, due to their high surface area, conductivity, and stability. They have also been effective in degrading recalcitrant pollutants such as pharmaceuticals, personal care products and endocrine disruptors. NCQDs have also been effective in removing heavy metals from wastewater. The high surface area of NCQDs provides a large area for the adsorption of heavy metals. Their high conductivity allows for the efficient transfer of electrons to facilitate the reduction of heavy metals. Furthermore, NCQDs have been explored for their ability to enhance the photocatalytic activity of other materials, such as  $\text{TiO}_2$ , by acting as a co-catalyst. NCQDs have been found to increase the photocatalytic activity of  $\text{TiO}_2$  for the degradation of pollutants in wastewater by enhancing the separation of photogenerated electron-hole pairs.

It has been proved that CDs exhibit high photocatalytic activity under UV irradiation with dominant properties such as water solubility, non-toxicity, and high chemical stability compared with conventional photocatalysts. Some recent studies have demonstrated the photocatalysis of CDs for the decomposition of ampicillin antibiotics [138], organic/industrial dyes [26], NO [132], naproxen [139], and tetracycline [140]. In addition, it has been proved that the interaction of plasma with water produces UV light sources and reactive oxygen species (ROS) radicals. These species function as reducing agents, which can decompose complex structures in wastewater, such as dye compounds [141]. Therefore, a combination of N-doped carbon quantum dots and plasma is strongly believed to synergistically affect the decomposition of complex compounds in wastewater.

Overall, N-doped carbon quantum dots have shown great potential as photocatalysts in wastewater treatment due to their unique properties and ability to enhance the photocatalytic activity of other materials. However, research is ongoing to further understand the mechanism of action of NCQDs as photocatalysts and to optimize their performance in wastewater treatment applications.

### 1.3.8.3. N-doped carbon quantum dots as theranostic agents in biomedical applications

N-doped carbon quantum dots (NCQDs) have been studied as theranostic agents in biomedical applications due to their unique properties, such as high biocompatibility, low toxicity, and strong fluorescence. These properties make NCQDs suitable for use as both diagnostic and therapeutic agents in the biomedical field.

Research has shown that NCQDs have potential applications as imaging agents for in vivo imaging and diagnostic imaging. NCQDs have been found to have high fluorescence intensity and strong near-infrared (NIR) absorption, making them suitable for deep-tissue imaging. They have also been found to be biocompatible and non-toxic, making them suitable for use in vivo. Furthermore, NCQDs have been

explored for their potential therapeutic applications. Research has shown that NCQDs have potential applications in cancer therapy due to their ability to generate reactive oxygen species (ROS) and their ability to act as a photosensitizer. NCQDs have been found to have high cytotoxicity against cancer cells and have been found to induce apoptosis in cancer cells.

Additionally, NCQDs have been found to have potential applications in drug delivery systems. NCQDs have been found to have high stability and a large surface area, making them suitable for use in drug delivery systems. They have also been found to protect the drugs from degradation and enhance drug efficacy.

One area of research is in the field of biosensing. NCQDs have been found to have high sensitivity and selectivity in detecting biomolecules, such as DNA and proteins, making them suitable for use in biosensing applications. They also have high stability and a large surface area, making them suitable for biosensing devices.

Another area of research is in the field of regenerative medicine. NCQDs have been found to have potential applications in stem cell labelling and tracking due to their biocompatibility and fluorescence properties. They have also been found to have potential applications in promoting the proliferation and differentiation of stem cells, making them suitable for use in regenerative medicine applications.

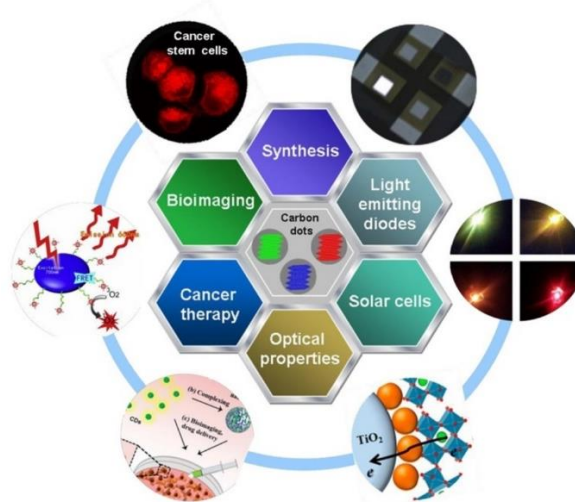


**Figure 11.** Potential applications of N-doped carbon quantum dots in biomedical applications (This figure is adapted from the original work [150], Copyright 2016 Elsevier Publishing)

It has been investigated that the wavelength range of carbon dots is from 330 nm to 475 nm. Reports have shown that carbon dots (CDs) possess high optical properties compared to other materials, such as quantum dots. In particular, strong fluorescence of carbon dots can be seen in blue and green to yellow (>460 nm). Unlike other traditional fluorescent materials, CDs show single-photon emission with down-

conversion fluorescence and two and multi-photon fluorescence emission with up-conversion fluorescence [142]. Based on such outstanding fluorescent properties, many studies indicated that carbon dots are one of the most effective theranostic agents in biomedical applications. Single photon fluorescence emission is used for imaging organs in living systems and cells in vitro [143]. Two-photon fluorescence emission is used for imaging live cells and tissues at different pH values [144]. Apart from their unique optical properties, CDs also possess some important features which make them an exceptional vehicle for fluorescence labelling and imaging: low toxicity [145], fairly good biocompatibility and permeability [146], weak interactions with proteins [147], resistance to swelling and photobleaching [148], low cost [149]. These features make them a solid base for diagnostics. N-doped carbon quantum dots are a new type of CDs in which nitrogen is doped onto the surface to enhance their optical properties [18]. In addition, the existence of -COOH and -NH<sub>2</sub> on the surface enables N-doped carbon quantum dots to conjugate with drugs for various disease treatments [86]. Therefore, it is strongly believed that N-doped carbon quantum dots are potential for theranostic applications.

Overall, N-doped carbon quantum dots have shown great potential as theranostic agents in biomedical applications (Figure 11) due to their unique properties, such as high biocompatibility, low toxicity, and strong fluorescence. They have many applications in imaging, therapy, and drug delivery systems. However, more research is needed to fully understand the mechanism of action of NCQDs as theranostic agents and to optimize their performance in biomedical applications.

### 1.4. Research aims and objectives

The primary aim of this thesis is to develop a new kind of microplasma to address the challenges associated with the large-scale production of N-fixation multifunctional N-doped carbon quantum dots (NCQD) for selected applications. A comprehensive literature review of the agricultural applications of NCQD was conducted. A comprehensive assessment of the current large-scale synthesis of NCQD in terms of substantivity was carried out using green chemistry and EcoScale metrics.

This research generally attempted to develop a new kind of microplasma reactor that can rationally design N-doped carbon quantum dots from folic acid (vitamin B9) for selected applications (nanopesticides and nanofertilizers). Large-scale synthesis of NCQD was also considered by the process intensification method. A deep insight into plasma catalysis in the production process characterised by optical emission spectroscopy was also concerned. From the recognized knowledge gaps in the microplasma synthesis of NCQD, the following research aims and objectives were developed:

**Aim 1:** To understand the potentials of plasma-assisted synthesis of N-doped nanoparticles (NPs) for pesticidal applications in crops (Paper 1) comprehensively

- Objective 1: to provide perspectives of promising applications of N-doped NPs as emerging nanopesticides.
- Objective 2: to review the opportunities plasma-enabled NP technology offers for the scalable production of N-doped NPs based on a green, eco-friendly and sustainable approach.

**Aim 2:** To assess the overall sustainability of the up-to-date large-scale synthesis processes of nitrogen-doped carbon quantum dots (Paper 2)

- Objective 1: To have an overview of the state-of-the-art synthesis technologies of nitrogen-doped carbon quantum dots
- Objective 2: To assess all large-scale synthesis processes of nitrogen-doped carbon quantum dots using green chemistry, circular and EcoScale metrics.

**Aim 3:** To develop a rational design concept to synthesise nitrogen-doped carbon quantum dots from Vitamin B9 (Paper 3)

- Objective 1: To develop a rational design strategy for fabricating nitrogen-doped carbon quantum dots from Vitamin B9.
- Objective 2: To fabricate NCQD from the rational design concept using the kINPen®IND microplasma jet.
- Objective 3: To prove the potential of the rationally designed NCQD towards selected applications by physicochemical characterisation.

**Aim 4:** To prove and achieve the fundamental concept to govern the mass-based intensification by process design (Paper 4)

- Objective 1: To explore the kINPen®IND microplasma jet reactor to synthesise N-doped carbon nanodots from folic acid (Vitamin B9) in an aqueous solution.
- Objective 2: To optimise the plasma jet-liquid distance, metal-plasma interaction, and recycling towards mass-based intensification.
- Objective 3: To explore the mechanism of the microplasma synthesis of N-doped carbon quantum dots.

## Chapter 1. Introduction

---

**Aim 5:** To decipher plasma-catalysis in triphasic microplasma synthesis for N-doped carbon quantum dots from vitamin B9 via optical emission spectroscopy (Paper 5)

Objective 1: To optimise excited species formation in different plasma-liquid-solid process designs

Objective 2: To optimise metallic catalysts for the triphasic microplasma synthesis of N-doped carbon dots

Objective 3: To explore the mechanism of plasma-liquid-catalysts synthesis of N-doped carbon quantum dots.

**Aim 6:** intensify reactivity via bespoke transient hydrodynamics in a plasma-activated three-phase catalyst system for formation of N-doped carbon quantum dots (Paper 6)

Objective 1: To understand how the interface between the plasma and the liquid is deformed and how that might be utilised to increase mass transport.

Objective 2: To study the effect of diffusivity of the liquid reactant on the reaction rate by changing the liquid viscosity.

Objective 3: To investigate catalytic activity using metal flakes as bed.



### 1.5. Thesis outline

This PhD thesis is organized into 8 chapters: an introduction, a literature review (review paper), four other chapters adapted from the original research publications, and finally, a chapter of conclusions and suggested future research works. A summary of each chapter is given below (Figure 12).

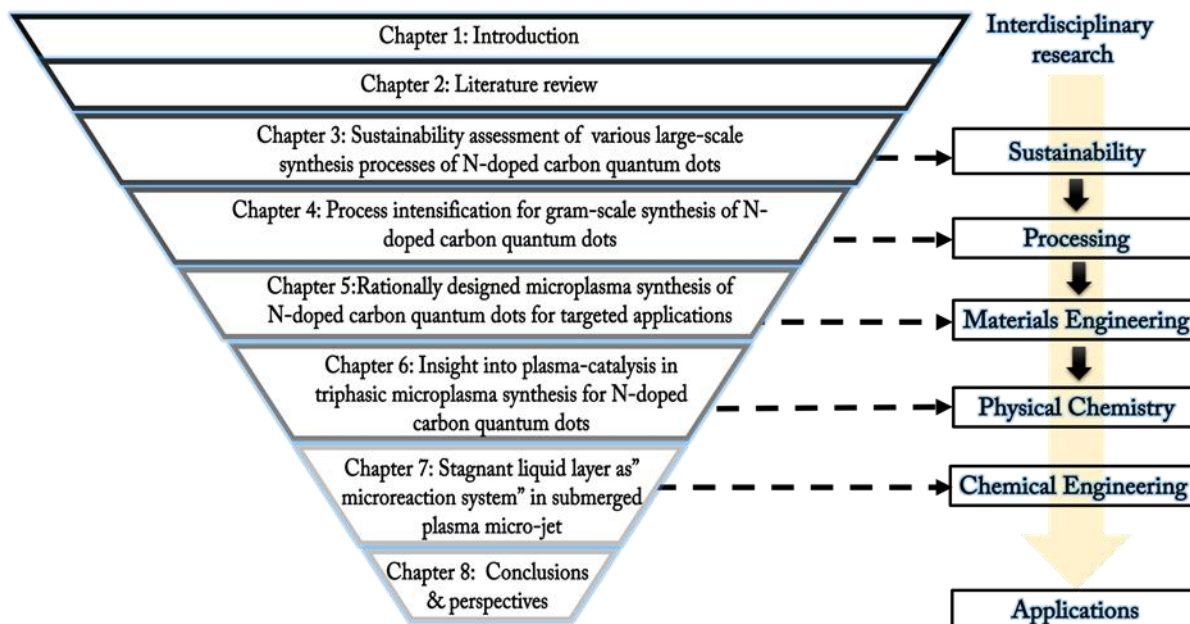


**Figure 12.** The overall outline of the dissertation with interdisciplinary research topics

**Chapter 1. Introduction.** This chapter introduces the emerging issue in global food demand due to huge crop loss and unsustainable agriculture production. This chapter highlights the potential and promise of using nitrogen-fixation microplasma technology to produce high-quality multifunctional nanoparticles, which are keys for an agritech revolution to achieve a more sustainable and resilient agriculture. Finally, this chapter discusses the motivation of this research topic, current research gaps, and research aims.

**Chapter 2. Literature review.** In this chapter, N-doped ZnO and N-doped TiO<sub>2</sub> NPs will be introduced and reviewed as the first examples of these nanomaterials that have been successfully proven as nanopesticides. Following the first demonstration and the application of N-doped carbon dots (N-doped carbon quantum dots), various agricultural applications such as nanopesticides, pesticide nanocarriers, disease detection, and pest targeting will be reviewed, showing their enormous potential to be translated into real applications. The plasma technology comes into play when the focus is on the manufacturing process of these nanomaterials since, in pest control, producing high-quality nanopesticides is indispensable and challenging. The implementation of this technology and the introduction of N-doped NPs as new powerful pesticidal agents could make a significant impact on improved crop production.

*The main contribution of this chapter is to provide perspectives of promising applications of N-doped NPs as emerging nanopesticides and a comprehensive overview on the opportunities that plasma-enabled NP technology offers for the scalable production of N-doped NPs based on a green, eco-friendly and sustainable approach.*

**Chapter 3. Sustainability assessment of various large-scale synthesis processes of N-doped carbon quantum dots.** In this chapter, six of the most promising lab-scale synthesis process methodologies for N-doped carbon dots (NCDs) are selected and compared in terms of green chemistry and circular and EcoScale/Good-Manufacturing Practice metrics. I compared a new innovative route, the low-temperature plasma-enabled synthesis of carbon dots, e.g., from citric acid and monoethanolamine, to more-established literature processes, such as thermochemical processes, from the same or other materials. Along with this study, the advantages and disadvantages of each method are depicted in manifold sustainability facets. It is shown how recycling/reuse of unconverted starting materials and solvents can improve the sustainability profile. In addition, safety constraints, cost analysis, and energy consumption are considered. The analysis showed that the thermal process from citric acid and monoethanolamine gives the best performance concerning the sustainability assessment chosen here.

*The main contribution of this chapter is to provide a comprehensive assessment of the most promising lab-scale synthesis process methodologies for N-doped carbon quantum dots to learn more about which of these methods are most promising for scaling-up and industrial manufacturing of N-doped carbon quantum dots.*

**Chapter 4. Process intensification for gram-scale synthesis of N-doped carbon quantum dots.** In this chapter, the distance of the tip of the microplasma jet to the water surface is changed in three steps, named distant, contact, and deflection modes. As a further variation, the liquid volume is either stirred or unstirred and may contain glass beads or metal flakes. In this way, the mass transfer, hydrodynamics, and the electrical field are influenced and create the specific gas-liquid interface, possibly including plasma-catalytic effects. A thermofluidic analysis confirms a uniform temperature profile and a positive temperature effect on mass transfer. In this way, the research achieves process intensification, bringing the synthesis towards 1 g per day and maximising the intended performance and the photoluminescence intensity. Recycling further increases the mass yield via centrifugation. An analysis by optical emission spectroscopy reveals the formation of the plasma species from which a reaction mechanism is proposed.

*The main contribution of this chapter is to achieve mass-based intensification by process design (the plasma jet-liquid distance, metal-plasma interaction, and recycling towards mass-based intensification).*

**Chapter 5. Rationally designed microplasma synthesis of N-doped carbon quantum dots for targeted applications.** In this chapter, N-doped carbon quantum dots (NCQD) are rationally designed and synthesised, for the first time, from folic acid (Vitamin B9) by a non-thermal microplasma jet. The structural and analytical characterisation confirmed an average size of 3.1 nm for the synthesised NCQD with the multi-functional groups (-OH, -COOH, -NH<sub>2</sub>) on their surface. The TEM results indicated that the core of NCQD was a multilayered structure, including single-defected graphene sheets of graphitic nitrogen and pyrrolic nitrogen. In addition, the fluorescence performance and stability of the as-prepared NCQD were determined. The quantum yield of NCQD was 35%, which is relatively high, with a strong blue fluorescence.

*The main contribution of this chapter is to provide a new conceptual strategy to rationally design and synthesise the desirable for three main applications (nanopesticides, water purification, and theranostic treatment).*

**Chapter 6. Insight into plasma-catalysis in triphasic microplasma synthesis for N-doped carbon quantum dots.** In this chapter, as an analytical method, optical emission spectroscopy (OES) investigations are appropriate to investigate the mechanism of how a plasma(-heterogeneous) catalyst in a multiphase reaction may affect the fabrication of NCQD from Vitamin B9. Seven steps are proposed for the reaction mechanism to yield the N-doped quantum dots. The temperature at the plasma-liquid-catalyst interface was lower than 25 °C, as determined by IR imaging.

*The contribution of this study is to understand the plasma-catalytic effect under the microplasma multiphase design and vice versa, to understand the multiphase design better. The key of this research is to determine and advance multiphase hydrodynamics and reaction by shaping a characteristic surface profile via deep penetration of the plasma jet into the liquid volume.*

**Chapter 7. Stagnant Liquid Layer as “Microreaction System” in Submerged Plasma Micro-Jet for Formation of Carbon Quantum Dots.** This study aims to improve reactivity in a plasma-activated three-phase catalyst system using bespoke transient hydrodynamics. Existing three-phase plasma systems are poorly designed, understood, and not commercially available. The study evaluated N-doped carbon quantum dots as fertilizers and wastewater treatment using a commercial plasma system generating a plasma microjet. The plasma can penetrate the catalyst bed via the stagnant thin liquid film and polarize the plasma-liquid interface, resulting in an increased reaction rate by reducing the solvent's viscosity and increasing liquid component diffusivity towards the catalyst bed.

## Chapter 1. Introduction

---

*The contribution of this study is to understand how the interface between the plasma and the liquid is deformed and how that might be utilised to increase mass transport. Then, this will be further studied in gas-liquid-solid microplasma process to investigate for catalytic activity to the synthesis reaction.*

**Chapter 8. Conclusion, challenges, and perspectives.** This chapter provides the summary of this thesis by highlighting the main findings obtained from the results. Next, this chapter discusses the possible future directions for employing this work.

### 1.6. Budget and Research Funding

All costs of experiments, accessories, equipment, chemicals, conference and travel in this research were financially supported based on the Joint PhD Award between Adelaide and Warwick University under the umbrella of the project “Surface-CONfined fast-modulated Plasma for process and Energy intensification in small molecules conversion” (SCOPE).

### 1.7. Thesis Editing & Format

The thesis entitled “A new kind of microplasma for nitrogen-fixation multifunctional nanoparticle synthesis towards selected applications” has been prepared as a portfolio of publications based on the requirements of The University of Adelaide. The printed and online versions of this thesis are identical.

### 1.8. References

1. Kah, M., N. Tufenkji, and J.C. White, Nano-enabled strategies to enhance crop nutrition and protection. *Nature nanotechnology*, 2019. 14(6): p. 532-540.
2. Shishoo, R., Introduction: trends in the global textile industry, in *The global textile and clothing industry*. 2012, Elsevier. p. 1-7.
3. Lellis, B., et al., Effects of textile dyes on health and the environment and bioremediation potential of living organisms. *Biotechnology Research and Innovation*, 2019. 3(2): p. 275-290.
4. Boretti, A. and L. Rosa, Reassessing the projections of the world water development report. *NPJ Clean Water*, 2019. 2(1): p. 1-6.
5. Baltes, N.J., J. Gil-Humanes, and D.F. Voytas, Genome engineering and agriculture: opportunities and challenges. *Progress in molecular biology and translational science*, 2017. 149: p. 1-26.
6. AL-Ahmadi, M.S., Pesticides, anthropogenic activities, and the health of our environment safety, in *Pesticides-use and misuse and their impact in the environment*. 2019, IntechOpen.

7. Crenna, E., T. Sinkko, and S. Sala, Biodiversity impacts due to food consumption in Europe. *Journal of cleaner production*, 2019. 227: p. 378-391.
8. Li, S., et al., Recent progress of plasma-assisted nitrogen fixation research: a review. *Processes*, 2018. 6(12): p. 248.
9. Fuller, J., et al., Reaction mechanism and kinetics for ammonia synthesis on the Fe (211) reconstructed surface. *Physical Chemistry Chemical Physics*, 2019. 21(21): p. 11444-11454.
10. Gafur, N.A., et al., A case study of heavy metal pollution in water of Bone River by Artisanal Small-Scale Gold Mine Activities in Eastern Part of Gorontalo, Indonesia. *Water*, 2018. 10(11): p. 1507.
11. Yaseen, D. and M. Scholz, Textile dye wastewater characteristics and constituents of synthetic effluents: a critical review. *International journal of environmental science and technology*, 2019. 16(2): p. 1193-1226.
12. Mudliar, R., et al., Energy efficient—Advanced oxidation process for treatment of cyanide containing automobile industry wastewater. *Journal of Hazardous Materials*, 2009. 164(2-3): p. 1474-1479.
13. Oturan, M.A. and J.-J. Aaron, Advanced oxidation processes in water/wastewater treatment: principles and applications. A review. *Critical Reviews in Environmental Science and Technology*, 2014. 44(23): p. 2577-2641.
14. Poyatos, J.M., et al., Advanced oxidation processes for wastewater treatment: state of the art. *Water, Air, and Soil Pollution*, 2010. 205(1): p. 187-204.
15. Fernández-Castro, P., et al., Insight on the fundamentals of advanced oxidation processes. Role and review of the determination methods of reactive oxygen species. *Journal of Chemical Technology & Biotechnology*, 2015. 90(5): p. 796-820.
16. Ou, R., et al., Improved photocatalytic performance of N-doped ZnO/graphene/ZnO sandwich composites. *Applied Surface Science*, 2022. 577: p. 151856.
17. Budak, M. and H. Segmen, *Cancer Genes and Breast Cancers*. 2022.
18. Song, J., et al., Effect of Nitrogen Doping on the Photoluminescence of Amorphous Silicon Oxycarbide Films. *Micromachines (Basel)*, 2019. 10(10).
19. Li, O.L., et al., Selective nitrogen bonding states in nitrogen-doped carbon via a solution plasma process for advanced oxygen reduction reaction. *RSC advances*, 2016. 6(111): p. 109354-109360.
20. Sharma, A. and J. Das, Small molecules derived carbon dots: synthesis and applications in sensing, catalysis, imaging, and biomedicine. *Journal of nanobiotechnology*, 2019. 17(1): p. 1-24.
21. Gomez, I.J., et al., Nitrogen-doped carbon nanodots for bioimaging and delivery of paclitaxel. *Journal of Materials Chemistry B*, 2018. 6(35): p. 5540-5548.

22. Li, X., et al., Recent advances in carbon nanodots: properties and applications in cancer diagnosis and treatment. *Journal of Analysis and Testing*, 2019. 3(1): p. 37-49.
23. Huang, X., et al., Fast microplasma synthesis of blue luminescent carbon quantum dots at ambient conditions. *Plasma Processes and Polymers*, 2015. 12(1): p. 59-65.
24. Wang, J., C.F. Wang, and S. Chen, Amphiphilic egg-derived carbon dots: Rapid plasma fabrication, pyrolysis process, and multicolor printing patterns. *Angewandte Chemie International Edition*, 2012. 51(37): p. 9297-9301.
25. Lv, P., D. Xie, and Z. Zhang, Magnetic carbon dots based molecularly imprinted polymers for fluorescent detection of bovine hemoglobin. *Talanta*, 2018. 188: p. 145-151.
26. Ma, Z., et al., One-step ultrasonic synthesis of fluorescent N-doped carbon dots from glucose and their visible-light sensitive photocatalytic ability. *New Journal of Chemistry*, 2012. 36(4): p. 861-864.
27. Qu, D., et al., Highly luminescent S, N co-doped graphene quantum dots with broad visible absorption bands for visible light photocatalysts. *Nanoscale*, 2013. 5(24): p. 12272-12277.
28. Mehta, A., et al., Carbon quantum dots/TiO<sub>2</sub> nanocomposite for sensing of toxic metals and photodetoxification of dyes with kill waste by waste concept. *Materials & Design*, 2018. 155: p. 485-493.
29. Manioudakis, J., et al., Effects of nitrogen-doping on the photophysical properties of carbon dots. *Journal of Materials Chemistry C*, 2019. 7(4): p. 853-862.
30. Lin, L. and Q. Wang, Microplasma: A New Generation of Technology for Functional Nanomaterial Synthesis. *Plasma Chemistry and Plasma Processing*, 2015. 35(6): p. 925-962.
31. Shah, J., et al., Ammonia synthesis by radio frequency plasma catalysis: revealing the underlying mechanisms. *ACS Applied Energy Materials*, 2018. 1(9): p. 4824-4839.
32. Rezaei, F., et al., Applications of plasma-liquid systems: A review. *Materials*, 2019. 12(17): p. 2751.
33. Weltmann, K.D., et al., The future for plasma science and technology. *Plasma Processes and Polymers*, 2019. 16(1): p. 1800118.
34. Lin, L., et al., Synthesis of metallic nanoparticles by microplasma. *Physical Sciences Reviews*, 2018. 3.
35. Lin, L., et al., Plasma-assisted nitrogen fixation in nanomaterials: fabrication, characterization, and application. *Journal of Physics D: Applied Physics*, 2020. 53(13): p. 133001.
36. Lin, L., et al., Plasma-electrochemical synthesis of europium doped cerium oxide nanoparticles. *Frontiers of Chemical Science and Engineering*, 2019. 13(3): p. 501-510.
37. Ma, X., et al., Synthesis of luminescent carbon quantum dots by microplasma process. *Chemical Engineering and Processing - Process Intensification*, 2019. 140: p. 29-35.

38. Lin, L., et al., Color-Tunable Eu<sup>3+</sup> and Tb<sup>3+</sup> Co-Doped Nanophosphors Synthesis by Plasma-Assisted Method. *ChemistrySelect*, 2019. 4(14): p. 4278-4286.
39. Lin, L., et al., Facile synthesis of lanthanide doped yttria nanophosphors by a simple microplasma-assisted process. *Reaction Chemistry & Engineering*, 2019. 4(5): p. 891-898.
40. Lin, L., et al., Synthesis of Ni nanoparticles with controllable magnetic properties by atmospheric pressure microplasma assisted process. *AIChE Journal*, 2018. 64(5): p. 1540-1549.
41. Lin, L., et al., Synthesis of metallic nanoparticles by microplasma. *Physical Sciences Reviews*, 2018. 3(10).
42. Reuter, S., T. Von Woedtke, and K.-D. Weltmann, The kINPen—A review on physics and chemistry of the atmospheric pressure plasma jet and its applications. *Journal of Physics D: Applied Physics*, 2018. 51(23): p. 233001.
43. Mariotti, D. and R.M. Sankaran, Microplasmas for nanomaterials synthesis. *Journal of Physics D: Applied Physics*, 2010. 43(32): p. 323001.
44. Patil, B.S., Plasma (catalyst) - assisted nitrogen fixation : reactor development for nitric oxide and ammonia production. 2017, Technische Universiteit Eindhoven.
45. Wang, W., et al., Nitrogen Fixation by Gliding Arc Plasma: Better Insight by Chemical Kinetics Modelling. *ChemSusChem*, 2017. 10(10): p. 2145-2157.
46. Priestley, J., *Experiments and Observations on Different Kinds of Air: The Second Edition, Corrected*. Cambridge Library Collection - Physical Sciences. Vol. 1. 2013, Cambridge: Cambridge University Press.
47. Cherkasov, N., A.O. Ibhadon, and P. Fitzpatrick, A review of the existing and alternative methods for greener nitrogen fixation. *Chemical Engineering and Processing: Process Intensification*, 2015. 90: p. 24-33.
48. Rusanov, V.D., A.A. Fridman, and G.V. Sholin, The physics of a chemically active plasma with nonequilibrium vibrational excitation of molecules. *Soviet Physics Uspekhi*, 1981. 24(6): p. 447.
49. Xu, X., et al., Electrophoretic analysis and purification of fluorescent single-walled carbon nanotube fragments. *Journal of the American Chemical Society*, 2004. 126(40): p. 12736-12737.
50. Sun, Y.-P., et al., Quantum-Sized Carbon Dots for Bright and Colorful Photoluminescence. *Journal of the American Chemical Society*, 2006. 128(24): p. 7756-7757.
51. Yan, Y., et al., Recent advances on graphene quantum dots: from chemistry and physics to applications. *Advanced materials*, 2019. 31(21): p. 1808283.
52. Liu, J., et al., Deep red emissive carbonized polymer dots with unprecedented narrow full width at half maximum. *Advanced materials*, 2020. 32(17): p. 1906641.

53. Jiang, K., et al., Facile, quick, and gram-scale synthesis of ultralong-lifetime room-temperature-phosphorescent carbon dots by microwave irradiation. *Angewandte Chemie International Edition*, 2018. 57(21): p. 6216-6220.
54. Dave, K. and V.G. Gomes, Carbon quantum dot-based composites for energy storage and electrocatalysis: mechanism, applications and future prospects. *Nano Energy*, 2019. 66: p. 104093.
55. Zhang, Z., et al., A minireview on doped carbon dots for photocatalytic and electrocatalytic applications. *Nanoscale*, 2020. 12(26): p. 13899-13906.
56. Behi, M., et al., Carbon dots: a novel platform for biomedical applications. *Nanoscale Advances*, 2022. 4(2): p. 353-376.
57. Guo, B., et al., The role of fluorescent carbon dots in crops: Mechanism and applications. *SmartMat*, 2022. 3(2): p. 208-225.
58. Guo, B., et al., The role of carbon dots in the life cycle of crops. *Industrial Crops and Products*, 2022. 187: p. 115427.
59. Sun, Y.-P., et al., Quantum-sized carbon dots for bright and colorful photoluminescence. *Journal of the American Chemical Society*, 2006. 128(24): p. 7756-7757.
60. Mu, X., et al., A sensitive “off-on” carbon dots-Ag nanoparticles fluorescent probe for cysteamine detection via the inner filter effect. *Talanta*, 2021. 221: p. 121463.
61. Huang, H., et al., Controllable synthesis of biocompatible fluorescent carbon dots from cellulose hydrogel for the specific detection of Hg<sup>2+</sup>. *Frontiers in Bioengineering and Biotechnology*, 2021. 9: p. 617097.
62. Wang, Y., Q. Zhuang, and Y. Ni, Facile microwave-assisted solid-phase synthesis of highly fluorescent nitrogen-sulfur-codoped carbon quantum dots for cellular imaging applications. *Chemistry-A European Journal*, 2015. 21(37): p. 13004-13011.
63. Li, D., et al., Far-red carbon dots as efficient light-harvesting agents for enhanced photosynthesis. *ACS applied materials & interfaces*, 2020. 12(18): p. 21009-21019.
64. Jana, J., et al., Blue emitting nitrogen-doped carbon dots as a fluorescent probe for nitrite ion sensing and cell-imaging. *Analytica Chimica Acta*, 2019. 1079: p. 212-219.
65. Qin, K., et al., Applications of hydrothermal synthesis of *Escherichia coli* derived carbon dots in in vitro and in vivo imaging and p-nitrophenol detection. *Analyst*, 2020. 145(1): p. 177-183.
66. Yuan, F., et al., Bright high-colour-purity deep-blue carbon dot light-emitting diodes via efficient edge amination. *Nature Photonics*, 2020. 14(3): p. 171-176.
67. Cao, Y., Y. Cheng, and M. Sun, Graphene-based SERS for sensor and catalysis. *Applied Spectroscopy Reviews*, 2023. 58(1): p. 1-38.



68. Liu, J., R. Li, and B. Yang, Carbon dots: A new type of carbon-based nanomaterial with wide applications. *ACS Central Science*, 2020. 6(12): p. 2179-2195.
69. Rabeya, R., et al., Structural defects in graphene quantum dots: A review. *International Journal of Quantum Chemistry*, 2022. 122(12): p. e26900.
70. Abbas, A., et al., High yield synthesis of graphene quantum dots from biomass waste as a highly selective probe for Fe<sup>3+</sup> sensing. *Scientific Reports*, 2020. 10(1): p. 21262.
71. Chen, S., et al., Tuning the optical properties of graphene quantum dots by selective oxidation: a theoretical perspective. *Journal of Materials Chemistry C*, 2018. 6(25): p. 6875-6883.
72. Pho, Q.H., et al., Rational design for the microplasma synthesis from vitamin B9 to N-doped carbon quantum dots towards selected applications. *Carbon*, 2022. 198: p. 22-33.
73. Tao, S., et al., Confined-domain crosslink-enhanced emission effect in carbonized polymer dots. *Light: Science & Applications*, 2022. 11(1): p. 56.
74. Seliverstova, E., N. Ibrayev, and E. Menshova, Modification of structure and optical properties of graphene oxide dots, prepared by laser ablation method. *Fullerenes, Nanotubes and Carbon Nanostructures*, 2022. 30(1): p. 119-125.
75. Qin, J., L. Zhang, and R. Yang, Solid pyrolysis synthesis of excitation-independent emission carbon dots and its application to isoniazid detection. *Journal of Nanoparticle Research*, 2019. 21(3): p. 1-11.
76. Li, X., et al., Microwave synthesis of nitrogen and sulfur co-doped carbon dots for the selective detection of Hg<sup>2+</sup> and glutathione. *Optical Materials*, 2020. 99: p. 109559.
77. Nguyen, V., et al., Double-pulse femtosecond laser ablation for synthesis of ultrasmall carbon nanodots. *Materials Research Express*, 2020. 7(1): p. 015606.
78. Nguyen, V., et al., Tuning photoluminescence of boron nitride quantum dots via surface functionalization by femtosecond laser ablation. *Journal of Molecular Structure*, 2021. 1244: p. 130922.
79. Wang, R., et al., Recent progress in carbon quantum dots: synthesis, properties and applications in photocatalysis. *Journal of Materials Chemistry A*, 2017. 5(8): p. 3717-3734.
80. Lu, S., et al., Near-infrared photoluminescent polymer-carbon nanodots with two-photon fluorescence. *Advanced materials*, 2017. 29(15): p. 1603443.
81. Liu, J., et al., One-step hydrothermal synthesis of nitrogen-doped conjugated carbonized polymer dots with 31% efficient red emission for in vivo imaging. *Small*, 2018. 14(15): p. 1703919.
82. Yuan, F., et al., Engineering triangular carbon quantum dots with unprecedented narrow bandwidth emission for multicolored LEDs. *Nature communications*, 2018. 9(1): p. 1-11.
83. Li, L., et al., Focusing on luminescent graphene quantum dots: current status and future perspectives. *Nanoscale*, 2013. 5(10): p. 4015-4039.

84. Sato, K., et al., Surface modification strategy for fluorescence solvatochromism of carbon dots prepared from p-phenylenediamine. *Chemical Communications*, 2020. 56(14): p. 2174-2177.
85. Mei, A., et al., Photocatalytic materials modified with carbon quantum dots for the degradation of organic pollutants under visible light: A review. *Environmental Research*, 2022. 214: p. 114160.
86. Mishra, V., et al., Carbon dots: emerging theranostic nanoarchitectures. *Drug Discovery Today*, 2018. 23(6): p. 1219-1232.
87. Xu, J., et al., Carbon dots as a luminescence sensor for ultrasensitive detection of phosphate and their bioimaging properties. *Luminescence*, 2015. 30(4): p. 411-415.
88. Liu, C., et al., Nano-carrier for gene delivery and bioimaging based on carbon dots with PEI-passivation enhanced fluorescence. *Biomaterials*, 2012. 33(13): p. 3604-3613.
89. Roy, P., et al., Photoluminescent carbon nanodots: synthesis, physicochemical properties and analytical applications. *Materials Today*, 2015. 18(8): p. 447-458.
90. Shi, Y., et al., Carbon dots: An innovative luminescent nanomaterial: Photovoltaics: Special Issue Dedicated to Professor Yongfang Li. *Aggregate*, 2022. 3(3): p. e108.
91. Cui, L., et al., Carbon Dots: Synthesis, Properties and Applications. *Nanomaterials (Basel)*, 2021. 11(12).
92. Zhu, S., et al., Investigation of photoluminescence mechanism of graphene quantum dots and evaluation of their assembly into polymer dots. *Carbon*, 2014. 77: p. 462-472.
93. Kim, S., et al., Anomalous behaviors of visible luminescence from graphene quantum dots: interplay between size and shape. *ACS nano*, 2012. 6(9): p. 8203-8208.
94. Tang, J., et al., Influence of group modification at the edges of carbon quantum dots on fluorescent emission. *Nanoscale Research Letters*, 2019. 14(1): p. 1-10.
95. Pan, D., et al., Hydrothermal route for cutting graphene sheets into blue-luminescent graphene quantum dots. *Advanced materials*, 2010. 22(6): p. 734-738.
96. Zhu, S., et al., Strongly green-photoluminescent graphene quantum dots for bioimaging applications. *Chemical communications*, 2011. 47(24): p. 6858-6860.
97. Lin, L. and S. Zhang, Creating high yield water soluble luminescent graphene quantum dots via exfoliating and disintegrating carbon nanotubes and graphite flakes. *Chemical communications*, 2012. 48(82): p. 10177-10179.
98. Jin, S.H., et al., Tuning the photoluminescence of graphene quantum dots through the charge transfer effect of functional groups. *ACS nano*, 2013. 7(2): p. 1239-1245.

99. Wang, L., et al., Unraveling Bright Molecule-Like State and Dark Intrinsic State in Green-Fluorescence Graphene Quantum Dots via Ultrafast Spectroscopy. *Advanced Optical Materials*, 2013. 1(3): p. 264-271.
100. Lin, Z., et al., Classical oxidant induced chemiluminescence of fluorescent carbon dots. *Chemical communications*, 2012. 48(7): p. 1051-1053.
101. Wang, J. and J. Qiu, A review of carbon dots in biological applications. *Journal of materials science*, 2016. 51(10): p. 4728-4738.
102. Wang, R., X. Wang, and Y. Sun, One-step synthesis of self-doped carbon dots with highly photoluminescence as multifunctional biosensors for detection of iron ions and pH. *Sensors and Actuators B: Chemical*, 2017. 241: p. 73-79.
103. Bacon, M., S.J. Bradley, and T. Nann, Graphene quantum dots. *Particle & Particle Systems Characterization*, 2014. 31(4): p. 415-428.
104. Liu, H., T. Ye, and C. Mao, Fluorescent Carbon Nanoparticles Derived from Candle Soot *Angewandte Chemie International Edition* Volume 46. 2007, Issue.
105. Peng, J., et al., Graphene quantum dots derived from carbon fibers. *Nano letters*, 2012. 12(2): p. 844-849.
106. Zhao, P., et al., Facile One-Pot Conversion of Petroleum Asphaltene to High Quality Green Fluorescent Graphene Quantum Dots and Their Application in Cell Imaging. *Particle & Particle Systems Characterization*, 2016. 33(9): p. 635-644.
107. Li, X., et al., Preparation of carbon quantum dots with tunable photoluminescence by rapid laser passivation in ordinary organic solvents. *Chemical Communications*, 2010. 47(3): p. 932-934.
108. Hu, S.-L., et al., One-step synthesis of fluorescent carbon nanoparticles by laser irradiation. *Journal of Materials Chemistry*, 2009. 19(4): p. 484-488.
109. Kang, S.H., et al., Ultrafast method for selective design of graphene quantum dots with highly efficient blue emission. *Scientific reports*, 2016. 6(1): p. 1-7.
110. Ren, X., et al., Synthesis of N-doped micropore carbon quantum dots with high quantum yield and dual-wavelength photoluminescence emission from biomass for cellular imaging. *Nanomaterials*, 2019. 9(4): p. 495.
111. Zhuo, S., M. Shao, and S.-T. Lee, Upconversion and downconversion fluorescent graphene quantum dots: ultrasonic preparation and photocatalysis. *ACS nano*, 2012. 6(2): p. 1059-1064.
112. Zhou, S., et al., Graphene quantum dots: recent progress in preparation and fluorescence sensing applications. *RSC advances*, 2016. 6(112): p. 110775-110788.

113. Huang, H., et al., A one-step ultrasonic irradiation assisted strategy for the preparation of polymer-functionalized carbon quantum dots and their biological imaging. *Journal of colloid and interface science*, 2018. 532: p. 767-773.
114. Park, S.Y., et al., Photoluminescent green carbon nanodots from food-waste-derived sources: large-scale synthesis, properties, and biomedical applications. *ACS applied materials & interfaces*, 2014. 6(5): p. 3365-3370.
115. Li, L.L., et al., A facile microwave avenue to electrochemiluminescent two-color graphene quantum dots. *Advanced Functional Materials*, 2012. 22(14): p. 2971-2979.
116. Wang, Q., et al., Microwave-assisted synthesis of carbon nanodots through an eggshell membrane and their fluorescent application. *Analyst*, 2012. 137(22): p. 5392-5397.
117. Yao, Y.-Y., et al., Magnetofluorescent carbon dots derived from crab shell for targeted dual-modality bioimaging and drug delivery. *ACS applied materials & interfaces*, 2017. 9(16): p. 13887-13899.
118. Pires, N.R., et al., Novel and fast microwave-assisted synthesis of carbon quantum dots from raw cashew gum. *Journal of the Brazilian Chemical Society*, 2015. 26: p. 1274-1282.
119. Bandi, R., et al., Facile and green synthesis of fluorescent carbon dots from onion waste and their potential applications as sensor and multicolour imaging agents. *RSC advances*, 2016. 6(34): p. 28633-28639.
120. Zhao, Y., et al., A facile and high-efficient approach to yellow emissive graphene quantum dots from graphene oxide. *Carbon*, 2017. 124: p. 342-347.
121. Halder, A., et al., One-pot green synthesis of biocompatible graphene quantum dots and their cell uptake studies. *ACS Applied Bio Materials*, 2018. 1(2): p. 452-461.
122. Mehta, V.N., S. Jha, and S.K. Kailasa, One-pot green synthesis of carbon dots by using *Saccharum officinarum* juice for fluorescent imaging of bacteria (*Escherichia coli*) and yeast (*Saccharomyces cerevisiae*) cells. *Materials Science and Engineering: C*, 2014. 38: p. 20-27.
123. Lu, W., et al., Economical, Green Synthesis of Fluorescent Carbon Nanoparticles and Their Use as Probes for Sensitive and Selective Detection of Mercury(II) Ions. *Analytical Chemistry*, 2012. 84(12): p. 5351-5357.
124. Deng, Y., J. Qian, and Y. Zhou, Solvothermal Synthesis and Inkjet Printing of Carbon Quantum Dots. *ChemistrySelect*, 2020. 5(47): p. 14930-14934.
125. Zhu, S., et al., Strongly green-photoluminescent graphene quantum dots for bioimaging applications. *Chemical Communications*, 2011. 47(24): p. 6858-6860.
126. Tian, R., et al., Solvothermal method to prepare graphene quantum dots by hydrogen peroxide. *Optical Materials*, 2016. 60: p. 204-208.

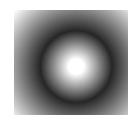
127. Liu, W., et al., Green synthesis of carbon dots from rose-heart radish and application for Fe<sup>3+</sup> detection and cell imaging. *Sensors and Actuators B: Chemical*, 2017. 241: p. 190-198.
128. Ma, C.-B., et al., A general solid-state synthesis of chemically-doped fluorescent graphene quantum dots for bioimaging and optoelectronic applications. *Nanoscale*, 2015. 7(22): p. 10162-10169.
129. Li, X., et al., Multicolour light emission from chlorine-doped graphene quantum dots. *Journal of Materials Chemistry C*, 2013. 1(44): p. 7308-7313.
130. Fan, L., et al., Direct Synthesis of Graphene Quantum Dots by Chemical Vapor Deposition. *Particle & Particle Systems Characterization*, 2013. 30(9): p. 764-769.
131. Vibhute, A., et al., Fluorescent carbon quantum dots: Synthesis methods, functionalization and biomedical applications. *Applied Surface Science Advances*, 2022. 11: p. 100311.
132. Carolan, D., et al., Environmentally friendly nitrogen-doped carbon quantum dots for next generation solar cells. *Sustainable Energy & Fuels*, 2017. 1(7): p. 1611-1619.
133. Li, O.L., et al., Synthesis of graphitic-N and amino-N in nitrogen-doped carbon via a solution plasma process and exploration of their synergic effect for advanced oxygen reduction reaction. *Journal of Materials Chemistry A*, 2017. 5(5): p. 2073-2082.
134. Bekeschus, S., et al., The plasma jet kINPen – A powerful tool for wound healing. *Clinical Plasma Medicine*, 2016. 4(1): p. 19-28.
135. Pho, Q.H., et al., Perspectives on plasma-assisted synthesis of N-doped nanoparticles as nanopesticides for pest control in crops. *Reaction Chemistry & Engineering*, 2020. 5(8): p. 1374-1396.
136. Anand, S.R., et al., Antibacterial Nitrogen-doped Carbon Dots as a Reversible “Fluorescent Nanoswitch” and Fluorescent Ink. *ACS Omega*, 2019. 4(1): p. 1581-1591.
137. Travlou, N.A., et al., S- and N-doped carbon quantum dots: Surface chemistry dependent antibacterial activity. *Carbon*, 2018. 135: p. 104-111.
138. Sharma, G., et al., Microwave assisted fabrication of La/Cu/Zr/carbon dots trimetallic nanocomposites with their adsorptional vs photocatalytic efficiency for remediation of persistent organic pollutants. *Journal of Photochemistry and Photobiology A: Chemistry*, 2017. 347: p. 235-243.
139. Wang, F., et al., Novel ternary photocatalyst of single atom-dispersed silver and carbon quantum dots co-loaded with ultrathin g-C<sub>3</sub>N<sub>4</sub> for broad spectrum photocatalytic degradation of naproxen. *Applied Catalysis B: Environmental*, 2018. 221: p. 510-520.
140. Xie, Z., et al., Construction of carbon dots modified MoO<sub>3</sub>/g-C<sub>3</sub>N<sub>4</sub> Z-scheme photocatalyst with enhanced visible-light photocatalytic activity for the degradation of tetracycline. *Applied Catalysis B: Environmental*, 2018. 229: p. 96-104.

141. Bruggeman, P. and C. Leys, Non-thermal plasmas in and in contact with liquids. *Journal of Physics D: Applied Physics*, 2009. 42(5): p. 053001.
142. Tang, J., et al., Carbon Nanodots Featuring Efficient FRET for Real-Time Monitoring of Drug Delivery and Two-Photon Imaging. *Advanced Materials*, 2013. 25(45): p. 6569-6574.
143. Cao, L., et al., Competitive performance of carbon "quantum" dots in optical bioimaging. *Theranostics*, 2012. 2(3): p. 295-301.
144. Kong, B., et al., Carbon Dot-Based Inorganic–Organic Nanosystem for Two-Photon Imaging and Biosensing of pH Variation in Living Cells and Tissues. *Advanced Materials*, 2012. 24(43): p. 5844-5848.
145. Molaei, M.J., Carbon quantum dots and their biomedical and therapeutic applications: a review. *RSC Advances*, 2019. 9(12): p. 6460-6481.
146. Kavitha, T. and S. Kumar, Turning date palm fronds into biocompatible mesoporous fluorescent carbon dots. *Scientific Reports*, 2018. 8(1): p. 16269.
147. Xu, Z.-Q., et al., Interactions between carbon nanodots with human serum albumin and  $\gamma$ -globulins: The effects on the transportation function. *Journal of hazardous materials*, 2015. 301: p. 242-249.
148. Wang, K., et al., Systematic safety evaluation on photoluminescent carbon dots. *Nanoscale Res Lett*, 2013. 8(1): p. 122.
149. Yoo, D., et al., Carbon Dots as an Effective Fluorescent Sensing Platform for Metal Ion Detection. *Nanoscale Res Lett*, 2019. 14(1): p. 272.
150. Yuan, F., et al., Shining carbon dots: Synthesis and biomedical and optoelectronic applications. *Nano Today*, 2016. 11(5): p. 565-586.

**BLANK PAGE**

# Chapter 2

## Literature review



---

**A**fter introducing the importance of nitrogen-fixation microplasma technology to generate advanced engineered multifunctional nanoparticles and their potential in agricultural applications to meet the high global food demand from the previous chapter. This second chapter will introduce a comprehensive overview and perspectives of promising applications of N-doped NPs as emerging nanopesticides and the opportunities which plasma-enabled NP technology offers for the scalable production of N-doped NPs based on a green, eco-friendly and sustainable approach.

The outcome of this chapter has been published as a review paper in “Reaction Chemistry & Engineering” journal as follows:

**Pho, Q.H.**, Losic, D., Ostrikov, K.K., Tran, N.N. and Hessel, V., 2020. Perspectives on plasma-assisted synthesis of N-doped nanoparticles as nanopesticides for pest control in crops. *Reaction Chemistry & Engineering*, 5(8), pp.1374-1396. (Q1, IF = 5.2)” <[Link](#)>


---



# Statement of Authorship

Title of Paper	Perspectives on plasma-assisted synthesis of N-doped nanoparticles as nanopesticides for pest control in crops
Publication Status	<input checked="" type="checkbox"/> Published <input type="checkbox"/> Accepted for Publication <input type="checkbox"/> Submitted for Publication <input type="checkbox"/> Unpublished and Unsubmitted work written in manuscript style
Publication Details	Pho, Q.H., Losic, D., Ostrikov, K.K., Tran, N.N. and Hessel, V., 2020. Perspectives on plasma-assisted synthesis of N-doped nanoparticles as nanopesticides for pest control in crops. Reaction Chemistry & Engineering, 5(8), pp.1374-1396.


## Principal Author


Name of Principal Author (Candidate)	Hue Quoc Pho		
Contribution to the Paper	Literature review, wrote, edited, and revised the manuscript.		
Overall percentage (%)	70%		
Certification:	This paper reports on original research I conducted during the period of my Higher Degree by Research candidature and is not subject to any obligations or contractual agreements with a third party that would constrain its inclusion in this thesis. I am the primary author of this paper.		
Signature		Date	28.01.2023

## Co-Author Contributions


By signing the Statement of Authorship, each author certifies that:


- i. the candidate's stated contribution to the publication is accurate (as detailed above);
- ii. permission is granted for the candidate to include the publication in the thesis; and
- iii. the sum of all co-author contributions is equal to 100% less the candidate's stated contribution.

Name of Co-Author	Dusan Losic		
Contribution to the Paper	Co-supervised and Writing- Review and Editing		
Signature		Date	2 feb 2023

Name of Co-Author	Kostya (Ken) Ostrikov		
Contribution to the Paper	Writing- Review and Editing		
Signature	 on behalf of co-author	Date	30.01.2023

Please cut and paste additional co-author panels here as required.

Name of Co-Author	Nam Nghiep Tran		
Contribution to the Paper	Writing- Review and Editing		
Signature		Date	28.01.2023

Name of Co-Author	Volker Hessel		
Contribution to the Paper	Supervised, Conceptualisation, Writing – review & editing, and is the corresponding author.		
Signature		Date	28.01.2023

Please cut and paste additional co-author panels here as required.

**BLANK PAGE**

# Chapter 3

## Sustainability assessment of various large-scale synthesis processes of NCQDs

---

In this chapter, a comprehensive literature review of the up-to-date gram-scale synthesis methods of N-doped carbon quantum dots to collect operational parameters for analysis. Then, green chemistry and circular and EcoScale/Good-Manufacturing-Practice metrics were used to compare all synthesis methods comprehensively. Along with this study, the advantages and disadvantages of each method are depicted in manifold sustainability facets. It is shown how recycling/reuse of unconverted starting materials and solvents can improve the sustainability profile. In addition, safety constraints, cost analysis, and energy consumption are considered.

This chapter has been published as a research paper in “*ACS Sustainable Chemistry and Engineering*” journal as follows:


**Pho, Q.H.**, Escriba-Gelonch, M., Losic, D., Rebrov, E.V., Tran, N.N. and Hessel, V., 2021. Survey of synthesis processes for N-doped carbon dots assessed by green chemistry and circular and EcoScale metrics. *ACS Sustainable Chemistry & Engineering*, 9(13), pp.4755-4770. [<Link>](#)

---

# Statement of Authorship

Title of Paper	Survey of Synthesis Processes for N-Doped Carbon Dots Assessed by Green Chemistry and Circular and EcoScale Metrics
Publication Status	<input checked="" type="checkbox"/> Published <input type="checkbox"/> Accepted for Publication <input type="checkbox"/> Submitted for Publication <input type="checkbox"/> Unpublished and Unsubmitted work written in manuscript style
Publication Details	Pho, Q.H., Escriba-Gelonch, M., Losic, D., Rebrov, E.V., Tran, N.N. and Hessel, V., 2021. Survey of synthesis processes for N-doped carbon dots assessed by green chemistry and circular and EcoScale metrics. ACS Sustainable Chemistry & Engineering, 9(13), pp.4755-4770.

## Principal Author

Name of Principal Author (Candidate)	Hue Quoc Pho		
Contribution to the Paper	Literature review, Conceptualization, Methodology, Formal analysis, Investigation, Data curation, Writing – original draft		
Overall percentage (%)	65%		
Certification:	This paper reports on original research I conducted during the period of my Higher Degree by Research candidature and is not subject to any obligations or contractual agreements with a third party that would constrain its inclusion in this thesis. I am the primary author of this paper.		
Signature		Date	28.01.2023


## Co-Author Contributions

By signing the Statement of Authorship, each author certifies that:

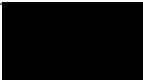
- the candidate's stated contribution to the publication is accurate (as detailed above);
- permission is granted for the candidate to include the publication in the thesis; and
- the sum of all co-author contributions is equal to 100% less the candidate's stated contribution.


Name of Co-Author	Marc Escriba-Gelonch		
Contribution to the Paper	Methodology, Formal analysis, Investigation, Data curation, Writing – original draft		
Signature	Marc Escribà Gelonch - DNI 43744099P (TCAT)	Date	01.02.2023

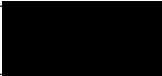
Digitally signed by Marc Escribà Gelonch - DNI 43744099P (TCAT)  
 DN: c=ES, o=Universitat de Lleida, 2.5.4.81744099P, ou=Empilat public  
 de nivell mig, ou=Escribà Gelonch - DNI 43744099P, givenName=Marc  
 escribà, serialNumber=D23243744099P, cn=Marc Escribà Gelonch - DNI 43744099P (TCAT)  
 Date: 2023.02.01 19:22:59 +01'00'

Name of Co-Author	Dusan Losic		
Contribution to the Paper	Co-supervised and Writing- Review and Editing.		
Signature		Date	2 feb 2023

Please cut and paste additional co-author panels here as required.

Name of Co-Author	Evgeny V. Rebrov		
Contribution to the Paper	Writing- Review and Editing.		
Signature		Date	06.02.2023

Name of Co-Author	Nam Nghiep Tran		
Contribution to the Paper	Writing- Review and Editing.		
Signature		Date	28.01.2023

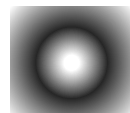
Name of Co-Author	Volker Hessel		
Contribution to the Paper	Supervised (scientific ideas, concepts, objectives, assessment of achievement degree, societal impact), Conceptualised, Writing – review & editing, and is the corresponding author.		
Signature		Date	28.01.2023

Please cut and paste additional co-author panels here as required.

**BLANK PAGE**

# Chapter 4

## Process intensification for gram scale synthesis of NCQDs



---

The results from Chapter 3 indicate that microplasma is one of the most sustainable methods in terms of energy efficiency while lacking mass efficiency. Chapter 4 focuses on mass-based intensification by process design to overcome this research gap. First, the distance of the tip of the microplasma jet to the water surface is changed in three steps, named distant, contact, and deflection modes. As a further variation, the liquid volume is either stirred or unstirred and may contain glass beads or metal flakes. In this way, the mass transfer, hydrodynamics, and the electrical field are influenced and create the specific gas–liquid interface, possibly including plasma-catalytic effects. A thermofluidic analysis confirms a uniform temperature profile and a positive temperature effect on mass transfer. By doing this way, the research achieves process intensification.

This chapter has been published as a research paper in “Chemical Engineering Journal” as follows:

Pho, Q.H., Lin, L., Rebrov, E.V., Sarafraz, M.M., Tran, T.T., Tran, N.N., Losic, D. and Hessel, V., 2023. Process intensification for gram-scale synthesis of N-doped carbon quantum dots immersing a microplasma jet in a gas-liquid reactor. *Chemical Engineering Journal*, 452, p.139164. [<Link>](#)


---



# Statement of Authorship

Title of Paper	Process intensification for gram-scale synthesis of N-doped carbon quantum dots immersing a microplasma jet in a gas-liquid reactor
Publication Status	<input checked="" type="checkbox"/> Published <input type="checkbox"/> Accepted for Publication <input type="checkbox"/> Submitted for Publication <input type="checkbox"/> Unpublished and Unsubmitted work written in manuscript style
Publication Details	Pho, Q.H., Lin, L., Rebrov, E.V., Sarafraz, M.M., Tran, T.T., Tran, N.N., Losic, D. and Hessel, V., 2023. Process intensification for gram-scale synthesis of N-doped carbon quantum dots immersing a microplasma jet in a gas-liquid reactor. Chemical Engineering Journal, 452, p.139164.


## Principal Author

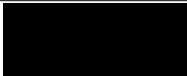
Name of Principal Author (Candidate)	Quoc Hue Pho
Contribution to the Paper	Conceptualization, Methodology, Formal analysis, Investigation, Data curation, Writing – original draft
Overall percentage (%)	65%
Certification:	This paper reports on original research I conducted during the period of my Higher Degree by Research candidature and is not subject to any obligations or contractual agreements with a third party that would constrain its inclusion in this thesis. I am the primary author of this paper.
Signature	 Date 28.01.2023

## Co-Author Contributions


By signing the Statement of Authorship, each author certifies that:


- i. the candidate's stated contribution to the publication is accurate (as detailed above);
- ii. permission is granted for the candidate to include the publication in the thesis; and
- iii. the sum of all co-author contributions is equal to 100% less the candidate's stated contribution.


Name of Co-Author	LiangLiang Lin
Contribution to the Paper	Investigation and Writing- Review and Editing.
Signature	 Date 30.01.2023


Name of Co-Author	Evgeny V. Rebrov
Contribution to the Paper	Formal analysis, Writing- Review and Editing.
Signature	 Date 06.02.2023

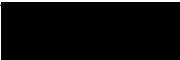
Please cut and paste additional co-author panels here as required.

Name of Co-Author	Mohammad Mohsen Sarafraz		
Contribution to the Paper	Formal analysis, Data curation, Writing- Review and Editing.		
Signature		<small>Digitally signed by Dr Mohammad Mohsen Sarafraz DN: cn=Dr Mohammad Mohsen Sarafraz, ou=Faculty of Science, ou=FATE ThermoFuels Group, email=Maecm.Sarafraz@gmail.com, c=AU Date: 2023.02.03 10:42:19 +11'00'</small>	Date 03.02.2023

Name of Co-Author	Thanh Tung Tran		
Contribution to the Paper	Formal analysis, Writing- Review and Editing.		
Signature		Date	1.2.2023

Name of Co-Author	Nam Nghiep Tran		
Contribution to the Paper	Writing- Review and Editing.		
Signature		Date	28.01.2023

Name of Co-Author	Dusan Losic		
Contribution to the Paper	Co-supervised andss Writing- Review and Editing.		
Signature		Date	2 feb 2023

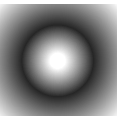
Name of Co-Author	Volker Hessel		
Contribution to the Paper	Supervised (scientific ideas, concepts, objectives, assessment of achievement degree, societal impact) Conceptualised, Writing – review & editing, and is the corresponding author.		
Signature		Date	28.01.2023

Please cut and paste additional co-author panels here as required.

**BLANK PAGE**

# Chapter 5

## Rationally designed microplasma synthesis of NCQDs for targeted applications



---

After successfully achieving the mass-based intensification for the microplasma synthesis of N-doped carbon quantum dots, the innovative contribution of this chapter is to provide a new conceptual strategy to rationally design and synthesise the desirable for three main applications (nanopesticides, water purification, and theranostic treatment). N-doped carbon quantum dots (NCQD) were rationally designed and synthesised, for the first time, from folic acid (Vitamin B9) by a non-thermal microplasma jet. Then, the morphology, size, crystallographic structure, and photoluminescence of the as-prepared NCQD, which plays a key role in selected applications, were investigated by various analytical characterisations such as HR, TEM, XPS, <sup>1</sup>HNMR, XRD, FTIR, UV-Vis, Raman spectroscopy, etc. Finally, The Derjaguin, Landau, Verwey, and Overbeek (DLVO) theory is conducted to understand their colloidal behaviours.

This chapter has been published as a research paper in “Carbon” journal as follows:

**Pho, Q.H.**, Lin, L., Tran, N.N., Tran, T.T., Nguyen, A.H., Losic, D., Rebrov, E.V. and Hessel, V., 2022. Rational design for the microplasma synthesis from vitamin B9 to N-doped carbon quantum dots towards selected applications. *Carbon*, 198, pp.22-33. [<Link>](#)

---

# Statement of Authorship

Title of Paper	Rational design for the microplasma synthesis from vitamin B9 to N-doped carbon quantum dots towards selected applications
Publication Status	<input checked="" type="checkbox"/> Published <input type="checkbox"/> Accepted for Publication <input type="checkbox"/> Submitted for Publication <input type="checkbox"/> Unpublished and Unsubmitted work written in manuscript style
Publication Details	Pho, Q.H., Lin, L., Tran, N.N., Tran, T.T., Nguyen, A.H., Losic, D., Rebrov, E.V. and Hessel, V., 2022. Rational design for the microplasma synthesis from vitamin B9 to N-doped carbon quantum dots towards selected applications. Carbon, 198, pp.22-33.

## Principal Author

Name of Principal Author (Candidate)	Quoc Hue Pho			
Contribution to the Paper	Conceptualization, Methodology, Formal analysis, Investigation, Data curation, Writing – original draft			
Overall percentage (%)	65%			
Certification:	This paper reports on original research I conducted during the period of my Higher Degree by Research candidature and is not subject to any obligations or contractual agreements with a third party that would constrain its inclusion in this thesis. I am the primary author of this paper.			
Signature	<table border="1" style="width: 100%;"> <tr> <td style="width: 60%;"></td> <td style="width: 40%;">Date</td> <td>28.01.2023</td> </tr> </table>		Date	28.01.2023
	Date	28.01.2023		

## Co-Author Contributions


By signing the Statement of Authorship, each author certifies that:


- i. the candidate's stated contribution to the publication is accurate (as detailed above);
- ii. permission is granted for the candidate to include the publication in the thesis; and
- iii. the sum of all co-author contributions is equal to 100% less the candidate's stated contribution.


Name of Co-Author	LiangLiang Lin			
Contribution to the Paper	Conceptualization, Writing- Review and Editing			
Signature	<table border="1" style="width: 100%;"> <tr> <td style="width: 60%;"></td> <td style="width: 40%;">Date</td> <td>30.01.2023</td> </tr> </table>		Date	30.01.2023
	Date	30.01.2023		


Name of Co-Author	Nam Nghiep Tran			
Contribution to the Paper	Writing- Review and Editing			
Signature	<table border="1" style="width: 100%;"> <tr> <td style="width: 60%;"></td> <td style="width: 40%;">Date</td> <td>28.01.2023</td> </tr> </table>		Date	28.01.2023
	Date	28.01.2023		

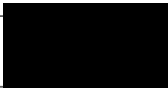
Please cut and paste additional co-author panels here as required.

Name of Co-Author	Thanh Tung Tran		
Contribution to the Paper	Formal analysis, Writing- Review and Editing		
Signature		Date	1.2.2023

Name of Co-Author	An Hoa Nguyen		
Contribution to the Paper	Data curation		
Signature		Date	28.01.2023

Name of Co-Author	Dusan Losic		
Contribution to the Paper	Co-supervised and Writing- Review and Editing.		
Signature		Date	2 feb 2023

Name of Co-Author	Evgeny V.Rebrov		
Contribution to the Paper	Writing- Review and Editing.		
Signature		Date	06.02.2023

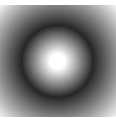
Name of Co-Author	Volker Hessel		
Contribution to the Paper	Supervised (scientific ideas, concepts, objectives, assessment of achievement degree, societal impact), conceptualised, Writing – review & editing, and is the corresponding author.		
Signature		Date	28.01.2023

Please cut and paste additional co-author panels here as required.

**BLANK PAGE**

# Chapter 6

## Insight into plasma-catalysis in triphasic microplasma synthesis for NCQDs



---

In chapter 6, the aim of this study is to understand the plasma-catalytic effect under the microplasma multiphase design and vice versa, to understand the multiphase design better. As an analytical method, optical emission spectroscopy (OES) investigations are appropriate to investigate the mechanism of how a plasma(-heterogeneous) catalyst in a multiphase reaction may affect the fabrication of NCQD from Vitamin B9. The key of this research is to determine and advance multiphase hydrodynamics and reaction by shaping a characteristic surface profile via deep penetration of the plasma jet into the liquid volume.

This chapter has been prepared as a research paper manuscript and supposed to be submitted to “Chemical Engineering Journal” as follows:

**Pho, Q.H.,** Tran, H.Q., Zhuang C.P., Nguyen, V.L., Tran, N.N., Tran, T. T., Rebrov, E.V., Losic, D., and Hessel, V., 2023. Deciphering Plasma-Catalysis in Triphasic Microplasma for N-doped Carbon Quantum Dots from Vitamin B9 via Optical Emission Spectroscopy. (Ready manuscript)

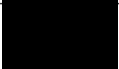
---



# Statement of Authorship

Title of Paper	Deciphering Plasma-Catalysis in Triphasic Microplasma for N-doped Carbon Quantum Dots from Vitamin B9 via Optical Emission Spectroscopy
Publication Status	<input type="checkbox"/> Published <input type="checkbox"/> Accepted for Publication <input type="checkbox"/> Submitted for Publication <input checked="" type="checkbox"/> Unpublished and Unsubmitted work written in manuscript style
Publication Details	Pho, Q.H., Tran, H.Q., Zhuang, C.P., Nguyen, V.L., Tran, N.N., Tran, T. T., Rebrov, E.V., Losic, D., Malacha, D., and Hessel, V., 2023. Deciphering Plasma-Catalysis in Triphasic Microplasma for N-doped Carbon Quantum Dots from Vitamin B9 via Optical Emission Spectroscopy. (Ready manuscript)

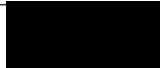
## Principal Author


Name of Principal Author (Candidate)	Quoc Hue Pho
Contribution to the Paper	Conceptualization, Methodology, Formal analysis, Investigation, Data curation, Writing – original draft
Overall percentage (%)	65%
Certification:	This paper reports on original research I conducted during the period of my Higher Degree by Research candidature and is not subject to any obligations or contractual agreements with a third party that would constrain its inclusion in this thesis. I am the primary author of this paper.
Signature	 Date 28.01.2023

## Co-Author Contributions

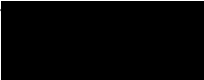
By signing the Statement of Authorship, each author certifies that:


- i. the candidate's stated contribution to the publication is accurate (as detailed above);
- ii. permission is granted for the candidate to include the publication in the thesis; and
- iii. the sum of all co-author contributions is equal to 100% less the candidate's stated contribution.


Name of Co-Author	Quan Hoang Tran
Contribution to the Paper	Investigation and data curation
Signature	 Date 28.01.2023

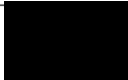
Name of Co-Author	Changping Zhuang
Contribution to the Paper	Investigation and data curation
Signature	 Date 28.01.2023

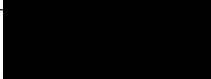
Please cut and paste additional co-author panels here as required.

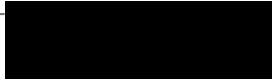
Name of Co-Author	Nguyen Van Duc Long		
Contribution to the Paper	Investigation and data curation		
Signature		Date	31.01.2023

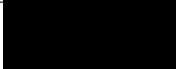
Name of Co-Author	Nam Nghiep Tran		
Contribution to the Paper	Conceptualization, Writing- Review and Editing.		
Signature		Date	28.01.2023

Name of Co-Author	Thanh Tung Tran		
Contribution to the Paper	Conceptualization, Writing- Review and Editing		
Signature		Date	1.2.2023

Name of Co-Author	Evgeny V. Rebrov		
Contribution to the Paper	Writing – review & editing		
Signature		Date	

Name of Co-Author	Dusan Losic		
Contribution to the Paper	Co-supervised and Writing- Review and Editing		
Signature		Date	2 feb 2023

Name of Co-Author	Zdenko Machala		
Contribution to the Paper	Investigation and data curation. Writing- Review.		
Signature		Date	06.02.2023

Name of Co-Author	Volker Hessel		
Contribution to the Paper	Supervised (scientific ideas, concepts, objectives, assessment of achievement degree, societal impact), Conceptualised, Writing – review & editing, and is the corresponding author.		
Signature		Date	28.01.2023

## Deciphering Plasma-Catalysis in Triphasic Microplasma for N-doped Carbon Quantum Dots from Vitamin B9 via Optical Emission Spectroscopy

Quoc Hue Pho <sup>a,c</sup>, Quan Hoang Tran <sup>a</sup>, Changping Zhuang <sup>a</sup>, Nguyen Van Duc Longs <sup>a</sup>, Nam Nghiep Tran <sup>a</sup>, Thanh Tung Tran <sup>a,b</sup>, Evgeny V. Rebrov <sup>c</sup>, Dusan Losic <sup>a,b</sup>, Zdenko Machala <sup>d</sup>, Volker Hessel <sup>a,c</sup>

<sup>a</sup> School of Chemical Engineering, The University of Adelaide, Adelaide, SA 5005, Australia

<sup>b</sup> The ARC Graphene Research Hub, School of Chemical Engineering and Advanced Materials, The University of Adelaide, SA 5005, Australia

<sup>c</sup> School of Engineering, University of Warwick, Library Rd, Coventry CV4 7AL, England, UK

<sup>d</sup> Department of Astronomy, Earth Physics and Meteorology, Comenius University, Bratislava, Slovakia

E-mail: [volker.hessel@adelaide.edu.au](mailto:volker.hessel@adelaide.edu.au)

### Abstract

Multiphase plasma catalysis is applied to fabricate N-doped carbon quantum dots by exposing a submerged plasma jet deep into a small liquid volume with the precursor and catalytic alloy flakes. Optical emission spectroscopy at the plasma-liquid-catalyst interface was used to investigate and understand the reaction mechanism, particularly the role of the plasma catalysis effect. Depending on the penetration depth of the jet, defining its contact with the liquid medium and the catalyst just underneath in a generic hydrodynamic regime, the deepest penetration, the ‘deflection mode’, generated more positively charged species from the metal catalyst. The bimetallic catalyst Ni<sub>80</sub>Cr<sub>20</sub> demonstrated the strongest effect, which is correlated to the highest electric potential among the three alloy catalysts investigated. Seven steps are proposed for the reaction mechanism to yield the N-doped quantum dots. The temperature at the plasma-liquid-catalyst interface was lower than 25 °C, as determined by IR imaging. Nonetheless, notable water evaporation happens at the surface surrounded by highly convective phases.

**Keywords:** nonthermal microplasma, N-doped quantum carbon dots, optical emission spectroscopy, plasma catalysis, multiphase reaction

### Highlights

- Optical emission spectroscopy at the plasma-liquid-catalyst interface was used to investigate and understand the reaction mechanism, particularly the role of the plasma catalysis effect.
- The deepest penetration, the 'deflection mode', generated more positively charged species from the metal catalyst.
- The bimetallic catalyst Ni<sub>80</sub>Cr<sub>20</sub> demonstrated the strongest effect, which is correlated to the highest electric potential among the three alloy catalysts investigated.
- The temperature at the plasma-liquid-catalyst interface was lower than 25 °C, as determined by IR imaging.
- Seven steps are proposed for the reaction mechanism to yield the N-doped quantum dots.

### 1. Introduction

Since their initial discovery in 2004, carbon dots (CD) have attracted attention in research for various potential applications due to their unique properties, such as low toxicity, biocompatibility, water solubility, and excellent optical properties [1-3]. N-doped carbon quantum dots (NCQD) have the potential as multifunctional nanopesticides (pesticide nanocarriers [4], pesticides [5], pathogen targeting [6], and phytopathogen detecting [7]), are considered as a tool of the “agri-tech revolution” [8], which aims to enhance crop efficiency and meet the growing global demands for food [8, 9].

Extensive research studies on N-doped carbon quantum dots have been conducted, reporting a large number of diverse structures of this nanomaterial class with distinct properties, made *via* various synthetic techniques [10], including laser ablation [11], arc discharge [12], hydrothermal [13], pyrolysis [14], solvothermal [15] and ultrasonic [16] processing. Those manufacturing technologies differ in sustainability. In our previous research, green chemistry, circular and ecoScale metrics were used to assess those methods, which are common to judge sustainability for industrial-scale production of chemical processes [17], in particular in the pharmaceutical industry with similarly high-quality needs for functional nanomaterials. Among the six NCQD manufacturing routes, plasma synthesis had the best energy efficiency while lacking in mass efficiency [17]; meaning it does not have the productivity as the other processes, typically run in macroscopic reactors, whereas the plasma considered was a tiny jet.

Alike for microchannels, small reaction volumes do not inhibit productivity. Striving for process intensification to overcome the problem of low productivity of jet microplasmas, we designed a genuine process around enhancing mass transport in intensified gas (plasma)–liquid regimes and the facilitation of catalysis on metal particles in the liquid microvolume, achieving gram-scale synthesis, which is significant for a tailored nanomaterial [18]. This study will provide a closer look at the fundamentals to better understand plasma catalysis in a multiphase processing mode, including deciphering plasma-excited species and their reaction mechanism. This is motivated by our recent finding that the photoluminescence of the as-prepared NCQD increases by 18.4% in the presence of metal flakes as catalysts [18]. This evidence indicates a research gap in how these metal catalysts interact with plasma to enhance the production efficiency of NCQD.

The impact of this study is underlined by recent reports about the progress of plasma catalytic processes, for example, on the conversion of light hydrocarbons [19], CO<sub>2</sub> [20], and volatile organic compounds (VOCs) [21]. Meng et al. developed a process combining nonthermal plasma with a photocatalyst to improve product yield and limit coke formation in a simulated natural gas conversion to C<sub>6</sub>–C<sub>9</sub> branched-chain paraffins [22]. Ahmad et al. used a Ni/Al<sub>2</sub>O<sub>3</sub> catalyst for the methanation of CO<sub>2</sub>. The plasma-catalytic process achieved similar conversions and selectivities at lower temperatures than the thermal

process [23]. Erik et al. also mentioned that plasma catalytic processes are already a highly successful approach for the small-scale fabrication of expensive materials such as CNTs [24-26] or inorganic nanowires [27, 28]. This evidences that the plasma-catalysis effect is also key in fabricating NCQD from folic acid (vitamin B9). However, the underlying plasma-catalyst effect and mechanism in the formation of NCDQ are unclear, which is tackled in this study.

For this reason, this study aims to understand the plasma-catalytic effect under that microplasma multiphase design and vice versa, to understand the multiphase design better. As an analytical method, optical emission spectroscopy (OES) investigations are appropriate to investigate the mechanism of how a plasma-(heterogeneous) catalyst in a multiphase reaction may affect the fabrication of NCQD from Vitamin B9. The key of our experiment is to determine and advance multiphase hydrodynamics and reaction by shaping a characteristic surface profile *via* deep penetration of the plasma jet into the liquid volume ('crater'). The jet can reach down to the bed of heterogeneous catalysts, metallic flakes, which are static, while exposed to a plasma flow field of very high velocity and drag force. The jet may likely contact both the thin liquid layer and the catalyst, meaning a genuine tri-phase process design possibly is generated, which is new to the literature and magnified by miniature dimensions, coined as 'micro-plasma'. Subtle details need a better understanding, e.g., how the fine droplet spray that has been detected under such conditions [29, 30], can add to reaction advancement.

## 2. Materials and methodology

### 2.1. Reactor configuration and experimental setup

Our experimental design is inspired by the concept of high-intensity gas-liquid reactors with powerful gas jets, which are known to improve phase mixing [31]. A high-velocity impinging flow reactor was developed to enter a small reactor volume and travel in counter current. Guided by a small nozzle, the gas and liquid streams meet in a small reactor volume, leading to a highly turbulent distribution of the gas phase in the liquid. The formation and collapse of gas bubbles enhance substance exchange. Another high-intensity gas-liquid reactor design consists of a pump, an orifice, a vertical tube coaxial with the orifice, and a baffle plate [31]. The pump creates a downward vertical jet of liquid through the orifice, creating a gas-liquid dispersion in the tube. The two-phase jet is directed onto a baffle near the bottom of the tank and distributed throughout the liquid. The liquid is drawn under the baffle plate and recycled.

Our experimental design follows these high-intensity gas-liquid reactor concepts but should be simplified. It means that the plasma gas phase exists over long distances, which is difficult to achieve. Instead, we use a micro-plasma jet aimed at the liquid (Figure 1). We also withhold flow feedback for repeated gas-liquid interactions, as single contact is better shown to be fundamental for the process intensification [32].

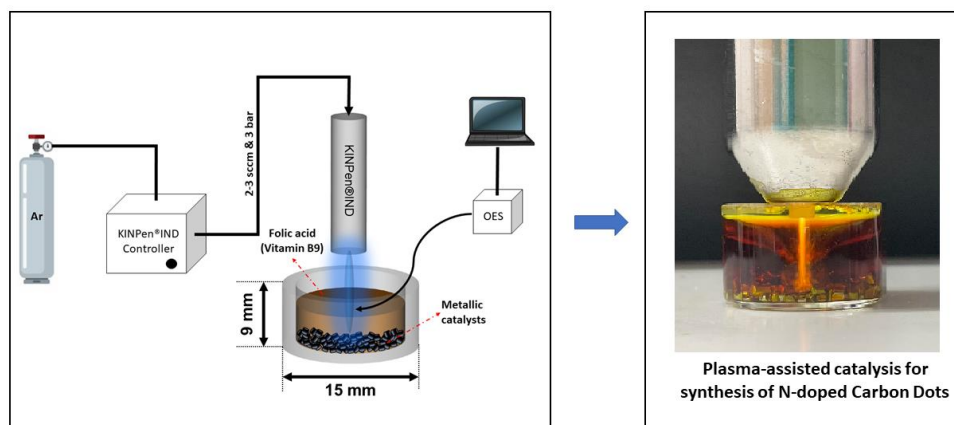


**Figure 1.** Reactor configurations and experimental setup of the synthesis process of NCQD.

The reactor configuration and experimental synthesis process were adopted from previous studies [31]. Simply put, the synthesis reactor consists of two parts: (1) A kINPen®IND microplasma jet with dimensions 105 × 180 × 330 mm (H × W × D) was purchased from Neoplas GmbH, Germany, and (2) a 9 mm open glass reactor was used in our study with designed and manufactured in-house 15mm (W x H) dimensions. A 110 VAC (50 Hz) power supply is connected to the kINPen®IND microplasma jet. A continuous gas stream of Ar (99.9%) was connected to the microplasma nozzle. A stable microplasma stream with a length of 1 cm was formed under Ar gas flow and a control pressure of 3 bar. To understand the reaction mechanism, we installed an optical fibre in the plasma-liquid-catalyst interface and detected the reactive species generated from the microplasma. The general synthetic procedure is also described in Figure 1. Briefly, a folic acid (FA) solution (0.1 g/mL) as a starting carbon source was obtained by dissolving 2 g of folic acid (98%) in 20 mL of NaHCO<sub>3</sub> (0.5 M) as a solvent, resulting in an orange colour and prepared by stirring until the solution was evenly mixed. Then 1 ml of FA solution (0.1 mg/ml) was transferred to the open reactor and treated under microplasma with 0.5 g of various metal flakes (Sn coated Cu, Ni<sub>90</sub>Ni<sub>10</sub>, and Ni<sub>180</sub>Cr<sub>20</sub>) as catalysts.

## 2.2. Optical emission spectroscopy analysis

Optical emission spectroscopy (OES) is an essential technique for the multi-element analysis of various materials. This technology monitors the levels of various chemicals and trace elements in the environment and determines the composition of solids, liquids and gases. In optical emission spectroscopy, electrical energy is applied as a spark, created between an electrode and a metal sample, driving vaporised atoms into a high-energy state in a so-called 'discharge plasma'.

Plasma emissions with different flow velocities generated by the atmospheric pressure of the plasma jet system were recorded. The resulting spectral distribution was plotted as amplitude versus wavelength. The



emission spectra of the synthesis reaction of NCQDs under microplasma were recorded using the OES technique. The spectrum consists of several characteristic spectral lines of specific atoms and ions of Ar. In this study, to observe the signals of nickel ions, the emission spectra were measured using an HR2000 + E.S. spectrometer (Ocean Optics, Inc.) during the reaction process (Figure 1).

### 2.2.1. Reaction setup

To carry out the OES measurements in the synthesis reaction of NCQDs, a 400- $\mu\text{m}$ -in-diameter glass optical fibre with a length of 1 meter was connected to an HR2000 + E.S. spectrometer (Ocean Optics, Inc.). This optical fibre functions as a detection probe. The HR2000 + E.S. spectrometer was then connected to a computer where Oceanview 2.0.8 software was installed for data recording and control. Briefly, in each OES measurement, the optical fibre was positioned and fixed by a holder at a distance of 1 mm above the plasma-liquid-catalyst interface. The OES signal was recorded in a dark room to avoid systematic errors due to the noise from the visible light background. All spectra were recorded in the wavelength range 200 nm to 1000 nm, with an integration time of 100 ms and averaged over 20 measurements per spectrum. The experimental measurements were triplicated to avoid systematic errors.

### 2.2.2. Validating various bimetallic catalysts on fabrication reaction of NCQDs

In this study, different types of multi-element metal catalysts (Sn-coated Cu,  $\text{Cu}_{90}\text{Ni}_{10}$ , and  $\text{Ni}_{80}\text{Cr}_{20}$ ) were used to understand better the effect of plasma catalysis on the NCQDs synthesis. The experimental design for NCQDs plasma-assisted microplasma synthesis is shown in Table 1.

**Table 1.** Experimental configuration of plasma-assisted microplasma synthesis of NCQD

Configuration	Distant	Contact	Deflection
Plasma length	10 mm	10 mm	4 mm
Catalyst size	500 $\mu\text{m}$	500 $\mu\text{m}$	500 $\mu\text{m}$
Catalyst layer thickness	2 mm	2 mm	2 mm
Mass	0.5 g	0.5 g	0.5 g

### 2.3. Electric potential analysis of bimetallic catalysts

Electric potential is created between two dissimilar metals in an electrochemical reaction. This potential measures the energy per unit charge available from the oxidation/reduction reactions to drive the reaction. It is customary to visualise the cell reaction in terms of two half-reactions, an oxidation half-reaction and a reduction half-reaction. The electrochemical potentials of the catalysts can be calculated as follows (1):

$$E_{\text{Catalyst}}^0 = E_{\text{Oxidation}}^0 - E_{\text{Reduction}}^0 \quad (1)$$

### 2.4. Thermal Imaging using FLIR camera and surface profile

Regarding thermal imaging, a FLIR camera was set up to capture the thermal graphs of pure plasma, plasma-Ni<sub>80</sub>Cr<sub>20</sub>, and plasma-liquid-Ni<sub>80</sub>Cr<sub>20</sub> interaction, by infrared imaging. The camera captured images of the reactor to reproduce the liquid surface profile. The plasma-liquid-catalyst interface was re-drawn by Adobe Photoshop 2020 software. These surface curves are digitalised for further surface profile investigation.

## 3. Results and discussion

### 3.1. Setting of thin liquid layer and plasma-liquid-catalyst interfaces

As the main motivation, we aimed to advance multiphase plasma design to promote phase-physical properties and fluid/interfacial transport for chemical reactions. The chemical engineering literature often overlooks the plasma pre-determination of process design. Microfluidic operation and flow chemistry [33-37], have proven to be particularly beneficial in the defined process setting and to intensify reactions. Our process design is driven by the microfluidic microplasma [35]. Micro-scale phenomena have been reported in plasma processing, including their impact on Brownian motion gas-liquid, ‘multiphase’) [38] and thermophoresis, selective particle movement along a temperature gradient [39].

As second motivation, our experiments are inspired by OES's reported monitoring effectiveness to steer multiphase plasma reactions [40] Aadim et al. reported that changing the gas flow can change the emission intensity, which means that the number of excited species can be tuned [40].

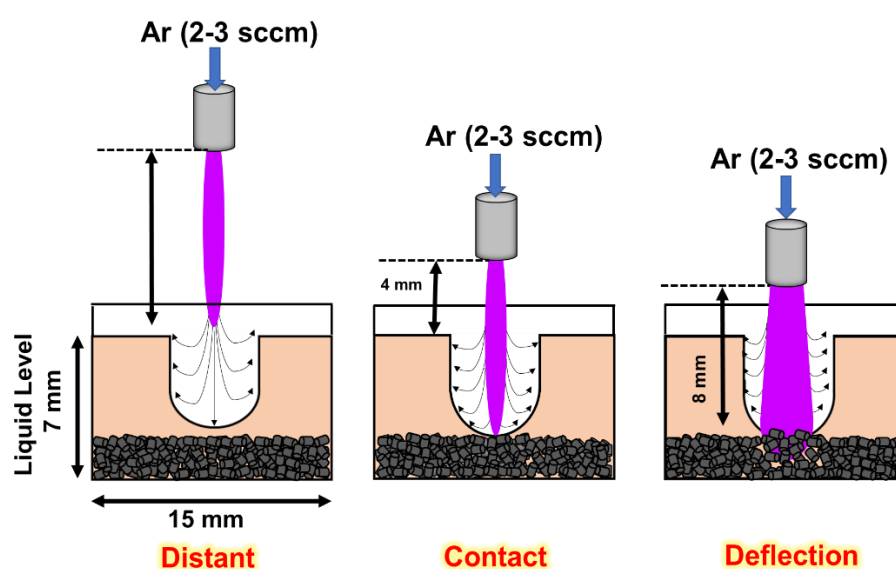


**Figure 2.** Generic configurations of the microplasma jet-liquid system at different operational modes with various metal catalysts.

We choose three generic configurations for positioning the plasma jet relative to the liquid surface (Figure 2). In the 'distant' position, the most protruding part, the tip of the microplasma jet, does not contact the liquid surface but rather generates only a small crater. The reaction is assumed to be essentially gas-liquid. It is believed to have little effect on liquid-phase hydrodynamics and mass transfer. In the 'contact' position, we emulate the high-intensity gas-liquid reactor, as reported on a macroscopic scale by Wild et al. [31]. The plasma jet penetrates deeper, forming a liquid film above the catalyst surface. In the "deflection" position, it emulates a "fast impinging jet reactor", a plasma reactor configuration proposed by Botes [32]. The liquid film is further thinned, the diameter of the plasma jet hitting the liquid is larger, and the plasma might penetrate the catalyst. The plasma jet is maximally harshly re-directed, creating a turbulence plasma-gas phase and potentially inducing recirculation of the bulk liquid to support the transport of folic acid reactant to the film reaction zone and transport of carbon quantum dots out of it in the bulk liquid volume. What is expected is a multiphase system with the continuous renewal of the interface, possibly assisted by the generation and breakup of small droplets from the water surface, following the literature report [41].

### 3.1.1. Shaping surface profile by metallic flake catalysts

The plasma jet in the deflection mode is stopped at the metal ( $\text{Ni}_{80}\text{Cr}_{20}$ ) flakes interface surrounded by a liquid, giving rise to a different surface profile than water alone, Figure 3. Thus, the flakes drain a liquid microvolume with a large specific interface to the plasma. This phenomenon is not given for the pure water phase. The metal flakes are needed for their catalytic function and to entrain the reaction solvent in a stationary bed by wetting and shaping the multiphase reaction design. Both 'deflection impingement' with and without flakes demonstrates the formation of a deep crater, which is only possible in a microvolume and would not occur with a conventional laboratory beaker size, e.g. 50 or 100 ml, and/or a larger plasma jet.

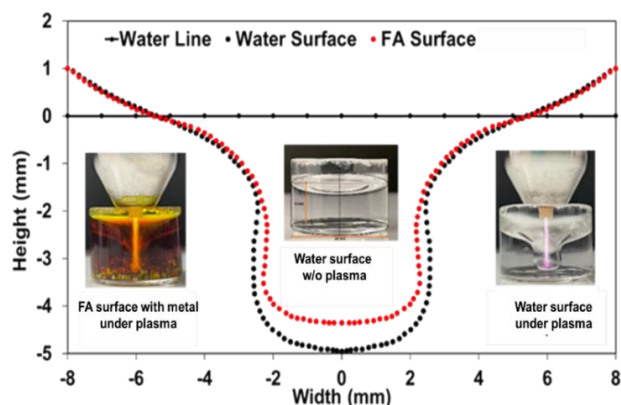


**Figure 3.** Surface profile of reaction liquid (folic acid) in the presence of  $\text{Ni}_{80}\text{Cr}_{20}$  as compared with water surface with or without plasma at the deflection mode

### 3.2. Optimising argon ion and water-related excited species concentration at the plasma-liquid interface

The key is generating the right reactive species in great amounts and with high solubility, as the reaction is supposed to be mediated by the liquid phase.

Microfluidic operation is known to complete reactions in seconds which may otherwise take others. Thus, the first reaction experiment is motivated by maximising the number of reactive species per time. We assumed that the argon flow rate correlates with that, meaning the higher, the more reactive species. Our plasma system allows 2 and 3 sccm argon flow rate settings.

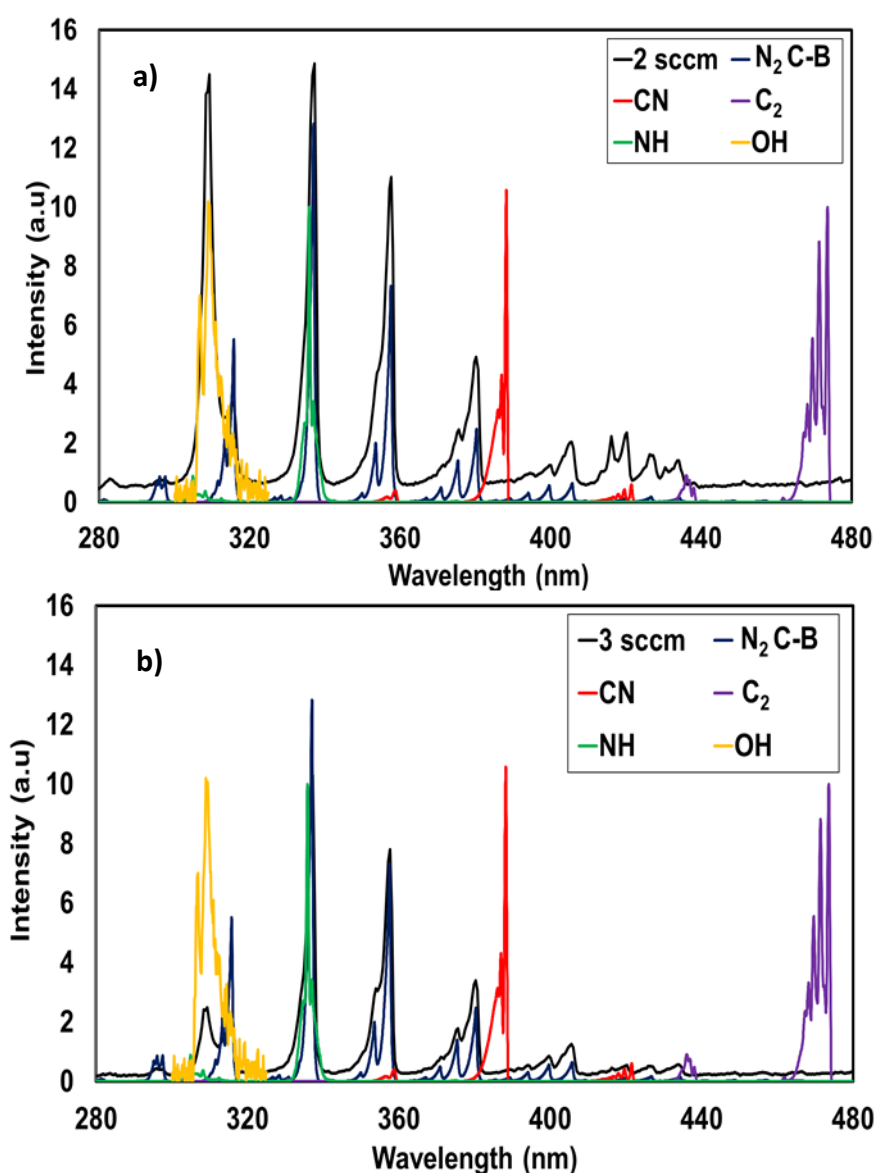


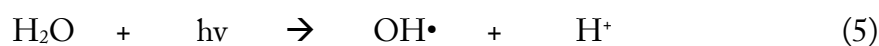
**Figure 4.** OES analysis of the flow-rate influence at (a) 2 sccm and (b) 3 sccm on the intensity of positively charged species in reaction at the plasma-liquid interface of the synthesis reaction of NCQD with the presence of  $Ni_{80}Cr_{20}$  catalysts, as compared with modelled positively charged species (using Specair software)

OES analysis was used for a semi-quantitative determination of the ionised species, as proposed by Bruggeman et al. [42]. Their intensity close to the plasma-liquid interface is higher at an argon flow rate of 2 sccm than that at a flow rate of 3 sccm, Figure 4 and Figure S1. The impact of longer residence time is more relevant than providing more reactive species. The OES spectrum at 2 sccm (Figure 4a) and 3 sccm (Figure 4b) detects a major share of N<sub>2</sub> C-B. The simulated N<sub>2</sub> 0-0 band (337 nm) is narrower than measured, and the left wing of N<sub>2</sub> 0-0 band is broader. This is explained by the measured gas temperature  $T_{\text{gas}}$  at the 2 sccm and 3 sccm being higher than as simulated at 700 K, which would raise the left wing.

The presence of N<sub>2</sub> C-B is because a protective shield was not used to avoid air entrapment to our reaction. Intentionally, we wanted to use N<sub>2</sub> from the air as an abundant source (78% in air) to be ionised by Ar<sup>+</sup> species to form primary N<sub>2</sub><sup>+</sup> species and other secondary ionised nitrogen species.

Besides Ar<sup>+</sup> as the primary reaction species of the plasma, oxygen-containing species such as OH• (309 nm) have to be considered as secondary reactive species from the reaction medium, water. Their concentration is higher at the 2 sccm argon flow rate, consistent with a higher Ar<sup>+</sup> concentration.

Bruggeman et al. reported that a stream of positively charged ions is generated in a plasma jet and bombarded into the plasma-liquid-catalyst interface, causing various reactions [43], given in the equations (2), (3), (4), and (5).



These generated reactive species (Ar<sup>+</sup>, N<sub>2</sub><sup>+</sup>, O<sup>+</sup>, OH•) can easily penetrate through the liquid surface because their potential energy is large compared to any activation energy barrier (such as surface tension) required to enter the liquid. So cations are mostly immediately solvated when striking the liquid [44]. In addition, these ionised reactive species carry high energy, which can cause reactions at the interface by breaking down the chemical bonding of folic acid in the liquid phase [44].

### 3.3. Excited species formation in different plasma-liquid-solid process designs

Our previous studies reported the impact of operational modes of the microplasma jet towards the production of NCQD throughout the photoluminescence performance [18]. In this study, we introduced the OES analysis approach to understand better how the operational modes influence the intensity of ionised Ar gases at the surface interface of plasma-liquid. The position of the jet was adjusted towards the bottom of the reactors at a flow rate of 2 sccm, as described in Figure 2. The intensity of ionised Ar gases

at the plasma-liquid-catalyst interface of the synthesis reaction of NCQD (from NIST atomic spectra database lines data) was recorded at distant, contact, and deflection mode (Figure 5).

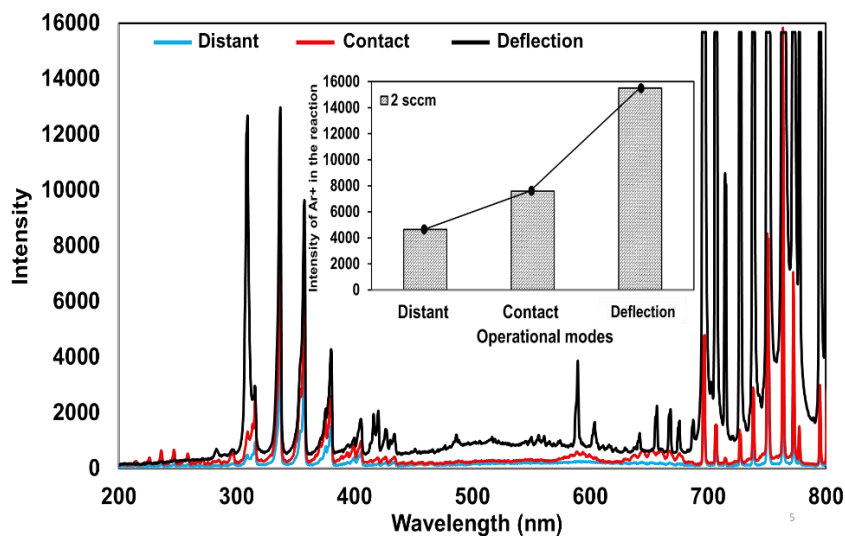


**Figure 5.** OES spectra of NCQD synthesis at various operational modes with the intensity of ionised Ar gases recorded from OES spectra at the plasma-liquid-catalyst interface (kINPen®IND microplasma jet, 25 °C, 0.1 g/mL folic acid solution, 0.5 g Ni<sub>80</sub>Cr<sub>20</sub>, 99.99 % Ar gas at 2 sccm).

Figure 5 shows that when shifting the ‘distant mode’ to ‘deflection mode’, the intensity of Ar<sup>+</sup> species increases significantly. In particular, the highest intensity of ionised Ar gases produced at the plasma-liquid-catalyst interface was recorded at “deflection” mode, which was nearly 4-fold higher than that at “distant mode”. This can be explained by the fact that once the distance of the jet is adjusted closer to the metal layer at the reactor bottom (Figure 2), the morphology of the plasma and plasma-liquid interface becomes unstable or oscillated due to enhanced mixing, convection, and the dissipation of energy into the liquid [45]. Bruggeman et al. reported that external forces associated with plasma production could significantly perturb the surface of the liquid and metal surface at the plasma-liquid-solid interface [43, 46, 47]. Energetic particles at the interface, both charged and uncharged, bombard the surface stronger [48, 49]. Electric fields resulting from the applied voltage and space charge can physically distort the surface [50, 51]. The interaction of streamers at the interface can also be a source of acoustic energy or even shock waves. These acoustic processes can drive radical production at the plasma-liquid interface or even within the bulk liquid [43]. As a result, the highest intensity of Ar<sup>+</sup> species can be detected in the ‘deflection mode’. These instabilities may explain enhanced diffusion leading to in-volume mixing.

After penetrating through the liquid surface, Ar<sup>+</sup> and positively charged ions will cause the decomposition of folic acid into reactive fragments. It can be explained that at “deflection” mode, there is a bulk gas convection associated with plasma, leading to the convection in the liquid with speeds of several cm.s<sup>-1</sup>,

sufficient to dominate over diffusion. The moving gas's shear stress caused this induced liquid flow at the interface. Therefore, it can be concluded that the “deflection” mode is the most effective for reactive species transfer from the plasma into the liquid in this reaction.

### 3.4. Catalyst investigations

#### 3.4.1. Optimising electric potential of bimetallic catalysts

We use metallic flakes of rod shape with mm length and diameter. Knowing from the literature that pure metals (copper) were not optimal for producing carbon quantum dots, we decided to investigate metal alloys. It is known that the electric potential determines the charge transfer capacity [52], and we hypothesised that it might impact the catalytic activity. Alloys provide a smart way to adjust this. This strategy may not only define the electric environment of the heterogeneous catalyst surface but also advance the capacity of the flakes to transfer charged ions from and to the microplasma source, adding homogeneous catalysts.

Metallic flakes have been used in heterogeneous catalyses, such as Pd-Cu alloy as acetylene hydrogenation catalysts [53] and Cu-Ni alloy heterogeneous catalysis water dissociation [54]. To our best knowledge, flakes have not been used in plasma catalysis.

The electric potentials of Sn-coated Cu, Cu<sub>90</sub>Ni<sub>10</sub>, and Ni<sub>80</sub>Cr<sub>20</sub> were computed as follows, using the equations (8), (9), and (10).

$$E_{Sn/Cu}^0 = E_{Cu^{2+}/Cu}^0 - E_{Sn^{2+}/Sn}^0 = (+0.34).(0.99) - (-0.14).(0.01) = + 0.338 \text{ (V)} \quad (8)$$

$$E_{Ni/Cu}^0 = E_{Cu^{2+}/Cu}^0 - E_{Ni^{2+}/Ni}^0 = (+0.34).(0.9) - (-0.25).(0.1) = + 0.331 \text{ (V)} \quad (9)$$

$$E_{Cr/Ni}^0 = E_{Ni^{2+}/Ni}^0 - E_{Cr^{3+}/Cr}^0 = (-0.25).(0.8) - (-0.75).(0.2) = + 0.350 \text{ (V)} \quad (10)$$

Ni<sub>80</sub>Cr<sub>20</sub> has the highest electric potential with +0.350 (V), as compared to Cu<sub>90</sub>Ni<sub>10</sub> with 0.331 (V) and Sn-coated Cu with 0.338 (V). Electrochemistry in Ni<sub>80</sub>Cr<sub>20</sub> is supposed to be facilitated as compared to Cu<sub>90</sub>Ni<sub>10</sub> and Sn-coated Cu. This also agrees with the results in Figure 6 that the microplasma changed the surface structure of Ni<sub>80</sub>Cr<sub>20</sub>, leading to enhanced catalytic activity.

The structure and components of these catalysts in Figure 6c also explain that Ni is more reactive in electrochemical series than Sn, Cr, and Cu. Therefore, Ni can be easily ionised by charged ions from the plasma to form Ni (I) and Ni (II) ions. On the other, Cu is considered less active than its element counterparts, meaning that its ionisation capacity is much less than Ni, Sn, and Cr. In addition, Cu accounts for a major part of Sn-coated Cu (99.99%) and Cu<sub>90</sub>Ni<sub>10</sub> (90%) (Figure 6a and Figure 6b). Therefore, the catalytic surface of these two materials is less activated in terms of electrochemistry.

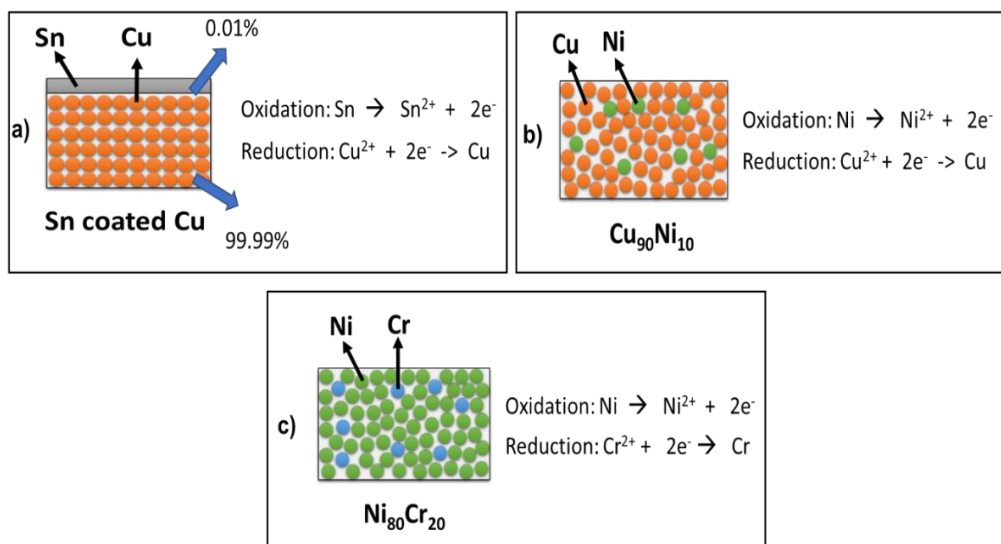


**Figure 6.** Structure, component, and electrochemistry reaction in (a) Sn-coated Cu, (b)  $\text{Cu}_{90}\text{Ni}_{10}$ , (c)  $\text{Ni}_{80}\text{Cr}_{20}$

### 3.4.2. Copper-based bimetallic catalyst

It has been demonstrated that Cu nanoparticles may act as a catalyst for carbon nanotube growth. Still, growing carbon nanomaterials directly on bulk Cu is only possible with an additional catalyst [55, 56]. Copper is a poor catalyst for carbon nanomaterials growth like CNTs, with smaller activity catalysing the decomposition of carbon stocks and lower carbon solubility [57]. In this study, Sn and Ni were used to add assumed advantageous electric properties to copper, see 3.1., in the form of coated Cu and  $\text{Cu}_{90}\text{Ni}_{10}$  catalysts, respectively [58, 59].

The bimetallic catalyst, Sn-coated Cu catalysis, has been reported to control the surface electronic state and binding energy in the electrocatalysis [60]. The introduction of Sn species in Cu changes the surface selectivity of the catalysts. As a result, the Cu–Sn bimetallic surface exhibited a highly selective and stable catalytic performance [61]. As Sn does not possess d-vacancies in their electron configuration, the Cu–Sn bimetallic catalysts have negligible affinity for carbon [62].

In the excited state, elemental lines of Cu and Sn were detected after exposure to plasma, Figure 7a and Figure 7b. The electron transition at the excited state is described in Table 2, using NIST atomic spectra database [15]. In particular, various typical peaks of Cu (I) at the excited state can be observed, which generates d-vacancies in their electron configuration, such as 507 nm, 516 nm, 456 nm, 521 nm, and 573 nm [ $3d^9(^2D)4s4p(^3P^o) \rightarrow 3d^94s(^3D)5s$ ]. In comparison, peaks at 296 nm [ $3d^9(^2D)4s4p(^3P^o) \rightarrow 3d^94s(^3D)5d$ ] and 298 nm [ $3d^94s^2 \rightarrow 3d^9(^2D)4s4p(^3P^o)$ ] are attributed to Cu (II). The typical peaks of Sn (II) at the excited state after exposure to plasma can also be observed at 556 nm [ $5s^26p\ 2P^o \rightarrow 5s^26d^2D$ ] and 289 nm [ $5s^25p^2 \rightarrow 5s^25p6d$ ]. Sn does not play an important role as a catalyst. However, Sn is introduced into Sn-



coated Cu to receive electrons from the d-orbital of Cu, leading to the generation of d-vacancies under microplasma treatment.

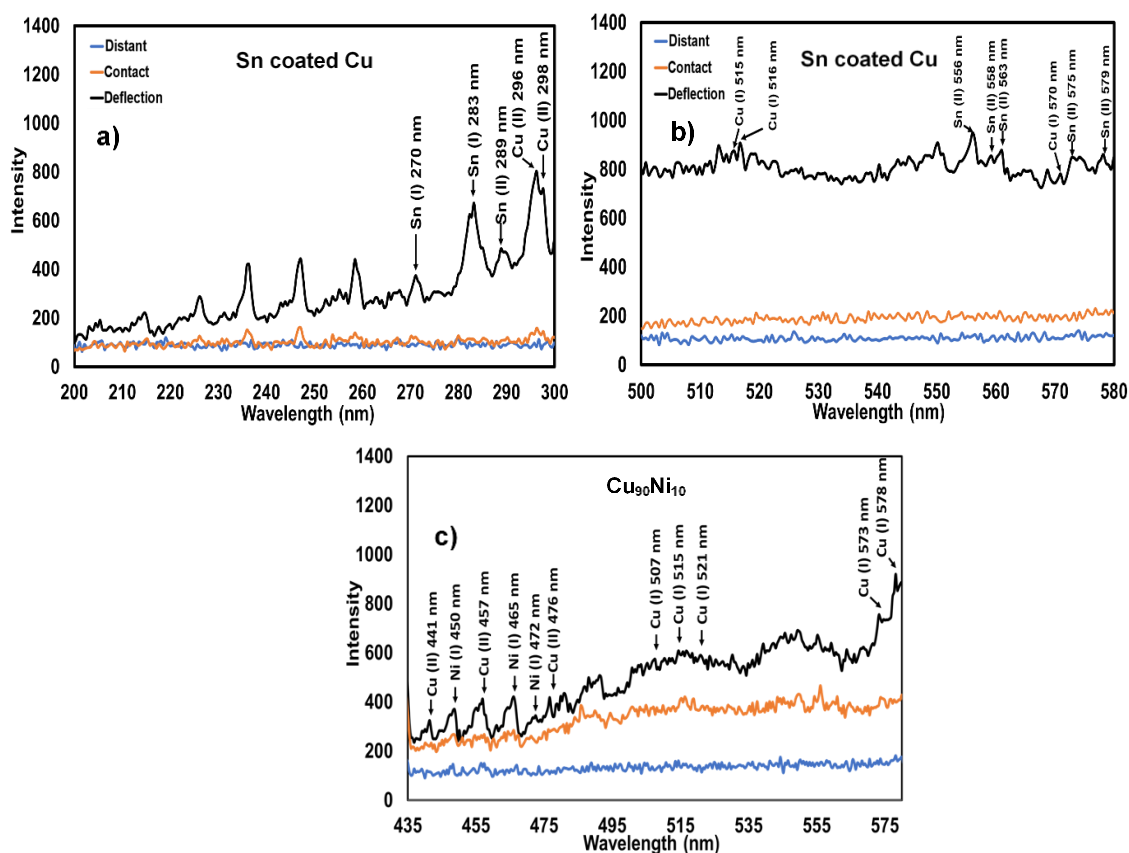


**Figure 7.** Detailed OES analysis of NCQD synthesis reaction using Sn coated Cu (a,b) and Cu<sub>90</sub>Ni<sub>10</sub> (c) under kINPen<sup>®</sup>IND microplasma jet at various operational modes with Ar flow rate of 2 sccm.

Previous studies demonstrated that Ni metals are a good catalyst candidate as they possess d-vacancies in their electron configuration [62-64]. Therefore, introducing Ni into Cu to form Cu<sub>90</sub>Ni<sub>10</sub> can also enhance the catalytic activity of pure Cu metals. The results in Figure 6c expressed Cu and Sn elemental lines at the excited state after exposure to plasma. The electron transition at the excited state is described in Table 2, using NIST atomic spectra database [15]. Figure 6c showed typical peaks of Ni (I) at 450 nm, 465 nm, and 472 nm [ $3d^9(^2D)4p \rightarrow 3d^84s(^4F)5s$ ], while typical peaks of Cu (II) can be observed at 441 nm [ $3d^9(^2D^{5/2})4d \rightarrow 3d^9(^2D^{5/2})6p$ ], 457 nm [ $3d^9(2D)4s4p(3P^{\circ}) \rightarrow 3d^94s(3D)5s$ ], 476 nm [ $3d8(3F)4s4p(3P^{\circ}) \rightarrow 3d9(2D_{3/2})5d$ ]. In addition, typical peaks of Cu (I) can be observed at 507 nm, 516 nm, 456 nm, 521 nm, and 573 nm [ $d^9(2D)4s4p(3P^{\circ}) \rightarrow 3d^94s(3D)5s$ ], 578 nm [ $3d^94s^2 \rightarrow 3d^{10}4p$ ].

Table 2. Summary of emission lines of Sn-coated Cu and Cu<sub>90</sub>Ni<sub>10</sub> from OES spectra

Ions	Transition	Wavelength
Cu (I)	$3d^{10}4p \rightarrow 3d^{10}4d$	515 nm
	$3d^9(2D)4s4p(^3P^o) \rightarrow 3d^94s(^3D)5s$	516 nm
	$3d94s^2 \rightarrow 3d^{10}4p$	570 nm
	$3d^9(2D)4s4p(^3P^o) \rightarrow 3d^94s(^3D)5s$	507 nm
	$3d^9(2D)4s4p(^3P^o) \rightarrow 3d^94s(^3D)5s$	521 nm
	$3d^9(2D)4s4p(^3P^o) \rightarrow 3d^94s(^3D)5s$	573 nm
	$3d^94s^2 \rightarrow 3d^{10}4p$	578 nm
Cu (II)	$3d^9(2D^{5/2})4d \rightarrow 3d^9(2D^{5/2})6p$	441 nm
	$3d^9(2D)4s4p(^3P^o) \rightarrow 3d^94s(^3D)5s$	457 nm
	$3d^8(3F)4s4p(^3P^o) \rightarrow 3d^9(2D^{3/2})5d$	476 nm
	$3d^94s^2 \rightarrow 3d^9(2D)4s4p(^3P^o)$	298 nm
	$3d^9(2D)4s4p(^3P^o) \rightarrow 3d^94s(^3D)5d$	296 nm
Sn (II)	$5s^26p\ 2P^o \rightarrow 5s^26d^2D$	556 nm
	$5s^25d\ ^2D \rightarrow 5s^24f$	558 nm
	$5s^25p^2 \rightarrow 5s^25p6s$	563 nm
	$5s^25p6s \rightarrow 5s^25p4f$	575 nm
	$5s^25d\ ^2D \rightarrow 5s^24f$	579 nm
	$5s^25p^2 \rightarrow 5s^25p6s$	270 nm
	$5s^25p^2 \rightarrow 5s^25p6s$	283 nm
Ni (I)	$3d^9(^2D)4p \rightarrow 3d^84s(^4F)5s$	450 nm
	$3d^8(^3F)4s4p(^3P^o) \rightarrow 3d^84s(^4F)5s$	465 nm
	$3d^8(^3F)4s4p(^3P^o) \rightarrow 3d^84s(^4F)5s$	472 nm

It can be concluded that the introduction of Sn and Ni metals can enhance the catalytic activity of Cu under plasma treatment. In addition, it can be seen in Figure 7 that increasing the distance of the jet to the “deflection” mode leads to a significant increase in the intensity of typical peaks with an election transition to the excited state, which then increases a negligible affinity for carbon species. At this position, the surface of Sn-coated Cu and Cu<sub>90</sub>Ni<sub>10</sub> bimetallic catalysts is more catalytically activated by the stream of charged particles in plasma.

### 3.4.3. Ni-based bimetallic catalyst

Ni<sub>80</sub>Cr<sub>20</sub> is a Ni-based bimetallic catalyst and alternative to Cu-based catalysts for the fabrication of NCQD. Unlike its copper counterpart, Ni is considered a transition metal with many d-vacancies in its electron configuration [62]. They have a high negligible affinity to attract reactive carbon species into their surface

to form intermediate binding between metal-carbon [65]. In this study, Cr is introduced into Ni to form  $\text{Ni}_{80}\text{Cr}_{20}$ , where Ni accounts for 80% of the mass.

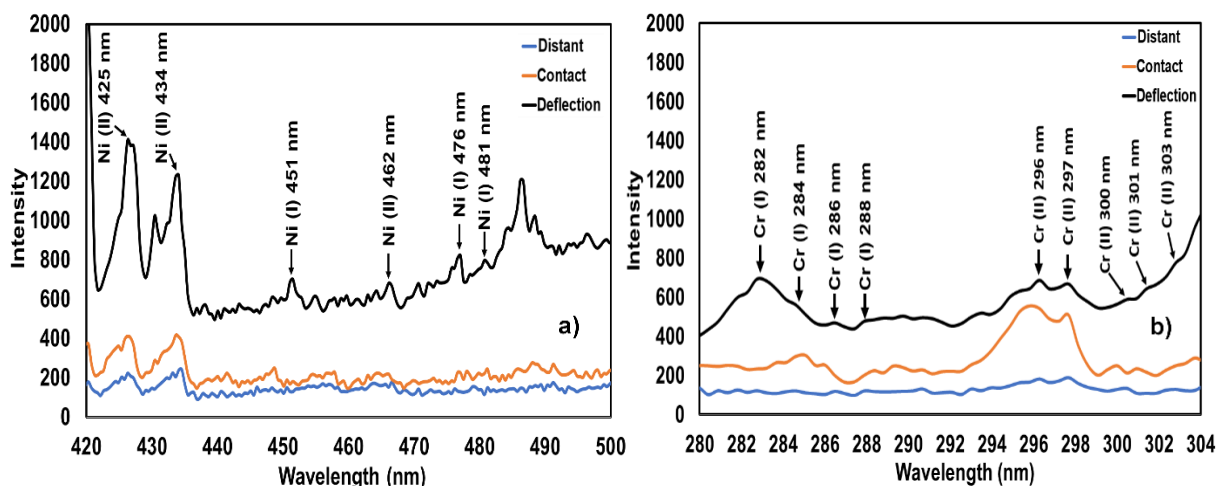


**Figure 8.** Detailed OES analysis NCQD synthesis reaction using nichrome catalyst under kINPen®IND microplasma jet at various operational modes with Ar flow rate of 2 sccm.

Elemental lines of Ni and Cr in the excited state are detected after exposure to plasma, Figure 8. The electron transition at the excited state is described in Table 3, using NIST atomic spectra database [15]. The results indicated that various strong peaks of Ni (II) at an excited state could be observed at 425 nm [ $3p^63d^72F \rightarrow 3p^63d^7\ ^2D_1$ ], 434 nm [ $3d^8(^1D)4s^2 \rightarrow 3d^8(^3F)4s4p(^3P^o)$ ], 462 nm [ $3p^63d^9\ ^2D \rightarrow 3p^63d^8(^3P)4s\ ^4P$ ]. Typical peaks of Ni (I) appeared at 451 nm, 476 nm [ $3d^9(^2D)4p \rightarrow 3d^84s(^4F)5s$ ], and 481 nm [ $3d^9(^2D)4p \rightarrow 3d^9(^2D_{3/2})4d$ ]. Typical peaks observed at 282 nm and 284 nm [ $3d^44s^2 \rightarrow 3d^5(^4F)4p$ ], 286 nm [ $3d^44s^2 \rightarrow 3d^44s4p$ ], and 288 nm [ $3d^5(^4P)4s \rightarrow 3d^5(^4F)4p$ ] represent for Cr (I) at the excited state, while peaks at 296 nm [ $3d^4(^3G)4s \rightarrow 3d^4(^3F)4p$ ], 297 nm [ $3d^4(^3H)4s \rightarrow 3d^4(^3H)4p$ ], 300 nm [ $3d^5 \rightarrow 3d^4(^3H)4p$ ], 301 nm [ $3d^4(^5D)4p \rightarrow 3d^4(^5D)5s$ ], and 303 nm [ $3d^5 \rightarrow 3d^4(^5D)4p$ ] are attributed at the excited state. In addition, as can be seen in Figure 8, the intensity of Ni (I) and Ni(II) is much higher than that of Cr (I) and Cr (II), meaning that Ni plays the main role in the catalytic activity of  $\text{Ni}_{80}\text{Cr}_{20}$ , while Cr (I) and Cr (II) is considered as a catalytic enhancer.

Table 3. Summary of elemental emission lines of  $\text{Ni}_{80}\text{Cr}_{20}$  from OES spectra

Species	Transition	Wavelength
Ni (I)	$3d^9(^2D)4p \rightarrow 3d^84s(^4F)5s$	451 nm
	$3d^9(^2D)4p \rightarrow 3d^84s(^4F)5s$	476 nm
	$3d^9(^2D)4p \rightarrow 3d^9(^2D_{3/2})4d$	481 nm

	$3p^63d^7\ ^2F \rightarrow 3p^63d^7\ ^2D_1$	425 nm
Ni (II)	$3d^8(^1D)4s^2 \rightarrow 3d^8(^3F)4s4p(^3P^o)$	434 nm
	$3d^9(^2D)4p \rightarrow 3d^8\ 4s(^4F)5s$	462 nm
Cr (I)	$3d^4\ 4s^2 \rightarrow 3d^5(^4F)4p$	282 nm
	$3d^4\ 4s^2 \rightarrow 3d^5(^4P)4p$	284 nm
	$3d^4\ 4s^2 \rightarrow 3d^4\ 4s4p$	286 nm
	$3d^5(^4P)4s \rightarrow 3d^5(^4F)4p$	288 nm
	$3d^4(^3G)4s \rightarrow 3d^4(^3F)4p$	296 nm
Cr (II)	$3d^4(^3H)4s \rightarrow 3d^4(^3H)4p$	297 nm
	$3d^5 \rightarrow 3d^4(^3H)4p$	300 nm
	$3d^4(^5D)4p \rightarrow 3d^4(^5D)5s$	301 nm
	$3d^5 \rightarrow 3d^4(^5D)4p$	303 nm

The elemental lines of Ni and Cr in the excited state indicate proficiency in d-vacancies in their electron configuration. This means that the microplasma changed the surface structure of Ni<sub>80</sub>Cr<sub>20</sub>, leading to enhanced catalytic activity.

The results in Figure 8 also indicated that the intensity of Ni and Cr increased significantly when shifting the operational modes from “distant” to “deflection”. This demonstrated that plasma enhanced catalytic activity to Ni<sub>80</sub>Cr<sub>20</sub> at “deflection” mode by bombarding an influx of electrically charged particles (electrons and ions) on this bimetallic catalyst's surface. The electrons in the surface of Ni<sub>80</sub>Cr<sub>20</sub> are excited from the ground state to form an activated surface for catalysis.

#### 3.4.4. Selection of catalysts for carbon quantum dot synthesis

It has been known that bimetallic catalysts can exhibit improvements over monometallic catalysts in various catalytic performance metrics for applications, including petrochemical processing, ammonia synthesis, and three-phase catalysis, among many others. Introducing a secondary metal atom to construct dual metallic, active sites is significantly effective in optimising the catalytic centres' adsorption–desorption behaviours. Copper-based and Ni-based bimetallic catalysts were investigated using OES analysis to select the best potential catalysts for plasma fabrication of NCQD.

In comparison with Sn-coated Cu and Cu<sub>90</sub>Ni<sub>10</sub> counterparts (Figure 7), Ni<sub>80</sub>Cr<sub>20</sub> catalysts (Figure 8) has a much higher intensity of Ni (I) and Cr (I) and Cr (II) at the excited state after exposure to microplasma with many typical sharp peaks. In particular, the intensity of Ni (I) can reach 1400 (a.u) in Ni<sub>80</sub>Cr<sub>20</sub>, while

the intensity of Cu (I) can only reach roughly 800 (a.u), meaning that the surface of  $\text{Ni}_{80}\text{Cr}_{20}$  is more catalytically activated than that of Sn coated Cu and  $\text{Cu}_{90}\text{Ni}_{10}$ . The results in Figure 8 also reflect the catalytic performance of  $\text{Ni}_{80}\text{Cr}_{20}$  compared to that of Sn-coated Cu and  $\text{Cu}_{90}\text{Ni}_{10}$ . This result is also in agreement with electric potential calculations in section 3.4.1 that is more active in terms of electrochemistry.

### 3.5. Thermal analysis of the plasma-catalysis system

Thermal imaging of the fabrication reactors was conducted to understand better how plasma influences heat transfer. Figure 9 shows thermal imaging of the plasma jet, plasma- $\text{Ni}_{80}\text{Cr}_{20}$  interaction and plasma-liquid- $\text{Ni}_{80}\text{Cr}_{20}$  interaction. Reuter et al. reported that the nonthermal kINPen<sup>®</sup>IND is pen-sized and can be held like a scalpel or pencil [66]. Its low gas temperature of less than 40 °C and highly reactive non-equilibrium chemistry [66].

The results in Figure 9a indicate that the plasma temperature in the kINPen<sup>®</sup>IND jet is about 28 °C, meaning the plasma is nonthermal. The temperature changes when interacting with liquid and metal catalysts were also investigated. Figure 9b shows that the temperature in the reactor increases up to about 37 °C. This means that the plasma- $\text{Ni}_{80}\text{Cr}_{20}$  interaction induces a thermal effect in the system. The plasma stream of particles (ionised gas, electron, etc.) with high-energy photons continuously bombards the surface of  $\text{Ni}_{80}\text{Cr}_{20}$  [43]. The electrons at the plasma- $\text{Ni}_{80}\text{Cr}_{20}$  interface absorb the energy from the plasma to a higher level (excited state) [67]. These excited electrons return to the ground state and emit the emission light [67], which is recorded by the OES spectroscopy, Figure 8 in section 3.3.2. Along with the emission being emitted, the extra energy was released as a heat [43].

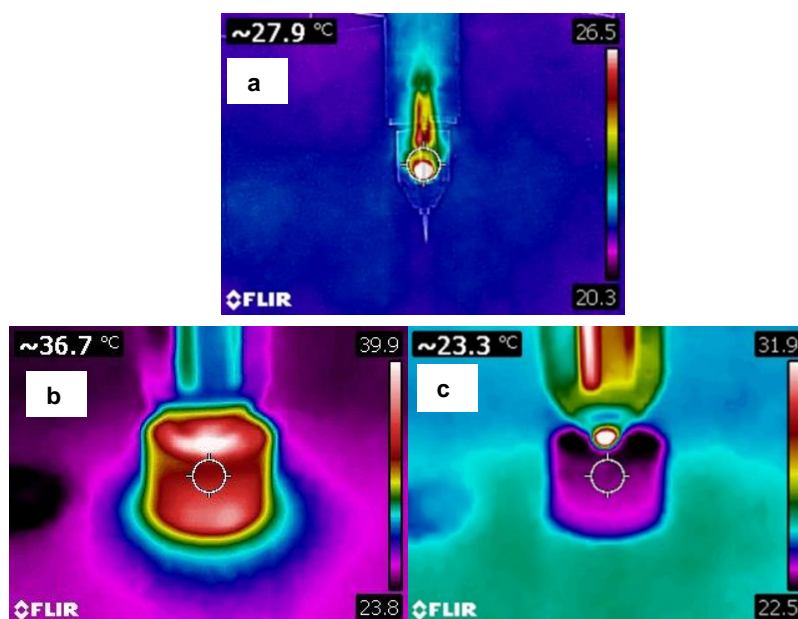


**Figure 9.** Thermal imaging of (a) pure plasma, (b) plasma- $\text{Ni}_{80}\text{Cr}_{20}$  interaction, (c) plasma-liquid- $\text{Ni}_{80}\text{Cr}_{20}$  interaction

However, the temperature of the plasma-Ni<sub>80</sub>Cr<sub>20</sub> interaction drops significantly to about 23 °C when the folic acid solution (as liquid) is added to the system (Figure 9c). Heat and mass transfer occur at the plasma-liquid-Ni<sub>80</sub>Cr<sub>20</sub> interface, causing the water evaporation process. Evaporation is an endothermic process decreasing the temperature [68].

### 3.6. Mechanism of plasma-liquid-catalysts synthesis of N-doped quantum dots

This study proposes a mechanism of the synthesis reaction of N-doped quantum dots in the plasma-liquid-catalyst system (Figure 10) based on the OES analysis and surface profile study provided in this manuscript. In the plasma catalysis [69], plasma affects the energy barrier of the reaction in synergy with the catalyst, thus changing the catalytic activity [27].

#### 3.6.1. Our results summary

The following results led us to propose the reaction mechanism.

- (1) A previous study demonstrated the presence of plasma catalysis, i.e. a higher conversion in the presence of a catalyst next to the plasma (reaction intensification) [69].
- (2) This study identified the flow rate for delivery of maximal argon ion, Ar<sup>+</sup> concentration, which are formed in the gas phase. We found that Ar<sup>+</sup> generates secondary reactive species at the plasma-water interface, and O<sup>+</sup> and O.H.\* were detected.
- (3) The formation is maximal in the 'deflection case' with the liquid layer thinned much, facilitating the transport of the Vitamin B9 precursor to the plasma-liquid surface as well as to the catalyst and the contact of the plasma with the catalyst.
- (4) The best catalyst was identified, meaning the right metals and their right dual composition to set the best electric potential.
- (5) Metal reactive species were also detected in the gas phase near the liquid surface; it is unclear if they play a role in the catalysis of the reaction or signal that the plasma-catalysis is intense (as a signal effect, yet of no relevance to the reaction). If these catalyse the reaction, a homogeneous pathway is opened beside the known heterogeneous one.

#### 3.6.2. Literature results summary

We add to our findings relevant knowledge from plasma-multiphase literature.

- (1) It has been reported that charged ions and particles can penetrate through a plasma-liquid interface [43], as the potential energy of positive and negatively charged particles is larger than the surface tension energy [43]. Charged particles (Ar<sup>+</sup>, N<sub>2</sub><sup>+</sup>, O<sup>+</sup>, e<sup>-</sup>, etc.) are immediately hydrated when striking the liquid [70].

- (2) Plasma is known for causing atomic abrasion of the surface of metal catalysts [71]. Photon, electron and ion deposition induces surface charging ( $\text{Ni}^{2+}$  and  $\text{Ni}^+$ ) to attract more water molecules to form a hydrate complex.
- (3) Water molecules absorb the UV energy photons to release more  $\text{OH}\cdot$  reactive species, leading to intensification of reactive species in the liquid.

### *3.6.3. Deduction of reaction mechanism from own results and literature*

Based on these experimental demonstrations and literature reports, seven steps are hypothesis for the mechanism of the plasma-catalytic Vitamin-B9 reaction.

- (1) Creation of excited species from plasma gas and water solvent.
- (2) Atomic abrasion of the metal surface of  $\text{Ni}_{80}\text{Cr}_{20}$  catalysts.
- (3) Mass transport of excited species ( $\text{Ar}^+$ ,  $\text{N}_2^+$ ,  $\text{O}^+$ , etc.) through the plasma-liquid interface and into the liquid film.
- (4) Ionisation on the surface of catalyst to form charged surface.
- (5) Nickel ions attracts water molecules to form a hydrate complex
- (6) Water molecules absorb the UV energy photons to release  $\text{OH}\cdot$  reactive species, leading to intensification of reactive species in the liquid.
- (7)  $\text{Ar}^+$ ,  $\text{N}_2^+$ ,  $\text{O}^+$  along with  $\text{OH}\cdot$  reactive species decompose folic acid to form N-doped carbon quantum dots.

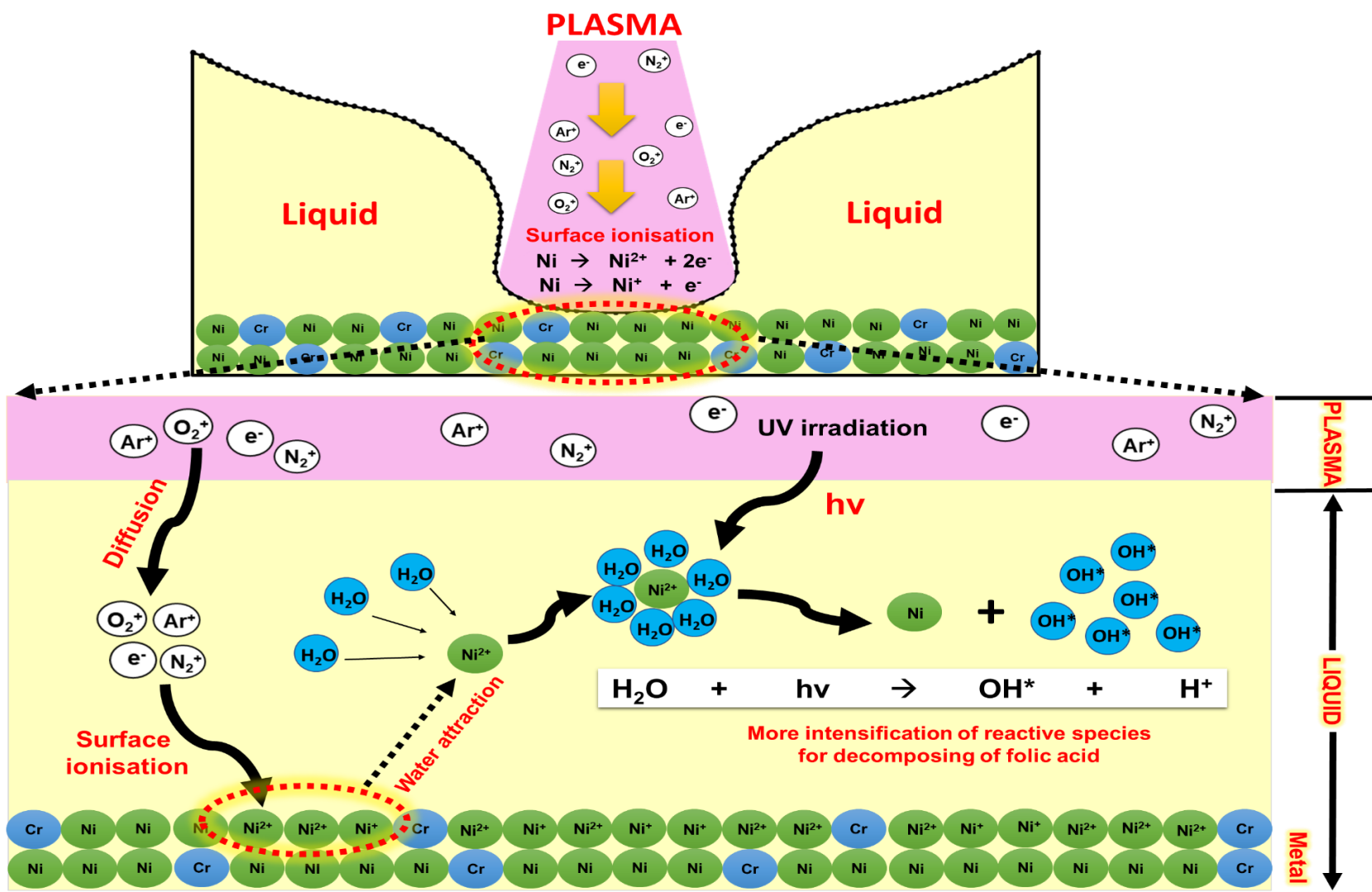


Figure 12. Proposed mechanism of plasma-liquid-catalyst synthesis of N-doped carbon quantum dots



### 4. Conclusions

The process of multiphase plasma catalysis, in this study, is utilized to synthesise N-doped carbon quantum dots. This is achieved by directing a submerged plasma jet into a small amount of liquid that contains the precursor and catalytic alloy flakes. Optical emission spectroscopy was used to observe and analyse the reaction mechanism, focusing on the role of plasma catalysis. The depth of the plasma jet's penetration affects the interaction with the liquid and catalyst in a typical hydrodynamic manner. The deepest penetration, referred to as the "deflection mode," produced more positively charged species from the metal catalyst. Among the three alloy catalysts examined, Ni<sub>80</sub>Cr<sub>20</sub> showed the strongest effect, which correlated with the highest electric potential. There are seven main steps in the proposed reaction mechanism leading to the production of N-doped Quantum Dots. IR imaging indicated that the temperature at the plasma-liquid-catalyst interface was below 25 °C, although significant water evaporation occurred at the surface due to high convective phases.

### 5. Outlook

Therefore, we could conduct a comprehensive chemical engineering study, focusing on plasma catalysis reaction, electro-plasma chemistry, thermal properties of reaction, heat mass transfer, and fluid mechanics in the way of traditional reactor engineering and process design. We added the point of view of using catalysts for the plasma synthesis of NCQD, followed by the concept of using OES analysis for a simple and quick characterisation of the reaction. We proposed a mechanism of plasma-liquid-catalysts synthesis of N-doped quantum dots for the first time, which will open a new window in the synthesis of NCQD at the plasma-liquid-catalyst (solid) interface.

### *Credit authorship contribution statement*

**Quoc Hue Pho:** Conceptualization, Methodology, Formal analysis, Investigation, Data curation, Writing – original draft. **Quan Hoang Tran, Changping Zhuang, Van Long Nguyen:** Investigation, Data curation. **Nam Nghiep Tran, Evgeny V. Rebrov:** Writing – review & editing. **Thanh Tung Tran:** Conceptualization, Writing- Review and Editing. **Dusan Losic:** Writing – review & editing, Supervision. **Zdenko Machala:** Formal analysis, Data curation. **Volker Hessel:** Conceptualization, Writing – review & editing, Supervision.

### *Conflict of Interest*

The authors declare that they have no conflict of interest.

### **Acknowledgements**

Mr. Hue Quoc Pho received the divisional ECMS and full-fee scholarships from the University of Adelaide, Australia. The authors acknowledge support from the ERC Grant Surface-Confined fast-modulated Plasma for process and Energy intensification (SCOPE) from the European Commission with grant number 810182.

### References

1. Döring, A., E. Ushakova, and A.L. Rogach, *Chiral carbon dots: synthesis, optical properties, and emerging applications*. Light: Science & Applications, 2022. **11**(1): p. 1-23.
2. Li, S., et al., *The development of carbon dots: From the perspective of materials chemistry*. Materials Today, 2021. **51**: p. 188-207.
3. Wang, B. and S. Lu, *The light of carbon dots: From mechanism to applications*. Matter, 2022. **5**(1): p. 110-149.
4. Beckers, S., S. Peil, and F.R. Wurm, *Pesticide-Loaded Nanocarriers from Lignin Sulfonates—A Promising Tool for Sustainable Plant Protection*. ACS Sustainable Chemistry & Engineering, 2020. **8**(50): p. 18468-18475.
5. Tran, N.N., et al., *Nanofertilizers and Nanopesticides for Crop Growth*, in *Plant and Nanoparticles*, J.-T. Chen, Editor. 2022, Springer Nature Singapore: Singapore. p. 367-394.
6. Li, X., et al., *Review on Structures of Pesticide Targets*. Int J Mol Sci, 2020. **21**(19).
7. Shivashakarappa, K., et al., *Nanotechnology for the detection of plant pathogens*. Plant Nano Biology, 2022. **2**: p. 100018.
8. Lowry, G.V., A. Avellan, and L.M. Gilbertson, *Opportunities and challenges for nanotechnology in the agri-tech revolution*. Nature nanotechnology, 2019. **14**(6): p. 517-522.
9. Pho, Q.H., et al., *Perspectives on plasma-assisted synthesis of N-doped nanoparticles as nanopesticides for pest control in crops*. Reaction Chemistry & Engineering, 2020. **5**(8): p. 1374-1396.
10. Omar, N.A.S., et al., *A Review on Carbon Dots: Synthesis, Characterization and Its Application in Optical Sensor for Environmental Monitoring*. Nanomaterials (Basel), 2022. **12**(14).
11. Kaczmarek, A., et al., *Luminescent Carbon Dots Synthesized by the Laser Ablation of Graphite in Polyethylenimine and Ethylenediamine*. Materials (Basel), 2021. **14**(4).
12. Chao-Mujica, F., et al., *Carbon quantum dots by submerged arc discharge in water: Synthesis, characterization, and mechanism of formation*. Journal of Applied Physics, 2021. **129**(16): p. 163301.
13. Zhu, Z., et al., *One-pot hydrothermal synthesis of fluorescent carbon quantum dots with tunable emission color for application in electroluminescence detection of dopamine*. Biosensors and Bioelectronics: X, 2022. **10**: p. 100141.
14. Otten, M., et al., *Pyrolysis and Solvothermal Synthesis for Carbon Dots: Role of Purification and Molecular Fluorophores*. Langmuir, 2022. **38**(19): p. 6148-6157.
15. Zhang, D., et al., *One-Step Green Solvothermal Synthesis of Full-Color Carbon Quantum Dots Based on a Doping Strategy*. The Journal of Physical Chemistry Letters, 2021. **12**(37): p. 8939-8946.

16. Xu, J., et al., *Ultrasonic-Assisted Synthesis of N-Doped, Multicolor Carbon Dots toward Fluorescent Inks, Fluorescence Sensors, and Logic Gate Operations*. *Nanomaterials* (Basel), 2022. **12**(3).
17. Pho, Q.H., et al., *Survey of Synthesis Processes for N-Doped Carbon Dots Assessed by Green Chemistry and Circular and EcoScale Metrics*. *ACS Sustainable Chemistry & Engineering*, 2021. **9**(13): p. 4755-4770.
18. Pho, Q.H., et al., *Process intensification for gram-scale synthesis of N-doped carbon quantum dots immersing a microplasma jet in a gas-liquid reactor*. *Chemical Engineering Journal*, 2023. **452**: p. 139164.
19. Taheraslani, M. and H. Gardeniers, *Plasma Catalytic Conversion of CH<sub>4</sub> to Alkanes, Olefins and H<sub>2</sub> in a Packed Bed DBD Reactor*. *Processes*, 2020. **8**(7): p. 774.
20. Zhang, Y., et al., *Plasma-coupled catalysis in VOCs removal and CO<sub>2</sub> conversion: Efficiency enhancement and synergistic mechanism*. *Catalysis Communications*, 2022. **172**: p. 106535.
21. Chang, T., et al., *A critical review on plasma-catalytic removal of VOCs: Catalyst development, process parameters and synergetic reaction mechanism*. *Science of The Total Environment*, 2022. **828**: p. 154290.
22. Meng, S., et al., *Nonthermal Plasma-Assisted Photocatalytic Conversion of Simulated Natural Gas for High-Quality Gasoline Production near Ambient Conditions*. *The Journal of Physical Chemistry Letters*, 2020. **11**(10): p. 3877-3881.
23. Ahmad, F., et al., *Low-Temperature CO<sub>2</sub> Methanation: Synergistic Effects in Plasma-Ni Hybrid Catalytic System*. *ACS Sustainable Chemistry & Engineering*, 2020. **8**(4): p. 1888-1898.
24. Szymanski, L., et al., *Synthesis of Carbon Nanotubes in Thermal Plasma Reactor at Atmospheric Pressure*. *Nanomaterials* (Basel), 2017. **7**(2).
25. Yanase, T., et al., *Synthesis of Carbon Nanotubes by Plasma-Enhanced Chemical Vapor Deposition Using Fe<sub>1-x</sub>MnxO Nanoparticles as Catalysts: How Does the Catalytic Activity of Graphitization Affect the Yields and Morphology?* *C*, 2019. **5**(3): p. 46.
26. Li, D., L. Tong, and B. Gao, *Synthesis of Multiwalled Carbon Nanotubes on Stainless Steel by Atmospheric Pressure Microwave Plasma Chemical Vapor Deposition*. *Applied Sciences*, 2020. **10**(13): p. 4468.
27. Neyts, E.C., et al., *Plasma Catalysis: Synergistic Effects at the Nanoscale*. *Chemical Reviews*, 2015. **115**(24): p. 13408-13446.
28. Dey, A., et al., *Ultrafast epitaxial growth of CuO nanowires using atmospheric pressure plasma with enhanced electrocatalytic and photocatalytic activities*. *Nano Select*, 2022. **3**(3): p. 627-642.
29. Joshi, E., et al., *Formation of droplets in weightless complex plasmas*. *Contributions to Plasma Physics*, 2021. **61**(10): p. e202100081.

30. Xiong, H. and W. Sun, *Investigation of Droplet Atomization and Evaporation in Solution Precursor Plasma Spray Coating*. Coatings, 2017. **7**(11): p. 207.
31. Botton, R., et al. *A simple gas-liquid mass transfer jet system*. in *8th World Congress of Chemical Engineering*. 2009.
32. Botes, F., L. Lorenzen, and J. Van Deventer, *The development of high intensity gas-liquid jet reactors*. Chemical Engineering Communications, 1998. **170**(1): p. 217-244.
33. CambiØ, D., et al., *2 3 4 5 6 7 8 9 T. No l*. Chem. Rev, 2016. **116**: p. 10276-10341.
34. Billaud, E.M.F., et al., *Micro-flow photosynthesis of new dienophiles for inverse-electron-demand Diels-Alder reactions. Potential applications for pretargeted in vivo PET imaging*. Chemical Science, 2017. **8**(2): p. 1251-1258.
35. Lin, L., et al., *Microfluidic plasmas: Novel technique for chemistry and chemical engineering*. Chemical Engineering Journal, 2021. **417**: p. 129355.
36. Lin, L., et al., *Microfluidic fabrication of fluorescent nanomaterials: A review*. Chemical Engineering Journal, 2021. **425**: p. 131511.
37. Serra, C.A., et al., *Microfluidic Production of Micro- and Nanoparticles*, in *Encyclopedia of Polymer Science and Technology*.
38. Arkar, K., et al., *Dynamics of active Brownian particles in plasma*. Molecules, 2021. **26**(3): p. 561.
39. Lee, N. and S. Wiegand, *Thermophoretic micron-scale devices: practical approach and review*. Entropy, 2020. **22**(9): p. 950.
40. Aadim, K.A., et al. *Influence of Gas Flow Rate on Plasma Parameters Produced by a Plasma Jet and its Spectroscopic Diagnosis Using the OES Technique*. in *IOP Conference Series: Materials Science and Engineering*. 2020. IOP Publishing.
41. Shui, L., J.C.T. Eijkel, and A. van den Berg, *Multiphase flow in microfluidic systems – Control and applications of droplets and interfaces*. Advances in Colloid and Interface Science, 2007. **133**(1): p. 35-49.
42. Bruggeman, P.J., et al., *Plasma-liquid interactions: a review and roadmap*. Plasma Sources Science and Technology, 2016. **25**(5): p. 053002.
43. Bruggeman, P., et al., *Plasma-liquid interactions: a review and roadmap*. Plasma sources science and technology, 2016. **25**(5): p. 053002.
44. Nikiforov, A.Y., *Plasma sputtering of water molecules from the liquid phase by low-energy ions: Molecular dynamics simulation*. High Energy Chemistry, 2008. **42**(3): p. 235-239.
45. Thompson, L., *LK Doraiswamy, "Sonochemistry*. Science and engineering" Ind. Eng. Chem. Res, 1999. **38**(4): p. 1215-1249.

46. Zeleny, J., *Instability of electrified liquid surfaces*. Physical review, 1917. **10**(1): p. 1.
47. Melcher, J.R. and C.V. Smith, *Electrohydrodynamic charge relaxation and interfacial perpendicular-field instability*. The Physics of Fluids, 1969. **12**(4): p. 778-790.
48. Watson, P., *Electrostatic and hydrodynamic effects in the electrical breakdown of liquid dielectrics*. IEEE Transactions on Electrical Insulation, 1985(2): p. 395-399.
49. Sugimoto, T. and Y. Higashiyama, *Production of water drops and corona due to rupture of air bubbles at water surface under a positive dc electric field*. Journal of Electrostatics, 2001. **53**(3): p. 209-219.
50. Hase, M., S.N. Watanabe, and K. Yoshikawa, *Rhythmic motion of a droplet under a dc electric field*. Physical Review E, 2006. **74**(4): p. 046301.
51. Bruggeman, P., et al., *Water surface deformation in strong electrical fields and its influence on electrical breakdown in a metal pin–water electrode system*. Journal of Physics D: Applied Physics, 2007. **40**(16): p. 4779.
52. Guo, Z.-Y., H.-Y. Zhu, and X.-G. Liang, *Entransy—A physical quantity describing heat transfer ability*. International Journal of Heat and Mass Transfer, 2007. **50**(13-14): p. 2545-2556.
53. Qin, F. and W. Chen, *Copper-based single-atom alloys for heterogeneous catalysis*. Chemical Communications, 2021. **57**(22): p. 2710-2723.
54. Ray, D., S. Ghosh, and A.K. Tiwari, *Controlling Heterogeneous Catalysis of Water Dissociation Using Cu–Ni Bimetallic Alloy Surfaces: A Quantum Dynamics Study*. The Journal of Physical Chemistry A, 2018. **122**(26): p. 5698-5709.
55. Kruszka, B., et al., *Synthesis of carbon nanotubes and nanotube forests on copper catalyst*. Materials Research Express, 2014. **1**(3): p. 035040.
56. Atthipalli, G., et al., *Nickel catalyst-assisted vertical growth of dense carbon nanotube forests on bulk copper*. The Journal of Physical Chemistry C, 2011. **115**(9): p. 3534-3538.
57. Li, Y., et al., *How catalysts affect the growth of single-walled carbon nanotubes on substrates*. Advanced Materials, 2010. **22**(13): p. 1508-1515.
58. Ji, Y., A. Guan, and G. Zheng, *Copper-based catalysts for electrochemical carbon monoxide reduction*. Cell Reports Physical Science, 2022. **3**(10): p. 101072.
59. Aflak, N., et al., *Recent Advances in Copper-Based Solid Heterogeneous Catalysts for Azide–Alkyne Cycloaddition Reactions*. International Journal of Molecular Sciences, 2022. **23**(4): p. 2383.
60. Kramida, A., et al., *NIST Atomic Spectra Database (Version 5.8) 2020*. National Institute of Standards and Technology: Gaithersburg, MD, USA, 2020.

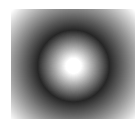
61. Sarfraz, S., et al., *Cu–Sn Bimetallic Catalyst for Selective Aqueous Electroreduction of CO<sub>2</sub> to CO*. ACS Catalysis, 2016. **6**(5): p. 2842-2851.
62. Jourdain, V. and C. Bichara, *Current understanding of the growth of carbon nanotubes in catalytic chemical vapour deposition*. Carbon, 2013. **58**: p. 2-39.
63. Meloni, E., M. Martino, and V. Palma, *A Short Review on Ni Based Catalysts and Related Engineering Issues for Methane Steam Reforming*. Catalysts, 2020. **10**(3): p. 352.
64. Oshchepkov, A.G., et al., *Recent Advances in the Understanding of Nickel-Based Catalysts for the Oxidation of Hydrogen-Containing Fuels in Alkaline Media*. ACS Catalysis, 2020. **10**(13): p. 7043-7068.
65. Zhu, M., et al., *Vacancy engineering of the nickel-based catalysts for enhanced CO<sub>2</sub> methanation*. Applied Catalysis B: Environmental, 2021. **282**: p. 119561.
66. Reuter, S., T. Von Woedtke, and K.-D. Weltmann, *The kINPen—A review on physics and chemistry of the atmospheric pressure plasma jet and its applications*. Journal of Physics D: Applied Physics, 2018. **51**(23): p. 233001.
67. Dorfs, D., et al., *Comprehensive Nanoscience and Technology (2011)*. Ch. **1**: p. 219.
68. Kim, Y., et al., *Novel mechanical vapor recompression-assisted evaporation process for improving energy efficiency in pulp and paper industry*. International Journal of Energy Research, 2022. **46**(3): p. 3409-3427.
69. Yan, C., et al., *Recent Advances in Plasma Catalysis*. The Journal of Physical Chemistry C, 2022. **126**(23): p. 9611-9614.
70. Gaisin, A.F. and E.E.e. Son, *Vapor-air discharges between Jet electrolytic cathode and metal anode at low pressure*. Teplofizika vysokikh temperatur, 2010. **48**(3): p. 470-472.
71. Hartl, H., et al., *Multiscale Plasma-Catalytic On-Surface Assembly*. Small, 2020. **16**(12): p. 1903184.

**BLANK PAGE**



# Chapter 7

## Stagnant Liquid Layer as “Microreaction System” in Submerged Plasma Micro-Jet



---

**T**his chapter aims to intensify reactivity via bespoke transient hydrodynamics in a plasma-activated three-phase catalyst system. In this hydrodynamic regime, plasma can penetrate the catalyst bed via the stagnant thin liquid film and polarise the plasma-liquid interface. Evidence for the effectivity of the new process regime is the determination of the enlargement of the reaction rate by increasing liquid component diffusivity towards the catalyst bed via reducing the solvent's viscosity.

This chapter has been prepared as a research paper manuscript and supposed to be submitted to “Chemical Engineering Journal” as follows:


**Pho, Q.H.**, Hessel, V., Rebrov, E.V., Lamichhane, P., Tran, N.N., and Losic, D., 2023. Stagnant Liquid Layer as “Microreaction System” in Submerged Plasma Micro-Jet for Formation of Carbon Quantum Dots. Chemical Engineering Journal. (Submitted).

---

# Statement of Authorship

Title of Paper	Stagnant Liquid Layer as “Microreaction System” in Submerged Plasma Micro-Jet for Formation of Carbon Quantum Dots
Publication Status	<input type="checkbox"/> Published <input type="checkbox"/> Accepted for Publication <input checked="" type="checkbox"/> Submitted for Publication <input type="checkbox"/> Unpublished and Unsubmitted work written in manuscript style
Publication Details	<b>Pho, Q.H.</b> , Hessel, V., Rebrov, E.V., Lamichhane, P., Tran, N.N., and Losic, D., 2023. Stagnant Liquid Layer as “Microreaction System” in Submerged Plasma Micro-Jet for Formation of Carbon Quantum Dots. Chemical Engineering Journal. <b>(Submitted)</b> .

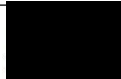
## Principal Author


Name of Principal Author (Candidate)	Quoc Hue Pho
Contribution to the Paper	Conceptualization, Methodology, Formal analysis, Investigation, Data curation, Writing – original draft
Overall percentage (%)	65%
Certification:	This paper reports on original research I conducted during the period of my Higher Degree by Research candidature and is not subject to any obligations or contractual agreements with a third party that would constrain its inclusion in this thesis. I am the primary author of this paper.
Signature	 Date 28.01.2023

## Co-Author Contributions

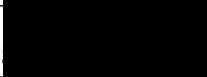
By signing the Statement of Authorship, each author certifies that:


- i. the candidate’s stated contribution to the publication is accurate (as detailed above);
- ii. permission is granted for the candidate to include the publication in the thesis; and
- iii. the sum of all co-author contributions is equal to 100% less the candidate’s stated contribution.


Name of Co-Author	Evgeny V. Rebrov
Contribution to the Paper	Conceptualization, Data curation, Writing – review & editing, Supervision.
Signature	 Date 08.02.2023

Name of Co-Author	Nam Nghiep Tran
Contribution to the Paper	Conceptualization, Writing- Review and Editing.
Signature	 Date 28.01.2023

Please cut and paste additional co-author panels here as required.

Name of Co-Author	Dusan Losic		
Contribution to the Paper	Co-supervised and Writing- Review and Editing		
Signature		Date	08.02.2023

Name of Co-Author	Pradeep Lamichhane		
Contribution to the Paper	Conceptualization, Writing- Review and Editing.		
Signature	 on behalf of co-author	Date	08.02.2023

Name of Co-Author	Volker Hessel		
Contribution to the Paper	Supervised ((scientific ideas, concepts, objectives, assessment of achievement degree, societal impact), Conceptualised, Writing – review & editing, and is the corresponding author.		
Signature		Date	28.01.2023

## Stagnant Liquid Layer as “Microreaction System” in Submerged Plasma Micro-Jet for Formation of Carbon Quantum Dots

Quoc Hue Pho<sup>a, c\*</sup>, Volker Hessel<sup>a, c\*\*,</sup>, Evgeny V. Rebrov<sup>c, d</sup>, Pradeep Lamichhane<sup>b</sup>, Nam Nghiep Tran<sup>a</sup>,  
Dusan Losic<sup>a, b</sup>

<sup>a</sup> School of Chemical Engineering, The University of Adelaide, Adelaide, SA 5005, Australia

<sup>b</sup> The A.R.C. Graphene Research Hub, School of Chemical Engineering and Advanced Materials, The University of Adelaide, SA 5005, Australia

<sup>c</sup> School of Engineering, University of Warwick, Library Rd, Coventry CV4 7AL, England, UK

<sup>d</sup> Department of Chemical Engineering and Chemistry, Eindhoven University of Technology, P.O. Box 513, 5600 MB, Eindhoven, the Netherlands

\* First author

\*\* Corresponding author: E-mail: volker.hessel@adelaide.edu.au

### Abstract

Reaction kinetics play a critical role in many chemical reactions and are essential for the cost and environmental profile of processes derived from the reactions. This study aims to intensify reactivity *via* bespoke transient hydrodynamics in a plasma-activated three-phase catalyst system. Likewise, three-phase plasma systems in literature are not well designed, understood and commercially available. The synthesised N-doped carbon quantum dots, with application as fertilisers and wastewater treatment was evaluated as a model reaction. We used a commercial plasma system generating a plasma microjet, creating an almost flat, large interface covering a thin stagnant liquid layer with a catalyst bed underneath. In this hydrodynamic regime, plasma can penetrate the catalyst bed *via* the stagnant thin liquid film and polarise the plasma-liquid interface. Evidence for the effectivity of the new process regime is the determination of the enlargement of the reaction rate by increasing liquid component diffusivity towards the catalyst bed via reducing the solvent's viscosity. The results show that the reaction rate is also determined by the interfacial area below the crater rather than the total gas-liquid interfacial area. The plasma process can compete energy-wise with the best dielectric barrier discharge (DBD) plasma processes and consumes lower energy than microfluidic processing in chemical microreactors. The high momentum transfer from the plasma jet to the liquid causes partial evaporation of volatile additives, other than water, which has to be considered in process design and reduced.

**Keywords:** plasma three-phase system, N-doped carbon quantum dots, reaction rate, kinetics, diffusivity-limited.

### 1. Introduction

Alike for highly productive chemical microreactors, applying process intensification principles to small plasma-chemical reaction volumes is essential to amplify productivity. On that backdrop, this submerged plasma jet study reports deciphering the engineering fundamentals of how to enhance mass transport and facilitate catalysis via a metal particle bed of alloy particles to increase reaction rate; beyond the performance achieved in [1]. Leverage is provided *via* bespoke hydrodynamics when penetrating the jet deeper into the reactor volume, displacing the liquid and demonstrating a massive increase in productivity [1]. Depending on the jet penetration into the liquid medium depth, different crater configurations (distant, contact, deflection) form in the liquid, each with different hydrodynamics. Leverage is also provided *via* the achievement of a gas (plasma)–liquid–solid three-phase contact for facilitating catalysis, for which a mechanism was proposed based on excited state analytics using optical emission spectroscopy [2].

Reaction kinetics is critical in chemical and biochemical processes [3, 4]. Hydrodynamics must be tailored to enable the 'best' intrinsic kinetics rather than leading to effective kinetics of reduced effectiveness. Learning can be taken from the principles of high-intensity gas–liquid two-phase reactors [5]. Applications of plasma jet reactors exposed to liquid media have been reported for applications, including wastewater treatment [6] and nanoparticle synthesis [7]; yet their engineering and hydrodynamic principles have not been explored in detail. Previous studies demonstrated that evaporation plays a key role in plasma-liquid systems which motivated the evaporation investigation reported herein [8, 9].

This study varies physico-chemical parameters of the liquid phase to study the hydrodynamics and mass transport, in the absence or in the presence of a catalyst bed of alloy flakes. With the latter, it is determined whether charging effect of the bottom layer by charged plasma species could play an additional role to accelerate the reaction kinetics. A commercial plasma equipment enables facile experimentation, the KINPen®IND reactor, providing a cold atmospheric-pressure microplasma jet with noble gases such as argon [10, 11]. This microplasma jet reactor has attracted considerable literature studies and documentation [5, 12, 13].

As test reaction we selected the formation of carbon quantum dots (CQDs), a recently discovered "zero-dimensional" carbon nanomaterial [14-17], which have applications in various fields such as agriculture [18, 19], environment [20, 21], biology [22, 23], chemistry [24], food science [25, 26], and

energy [27-30]. This is due to their favourable properties, such as low toxicity [31], intense luminescence [32], chemical stability [33], biocompatibility [34], and high specific surface area [35]. Extensive research studies on N-doped carbon quantum dots (NCQDs) have been conducted, reporting a large number of diverse structures of this nanomaterial class with distinct properties, made via various synthetic techniques such as pyrolysis [36], hydrothermal [37], solvothermal [38], microwave [39], chemical vapor deposition [40], electrochemical method [41], high-temperature combustion [42], etc.

A challenge still is the capacity for pilot or industrial production of these materials and how to fill this technology gap [43]; this paper explores fundamentals to transition. A techno-sustainability assessment compared six methods for producing NCQDs, with plasma synthesis having the highest energy efficiency but the lowest mass efficiency, resulting in lower productivity compared to the other processes; the latter being also due to the fact those processes are typically conducted in larger reactors. The approach of this study is to use a small reactor that can be numbered up, with high volume-specific productivity, both because of high mass and energy efficiency [44]. This submerged plasma microjet was previously shown to reach gram productivities in a few hours [1], compared to the best reactors in the field [43].

The goal of this study is to understand how the interface between the plasma and the liquid is deformed and how that might be utilised to increase mass transport. The latter effect is monitored via the NCQDs forming reaction rate (without presence of catalyst). In particular, the effect of diffusivity of the liquid reactant on the reaction rate is studied by changing the liquid viscosity. The effect of other physical parameters is also investigated, including density, polarity, and surface tension; in pure form and as combined effect. With that understanding, a fixed bed is placed on the floor of the reaction vessel, and operated in a mode that the bed is fully wetted and not dried out by the impinging plasma microjet. When using metal flakes as bed, the goal is to check for catalytic activity. In addition, the extent of evaporation of the liquid component is investigated, as Bruggeman et al. reported that evaporation plays a key role in plasma-liquid two-phase systems. We add volatile components to change the physico-chemical parameters of the liquid phase [45].

## 2. Methodology

### 2.1. Experimental setup

Our experimental design is based on the idea of high-intensity gas-liquid reactors that are equipped with forceful gas jets, which are known to enhance phase mixing [46]. We used a  $16\text{ m s}^{-1}$  downward vertical plasma jet that enters a small reactor volume via a nozzle with a diameter of 1.6 mm and after reaching the bottom it turns and moves in the upward direction along the gas-liquid interface. The plasma stream forms a crater in the liquid, resulting in a highly turbulent movement of liquid inside the reactor volume due to

gas to liquid momentum transfer. In addition, the creation and collapse of gas bubbles in the liquid enhances the mass transport between the two phases.

Another high-intensity gas-liquid reactor design includes a pump, an orifice, a vertical tube aligned with the orifice, and a baffle plate [46]. The pump produces a downward vertical jet of liquid through the orifice, generating a gas-liquid dispersion in the tube. The two-phase jet is directed onto a baffle near the bottom of the tank, distributing it throughout the liquid. The liquid is then collected and recycled under the baffle plate. Simplification of the high-intensity gas-liquid reactor concepts is required in our experimental design. The existence of the plasma phase over long distances is not achievable and poses a challenge. Instead, a micro-plasma jet aimed at the liquid is utilised, Figure 1. The flow feedback for repeated gas-liquid interactions is also withheld, as the fundamental nature of the process intensification is better demonstrated through single contact [46].

The experimental synthesis process and reactor configuration were taken, as reported in previous studies [1]. The synthesis reactor was comprised of two parts, a kINPen®IND microplasma jet (Neoplas GmbH, Germany), and a cylindrical glass reactor with a diameter of 15 mm, designed and manufactured in-house. An argon (99.9 vol.%) was fed via the nozzle with a mean velocity of  $16 \text{ m s}^{-1}$ . The jet length was 1 cm.

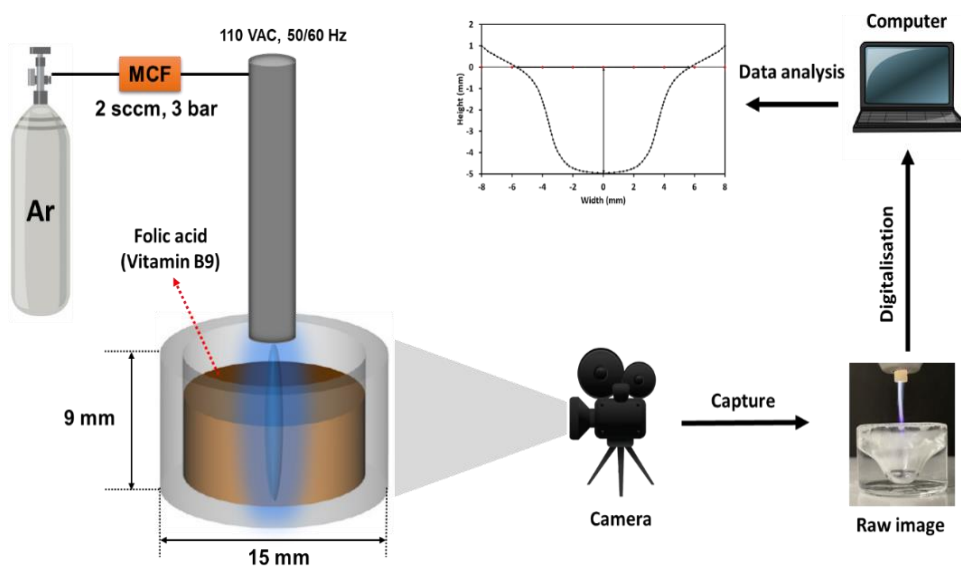


Fig. 1 Experimental setup with plasma-liquid reactor and interfacial profile analytics.

## 2.2. Physical parameter variation of the liquid reaction medium

In order to understand the influence of gas-liquid interfacial area and the diffusivity of the liquid reactant on the reaction rate, several solvents with different viscosity and surface tension were used as listed in Table 1.

Table 1. Physical parameters of solvents used.

Samples	Properties	
	Density (kg/m <sup>3</sup> )	Viscosity (mPa.s)
Water	997	1.002
Glycerol	1258	1011
Water with sodium oleate, C.M.C. = 10 <sup>-3</sup> mol L <sup>-1</sup>	997	1.01
Ethanol	785	1.1
Glycerol : Water = 1 : 3	1193	253
Water : Ethanol = 1 : 1	891	1.005
(Glycerol + Water) : Ethanol, indicated as Glycerol + Ethanol = 1 : 1	766	127
Surfactant : Ethanol = 1 : 1	891	1.055

### 2.3. Interfacial area of the crater and the liquid layer at the bottom

Calculation of specific surface area: When the plasma jet hits the liquid, a crater is formed. The total area of the crater was analysed by image analysis [47], Figure 1. It was assumed that the crater has an axisymmetric shape. The total interfacial area, as defined in Figure 4, was calculated as the outer surface area of the cone obtained by rotation of a curve about the vertical axis. The curve describing the interface was fitted using a polynomial function of degree 4 to the experimental curve obtained from the image analysis. The gas-liquid interface area of the bottom liquid layer, as defined in Figure 4, was estimated by a simplified method. The shape of the bottom liquid layer below the crater, typically with a thickness in the 200-300-micron range, was approximated with straight lines to the polynomial curve describing the crater shape. Then the area was calculated from the obtained shape of the thin liquid layer below the crater.

Calculation of stagnant layer thickness: Water properties are assumed. Viscosity is  $\mu = 0.001$  Pa s, density is  $\rho = 1000$  kg m<sup>-3</sup>, and the diameter of the reaction vessel is  $x = 0.003$  m. Then, the thickness  $\delta$  of the stagnant layer (L) is given as follows, equation 1 (Eq 1).

$$\delta_L = \frac{2.74 \cdot 10^{-4}}{\sqrt{v_L}} \text{ [m]} \quad (\text{Eq 1})$$

The liquid velocity near the interface can be estimated based on the equal pressure drop over the interface. As then the ratio of the velocities in the gas and in the liquid can be approximated as reciprocal ratio of their viscosities. For the case of water, equation 2 can be derived.

$$v_L \approx \frac{\mu_G}{\mu_L} v_G \approx \frac{1.8 \cdot 10^{-5}}{1 \cdot 10^{-3}} v_G \approx 0.018 \cdot v_G \text{ (m s}^{-1}\text{)} \quad (\text{Eq 2})$$



Then, the thickness of the stagnant layer  $\delta_L$  is given as follows.

$$\delta_L = \frac{2.74 \cdot 10^{-4}}{\sqrt{0.018 \cdot \nu_G}} \text{ (m)} \quad (\text{Eq 3})$$

## 2.4. Evaporation rate and reaction rate

An aqueous solution containing 20  $\mu\text{L}$  of folic acid (0.1 g/mL) 1 ml of a given liquid was transferred to the glass reactor. was added as a colour indicator and reactant to the liquid. The microplasma jet was vertically directed towards the reactor at three configurations (distant, contact, and deflection). After 10 minutes, the microplasma treatment of the liquid was stopped. The final volume of liquid was used to calculate the evaporation rate, Figure 2.

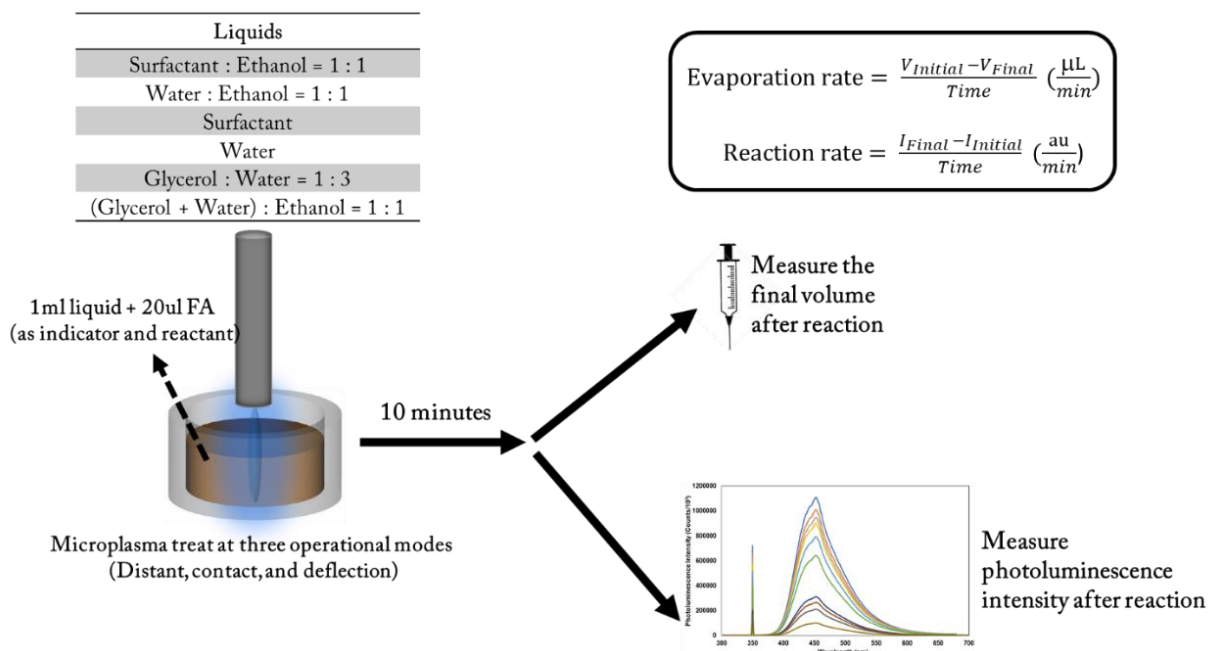


**Fig. 2** Schematic view of procedures applied for the calculation of evaporation and reaction rates in the synthesis of NCQDs.

The fluorescence emission is one of the most unique features of NCQDs, utilised in many fields [48]. In this study, fluorescence emission is used for calculating the reaction rate, Figure 2. Folic acid (20  $\mu\text{L}$ , 0.1 g/mL) was added to the liquid (1ml) in the reactor. The same three configurations of microplasma jet were used as those in our previous study [1]: (i) 'distant' (jet in contact with liquid with a weak momentum transfer), (ii) 'contact' (jet colliding deep into liquid, with a moderate impact on

hydrodynamics), and (iii) 'deflection' (jet perforating liquid completely down to reactor floor; a strong momentum transfer) [2], Figure 2.

After 10 minutes, the jet was stopped, and the colour of the solution changed from orange to brownish. The solution was analyzed with a photoluminescence spectrometer (FLS 1000, UK). The excitation and emission wavelengths were set at 360 and 450 nm, respectively. The photoluminescence intensity of NCQDs was used to obtain the reaction rate. In several experiments, 0.5 g of Ni<sub>80</sub>Cr<sub>20</sub> alloy flakes were placed at the bottom.

### 3. Results and Discussion

#### 3.1. Hydrodynamics for process intensification created by microjet plasma

Different depth of penetration of the plasma microjet into the liquid microvolume creates genuine hydrodynamic regimes, characterised by a large interfacial area, and the presence of a thin 'inner' liquid layer, at the floor of the reactor, with a moderate interfacial area. A catalyst can be added on the bottom as a fixed bed.

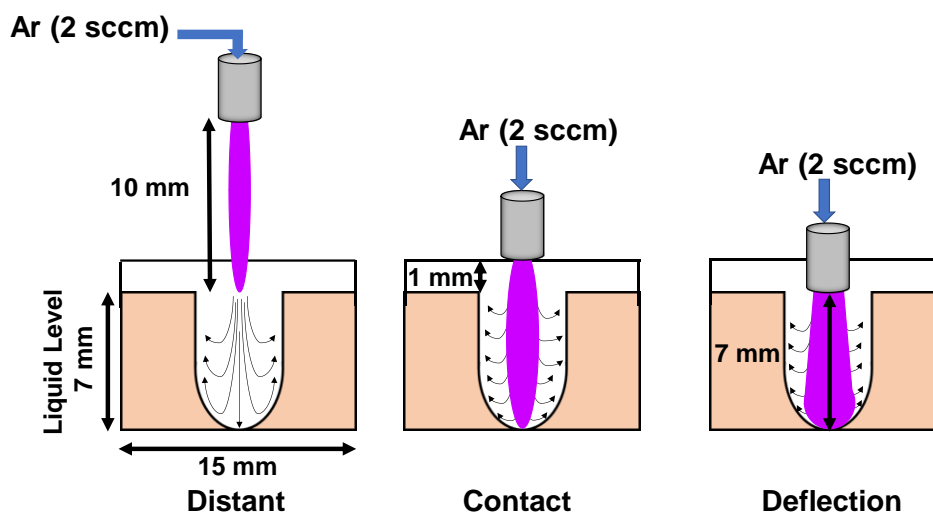


**Fig. 3** Hydrodynamic regimes by different depth of penetration of submerged microjet plasma into a liquid microvolume; termed distant (left), contact (middle), and deflection (right), [1].

In the 'distant' position, the tip of the microplasma jet, which is the most protruding part, does not contact the liquid surface and only generates a small crater. In the 'contact' position, the plasma jet penetrates deeper, forming a liquid film above the catalyst surface. The 'deflection' position resembles the "fast impinging jet reactor," a plasma reactor configuration proposed by Botes [5]. In this configuration, the liquid film is further thinned, and the plasma gas stream is redirected harshly, creating turbulence in the plasma-gas phase and potentially recirculation in the bulk liquid; intensifying mass transport in both

phases. As a result, a multiphase system with a continuous renewal of the interface is expected, possibly assisted by the generation and breakup of small droplets from the water surface, as reported in the literature [49].

We discovered that the highest intensity of charged (activated) species can be detected in the ‘deflection’ position [2]. The ‘deflection’ position is chosen as prime hydrodynamic setting for the study reported here, while the two other positions are co-investigated.

The new plasma microjet concept can compete energy-wise well with DBD plasma reactors and microreactors that are the standard in microfluidic processing. Only 1 W is consumed for the micro jet plasma in this study [10], although 56 W are needed for gas pumping at very high gas flow rate of 2 L h<sup>-1</sup> [50]. The latter may be optimised, as the deflection flow regime may be achieved by lower gas flow rates; yet manufacturer's restriction in flow rate setting prevents this study from testing this. For comparison, plasma generation of an energy-optimised laboratory DBD reactor takes 16 W (Pradeep et al., 2023), and pumping a gas flow rate of 0.2 L h<sup>-1</sup> consumes about 6 W [50]; together 22 W. For comparison, pumping a microreactor with two HPLC pumps (each 100 W [51]), consumes 200 W.

### *3.2 Effect of physical parameters of the liquid on the crater shape*

The plasma microjet displaces a major part of the liquid volume. It establishes a void gas volume that is characterized by a high-velocity gas downward that impinges on the liquid surface to be redirected upwards out of the void volume. Strong convection can be expected under those conditions ensuring good mass transport of the plasma to the gas-liquid interface. Relevant is that the use of the microjet secures that plasma contacts the liquid interface and potentially the catalyst beneath it. The high gas velocity transfers its momentum to the liquid phase to create a liquid recirculation loop, Figure 4. This liquid convection refreshes reactant in the stagnant layer from the ‘feed’ of the non-stagnant convective liquid zone; Figure 4a.

The stagnant liquid layer is controlled by diffusion, which is a slow process. Setting the stagnant layer to small dimensions, helps in fastening diffusion. Yet, a rough surface of a bed of Ni<sub>80</sub>Cr<sub>20</sub> flakes underneath the stagnant liquid layer may introduce turbulence and therefore increase convection towards the catalyst; Figure 4b.

Another concept might be ‘convective pumping’ of the plasma-activated species close to the catalyst; Figure 4c.

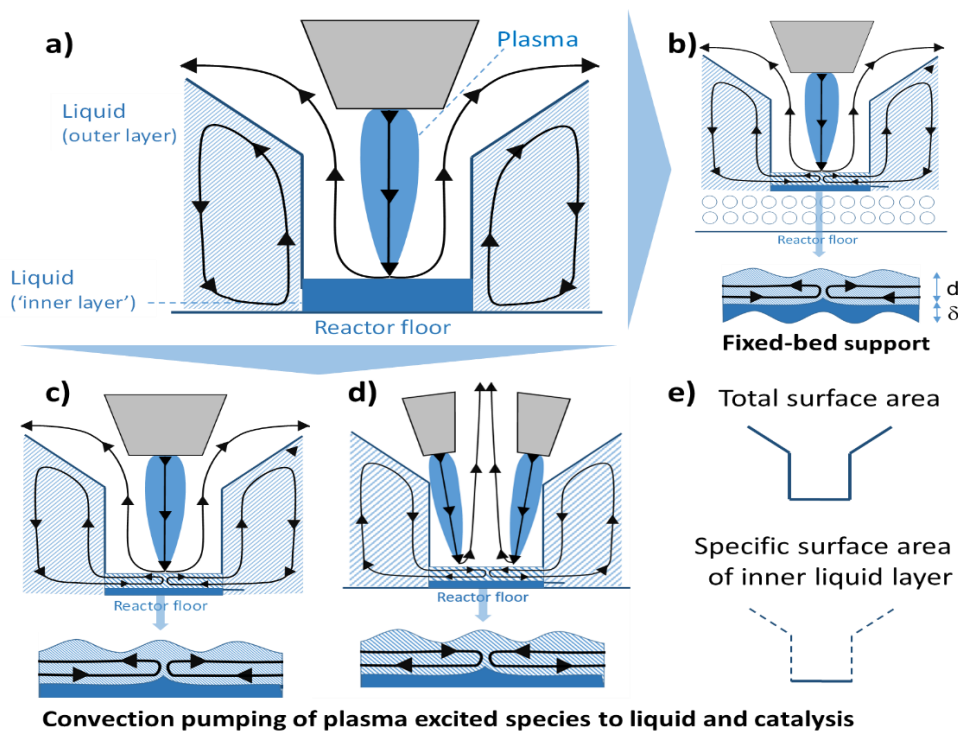


**Fig. 4** Schematic of the crater profile created by the submerged plasma microjet into a microvolume, showing hydrodynamic and reactor regions that determine the chemical engineering science. a) schematic profile as per experiments in this manuscript; b) same as a), yet with fixed bed support; c) same as a), yet with larger inner liquid layer to allow convection; d) same as a), yet with two jets placed at the outer part of the crater (instead of one jet in the crater centre); and e) schematics to define total surface area and specific surface area of inner liquid layer.

A layer thicker than the velocity boundary layer thickness ( $\delta$ ) allows a convective flow to enter into the ‘inner liquid surface area’, directly exposed to the plasma jet. As given in Figure 4c, this would actually pump the plasma-activated species away from the supposed reaction zone at the catalyst. This demands for a new positioning of the plasma jet from the centre position to an outside one; Figure 4d. A tilted arrangement of the jets is needed to achieve maximum transfer of gas momentum to the liquid. In this configuration, the convection flow would transfer plasma-excited species to the liquid stagnant (‘reaction’) zone and catalyst. Roughening of the stagnant liquid–solid interface would increase efficiency of this concept; extending use of concept in Figure 4b.

The surface profiles in the three positions were recorded (Figure 7), investigating phenomenally the shape of the interface and its total surface area and its specific surface area below the crater. The optimum configuration for interface shape would be a rather flat surface with a large surface area near the reactor floor (the potential position for a catalytic bed), Figure 4e.

To examine the magnitude of the effect, calculations of the gas velocity were done as a function of distance from the plasma-device outlet [10], Figure 5 Basic assumptions are (i) the velocity of air outside the plasma jet is considered as zero; (ii) temperature of gas is considered 300K; (iii) the diameter of nozzle is considered as 1.6 mm [10]; and the air flow rate is considered as 2 L.min<sup>-1</sup>.

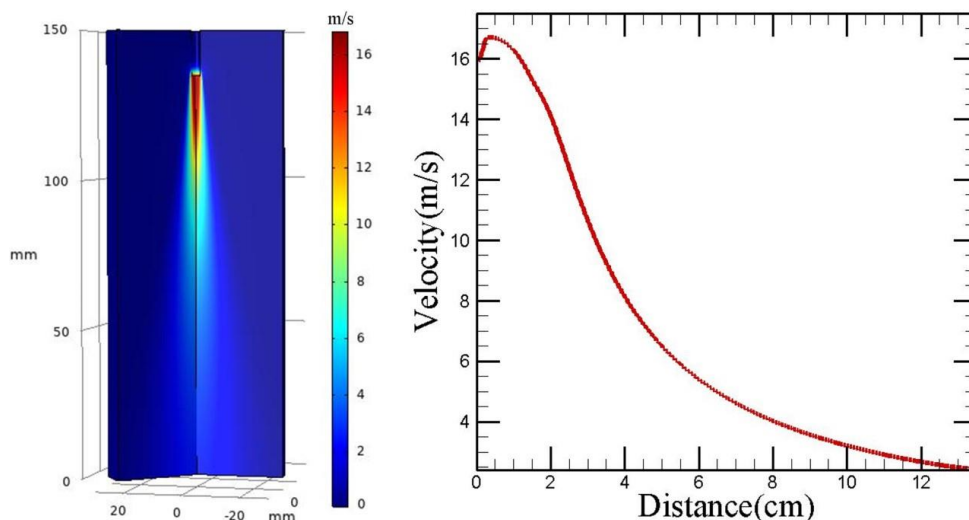


**Fig. 5** Gas velocity of the microjet plasma with distance; using the settings of the neoplas industrial plasma system [10].

The pressure decreases when gas leaves the nozzle, and its velocity increases, in line with the Bernoulli's principle, Figure 5. Then, the gas velocity decreases downstream the nozzle due to frictional losses and volumetric expansion of the jet.

The thickness of the stagnant layer needs to be determined to check on which time scale diffusion might be effective. With reference to Figure 5 and a gas velocity around 15-16 m s<sup>-1</sup>, the thickness of water velocity boundary layer around the solid surface (Eq. a1) is expected to be ca. 0.6 mm; meaning the plasma-activated species still need several minutes to reach the catalyst, Figure 6.

$$\delta_L = \frac{5x}{\text{Re}^{0.5}} = 5 \sqrt{\frac{\mu \cdot x}{\rho \cdot v_L}} \quad (\text{Eq.a1})$$

where x is the length of the solid surface in the flow direction (3 mm), and Re is the Reynolds number of the liquid.

This shows the need to roughen the catalyst surface, Figure 4 upper left scheme.

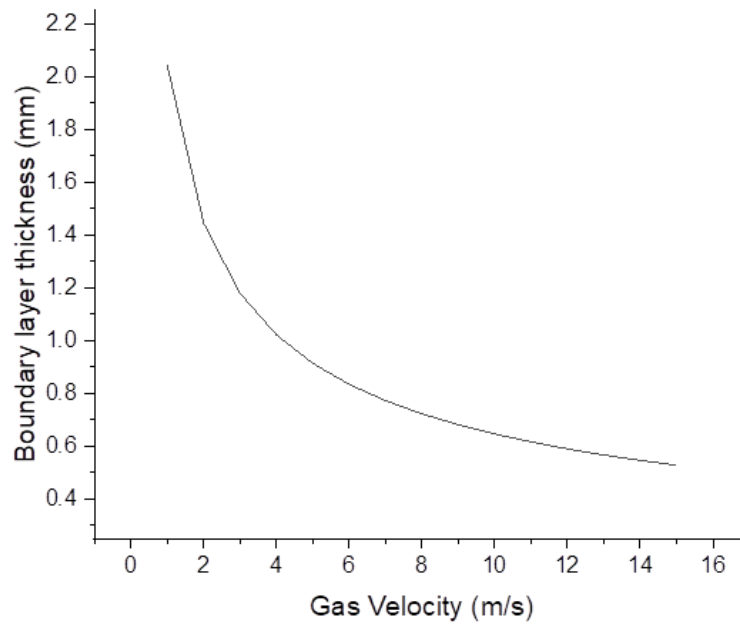


Fig. 6 Stagnant layer thickness with gas velocity.

To widen from using pure water only, glycerol, ethanol and sodium dodecyl sulphate (surfactant) were added to water to change viscosity, polarity, and surface tension of the liquid, respectively, and to study their impact on the crater surface area, liquid stagnant layer area and diffusivity of the reactant. The interface shape for different set of parameters was recorded and discussed below, Figure 7.

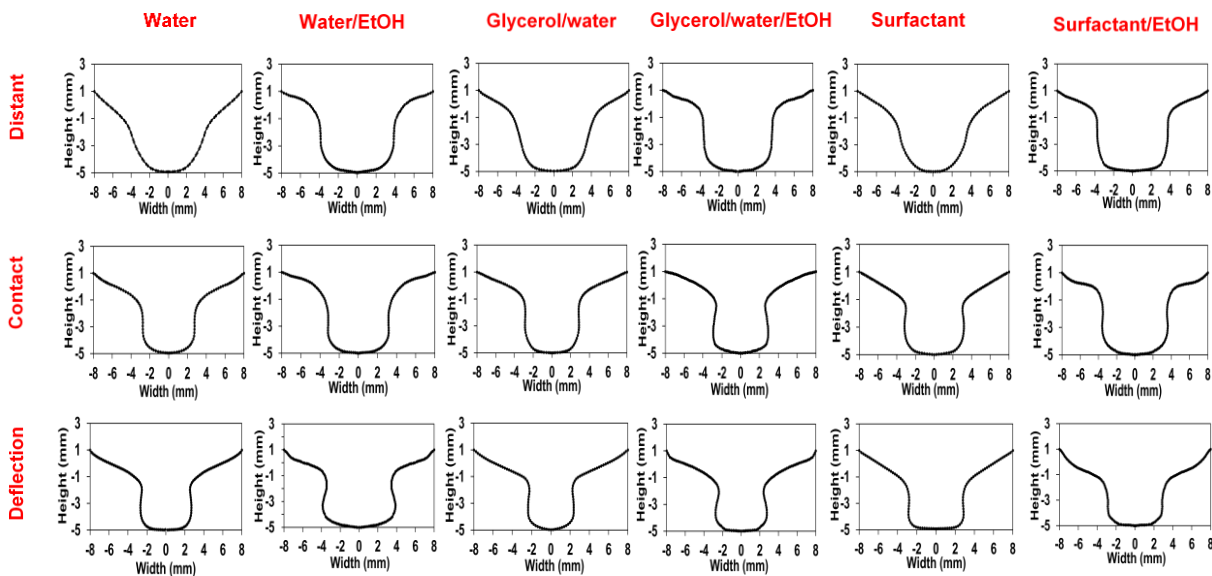
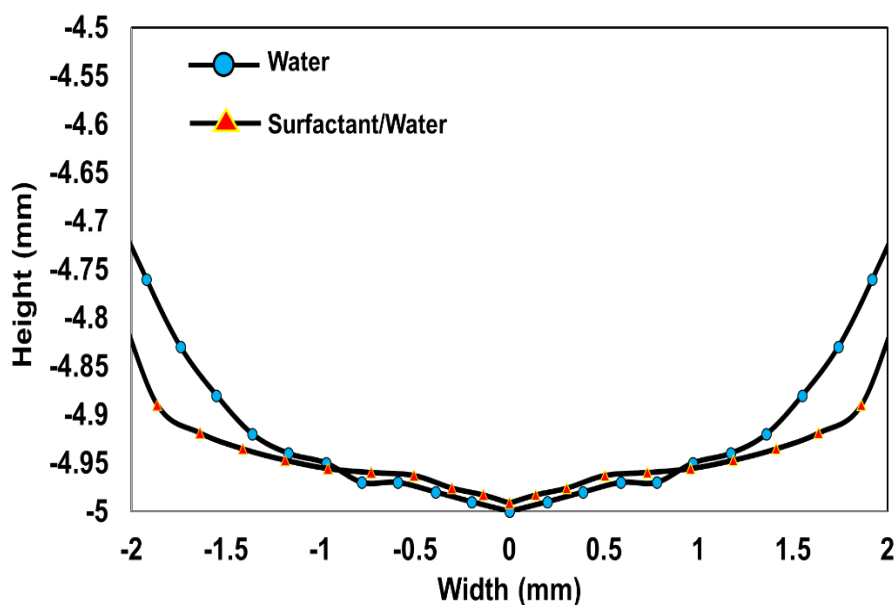


Fig. 7 Plasma-liquid interface profile for pure water (viscosity: 1.002 mPa.s), water/ethanol 1:1 (viscosity: 1.005 mPa.s), glycerol/water 1:3 (middle, viscosity: 253.42 mPa.s), glycerol-water-ethanol (right, viscosity 127.27 mPa.s), water/surfactant  $10^{-3}$  mol/l (viscosity: 1.01 mPa.s), and water/surfactant/ethanol (right, viscosity 1.055 mPa.s).

For pure water, the above given criterion of a good surface profile is better met for the contact mode as compared to the distant mode, with slight further improvement in the deflection mode, Figure 7.

Adding glycerol to the aqueous solutions increases viscosity and slightly changes density. The impact on the desired process design is low, meaning the surface profiles are similar to those with pure water. The interfacial surface area increases from 238 to 249 mm<sup>2</sup>, when moving to the deflection regime, Figure 7.

Adding ethanol alters polarity and adding surfactant surface tension. The profiles obtained are characterised by nearly vertical walls approaching a vertical well shape with a thin aqueous layer between the gas and the solid wall. This well shape is kept and the vertical alignment of the side walls improved when combining both or combining these with the glycerol (high viscosity) addition; for surfactant-ethanol (low surface tension – high polarity) it is found for all three positions (distant, contact, deflection).



**Fig. 8** Water-surfactant vs water interface profiles above the inner liquid layer, at a magnification of the height (y-axis) about 0.5 mm.

Adding ethanol and glycerol to the aqueous solutions increases both polarity and viscosity. The impact is more remarkable than changing viscosity alone. The gas-liquid interface gets more flattened, meaning the thin liquid layer has a rather constant thickness and a larger interfacial area. The large extent of flattening of the water-surfactant profile of the inner aqueous layer is evident when comparing the respective water profile; using large magnification of this 'micro-zone', Figure 8.

### 3.3 Effect of physical parameters of the liquid on total surface area

While the jet penetrates the liquid microvolume deeper, the total surface area of the crater is decreased to a small or medium extent, Figure 9; counter-intuitive to the expectation about strong impingement effect. The total surface area is largest for the deflection mode, followed by the contact and distant mode; with the contact mode being closer to the deflection one. The total surface area of the crater is the largest for pure water, while the lowest for water-surfactant. The specific (volume-rated) surface area is for pure water *ca.* 250 m<sup>-1</sup>, a value typical for advanced reactor equipment, yet lower than interfaces generated in microreactors (1,000 m<sup>-1</sup> to 10,000 m<sup>-1</sup>). The total surface is about 10 times larger than for a plain surface, non-perturbed by jet penetration.

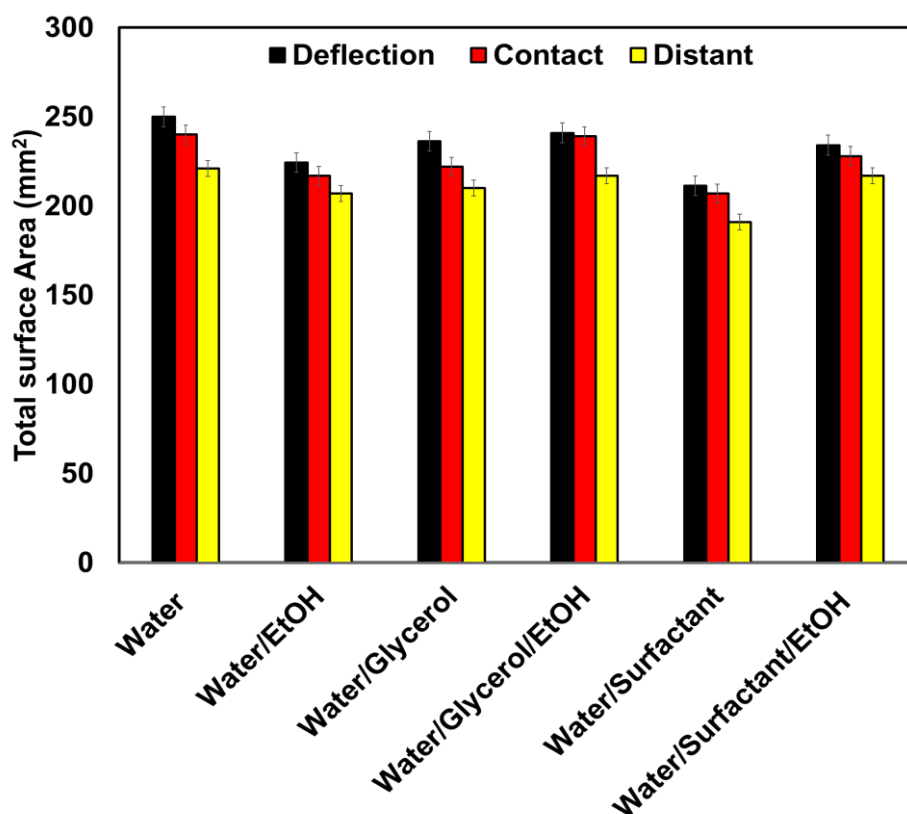


Fig. 9 Total surface area at different liquid properties; taken for all three hydrodynamic regimes with distinct plasma crater profiles.



## 3.4 Effect of physical parameters of the liquid on specific surface area of the inner liquid layer

We elucidated the specific interfacial area of the inner aqueous layer and the minimal water thickness of the inner water layer, the central point of the plasma cavity; revealing also the shape of the inner liquid layer surface. An ideal surface profile for chemical processing is flat (ultrathin) and thus constant in the water thickness, likely with diffusion being the governing mechanism of mass transport. This ultrathin liquid layer may also be ideal to employ reaction amplification by a catalyst.

The real inner surface profiles are curved, yet some are close to being ideal flat (water, water/surfactant, water/surfactant/ethanol, or water/glycerol/ethanol), Figure 9. While the surface areas differ, Figure 7, the average thickness of the inner water layer differs as well, Figure 6.

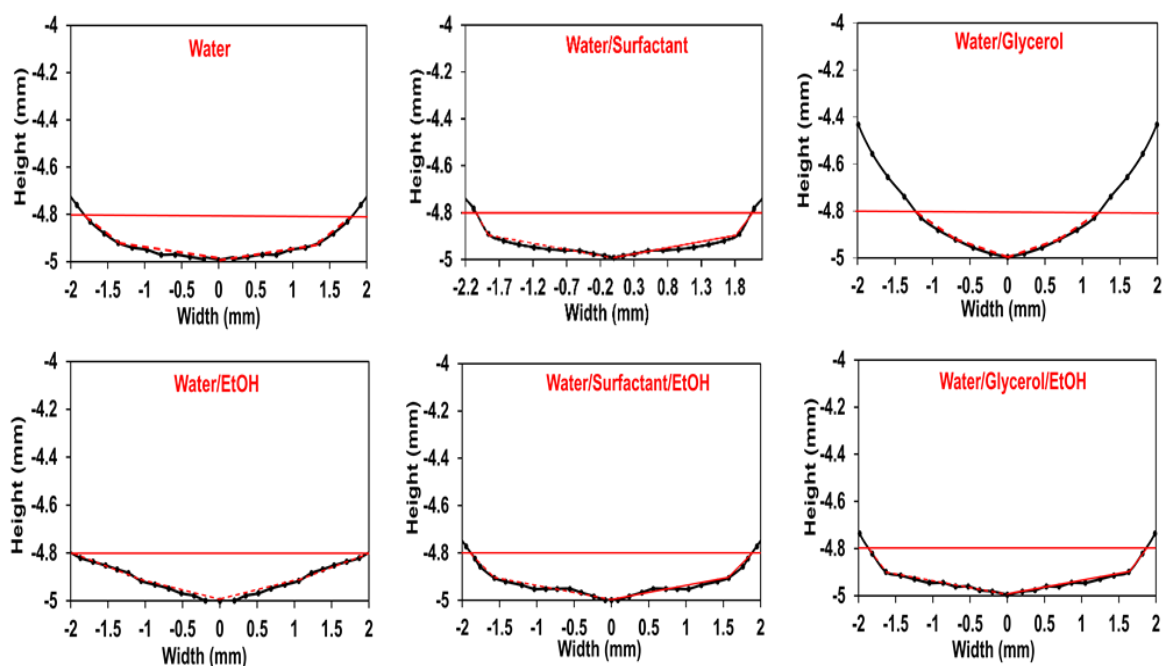


**Fig. 9** Schematic of the (experimentally determined) crater profile created by the submerged plasma microjet into a microvolume for systematic physico-chemical variation, determining hydrodynamics and reactor regions.

The scenarios considered have mostly mixed average hydrodynamic performance, e.g. having low average thickness of the inner water layer at low surface area, and vice versa. The scenarios water and water-surfactant have the best hydrodynamics. The profiles of aqueous systems with increased viscosity or reduced surface tension are close to an ideal flat surface, while having a larger depth of the inner layer throughout, and not only at the edges. Therefore, the plasma jet-liquid system can be fine-tuned in terms of having either a thin inner liquid layer (averaged over the span) or a flat layer.

The surface of the inner aqueous layer at the bottom (Figure 10) is 20-25% of the total surface area of the crater (Figure 7), which fits to the observation of five zones in Figure 5 of almost equal length and curvature. The addition of ethanol allows to make it still larger than for pure water, including admixture of surfactant and glycerol, whereas the addition of (only) glycerol halve the specific surface area. Taking 28 mm<sup>2</sup> as highest value (assuming averaged 0.1 mm layer thickness at 2.8 mm<sup>3</sup> volume), the specific (volume-rated) surface area for pure water is *ca.* 10,000 m<sup>-1</sup>, a value as high than the greatest interfaces reported for microreactors with capability for high capacity (1,000 m<sup>-1</sup> to 10,000 m<sup>-1</sup>); with up to 10,000 m<sup>-1</sup> reported for analytical microchip devices [52]. The specific volume of the inner aqueous layer is just 0.28 % of the total volume (2.8 vs. 1000 mm<sup>3</sup>), yet is supposed to make a major effort to the reaction outcome.

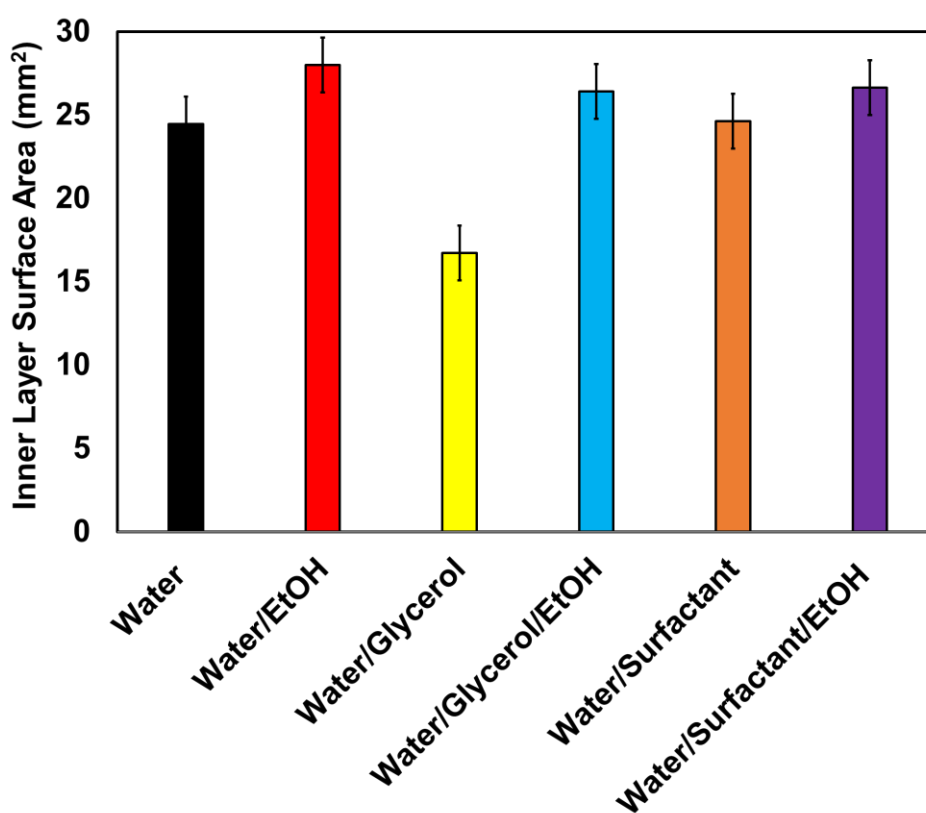
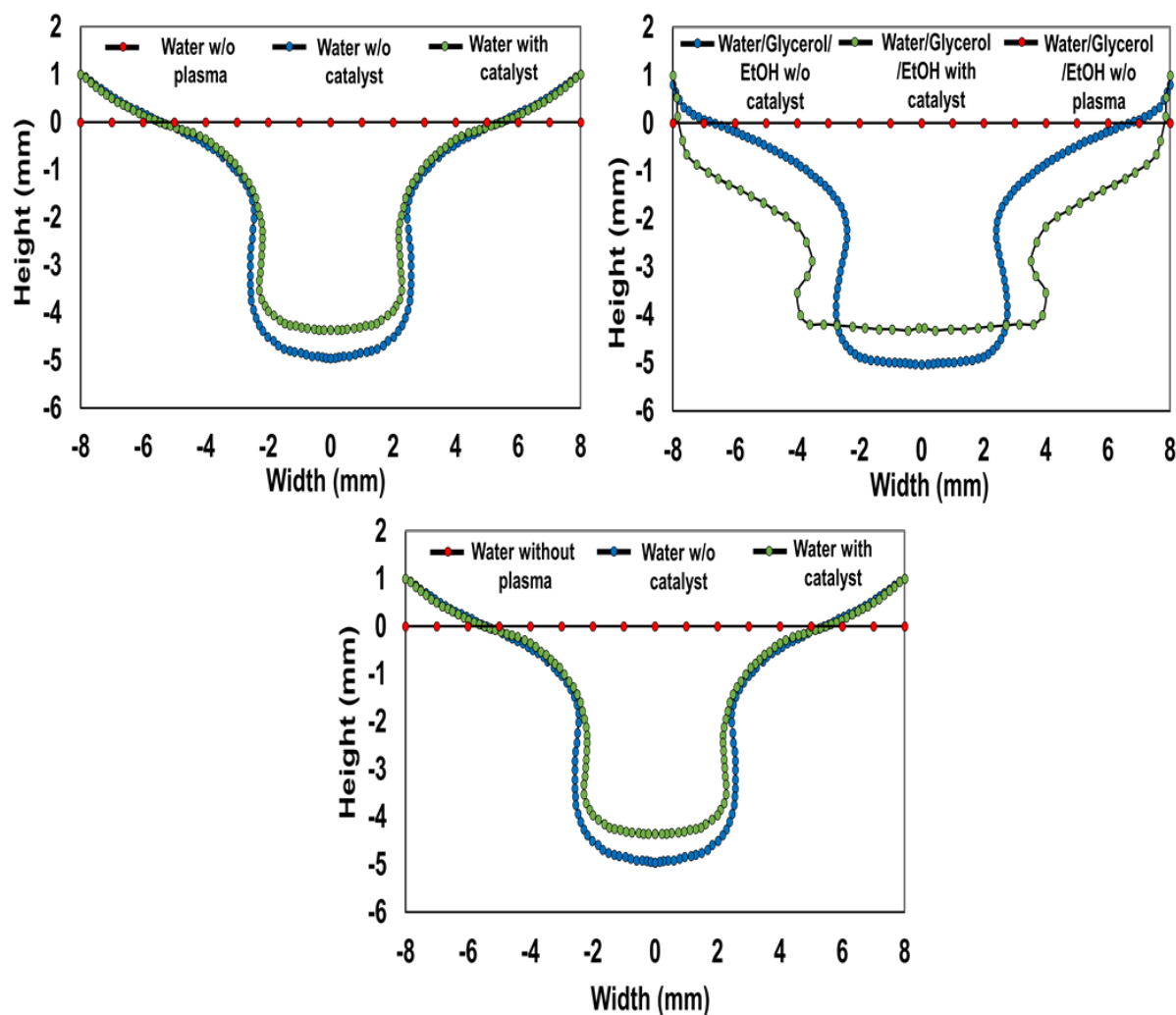


Fig. 10 Surface of the inner aqueous layer, depending on additives given to modify the physico-chemical properties (density, viscosity, surface tension).

### 3.5 Effect of physical parameters of the liquid on the inner liquid layer in the presence of a porous solid beneath

In order to achieve both a thin and flat inner liquid layer for one liquid system, the hydrodynamic profile is determined in the presence of a porous bed, composed of particles in the order of the size of the depth of the inner layer or somewhat larger; including glass spheres or metal flakes. The liquid will penetrate

that bed and the surface of the liquid is not expected to be influenced by wetting of the glass reaction vessel; assumed to cause the larger depth of the inner layer for the viscous and surface tension-reduced liquids.



**Fig. 11** Surface profile of (a) pure water, (b) glycerol and (c) glycerol-ethanol mixture as compared with surface without plasma treatment at the deflection mode.

The plasma jet in the deflection mode was exposed to a porous fixed bed of Ni-Cr alloy flakes draining a liquid, Figure 11. This changed the surface profile as compared to exposing the plasma microjet to water without fixed bed, Figure 10. An ideal flat profile is obtained for the glycerol (high viscosity) and glycerol-ethanol (high polarity- high viscosity) mixtures. In the case of glycerol-ethanol (high viscosity-high polarity), the surface area of the liquid inner layer is larger than for the case without fixed bed. In the case of pure water, no effect is observed. The profile is just elevated to higher position. It is suspected that high surface tension of the gas/water interface prevents to form a flat profile as given for the other two cases.

## 3.6 NCQDs reaction effect by liquid viscosity to test diffusion

This study intends to deploy the above-mentioned variation of physical properties for intensifying the chemistry of the NCQDs formation. Surface tension alteration does not show reaction rate dependency, while having best hydrodynamic surface profile with most extended surface of the thin layer. Polarity variation has no effect on the reaction rate either.

However, the NCQDs reaction rate was a strong function of viscosity and therefore diffusivity of the liquid reactant. The experiments were directed to detail this effect. The reaction rate increases as viscosity decreases and it increases largely from the distant to contact position, Figure 12. It can be seen that the ‘deflection’ mode is best in overcoming viscosity limitation. The ‘contact’ mode is close to this performance. The ‘distant’ mode is behind the performances of the three modes.

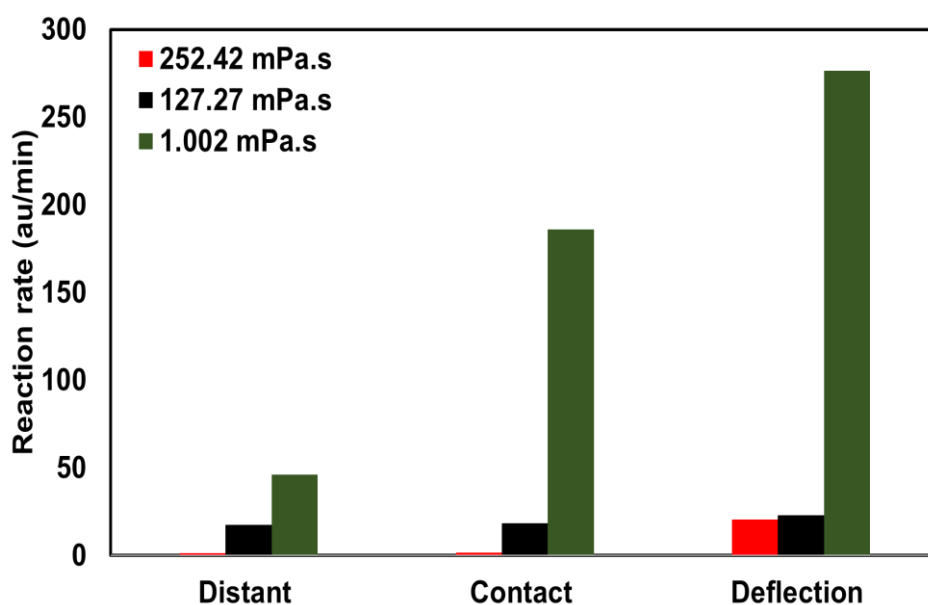


Fig. 12 Reaction rate as a function of the distance from the nozzle in three configurations.

Question is if that effect is related to unit operations (diffusivity) alone or transcribed by chemical effects (viscosity changing solvent polarity). The variation of viscosity, and the other physical parameters, do not follow the common effect of square dependency of reaction rate with co-solvent/ingredient concentration (see Supplementary Material). A chemistry-induced change of reactivity can therefore be excluded, and conclusion is the reaction rate reflect intrinsic dependencies of hydrodynamics and mass transfer on the reaction rate, i.e. diffusivity.

To further corroborate that the reaction rate is diffusion limited, the rate was plotted vs reciprocal viscosity of the solvent, which is proportional to diffusivity, Einstein's equation, Figure 13 [53].

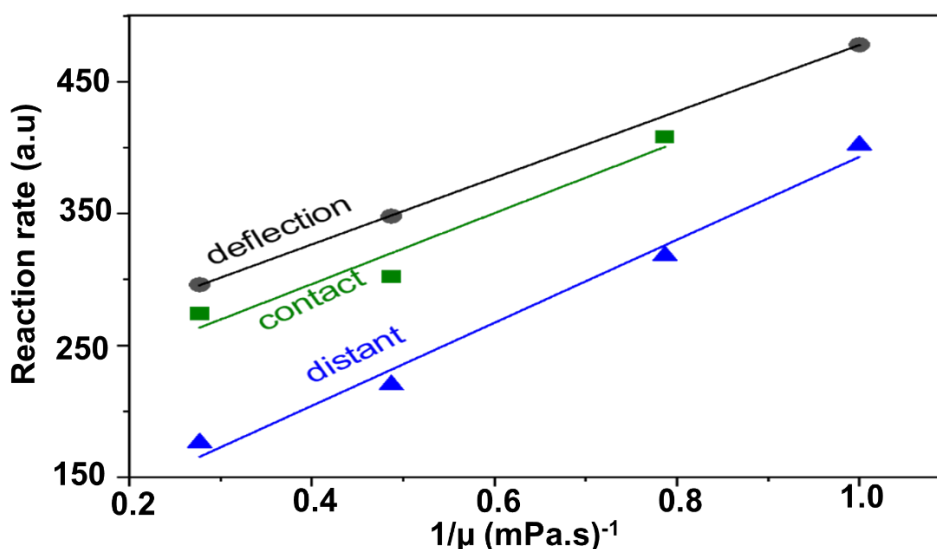


Fig. 13 Reaction rate as a function of reciprocal viscosity for the three jet configurations.

### 3.7 NCQDs reaction in presence of a metal flakes bed: test catalytic activity

A catalyst bed with the Ni-Cr alloy flakes was added. The effect of the Ni-Cr alloy catalyst to the plasma-liquid system to amplify the reaction rate was determined also for the combined viscosity-polarity effect, employing glycerol-ethanol-water mixtures. Hypothesis is that excited plasma species ( $\text{Ar}^+$ ,  $\text{N}_2^+$ ,  $\text{O}^+$ ,  $\text{OH}^*$ ) can diffuse faster to the catalyst beneath to induce the NCQDs formation [54, 55]. The deflection mode is best to utilise these plasma-excited species.

A rate enhancement of about 25% could be achieved for the catalyst-supported reaction experiment in the deflection position, Figure 14.

While this is not enough to justify proclaiming a catalytic effect in the classical meaning, it still marks a considerable process improvement. Of larger impact, in the order of five times intensification, the reaction rate increases from 76 to 387 (au/min) when changing the position from distant to deflection. Yet this effect can only be leveraged in pure water, meaning at low viscosity (1.002 mPa.s); the Ni-Cr catalyst cannot overrule the diffusion limitation and the formation of a relatively thicker layer above the catalyst. Yet for constant (high) viscosity, the catalyst is effective to increase reaction rate as the determined rates show for glycerol + water (252.42 mPa.s) and glycerol + ethanol (127.27 mPa.s). The catalyst effect is strongest in the deflection mode, as given for the non-catalysed experiments, Figure 11.

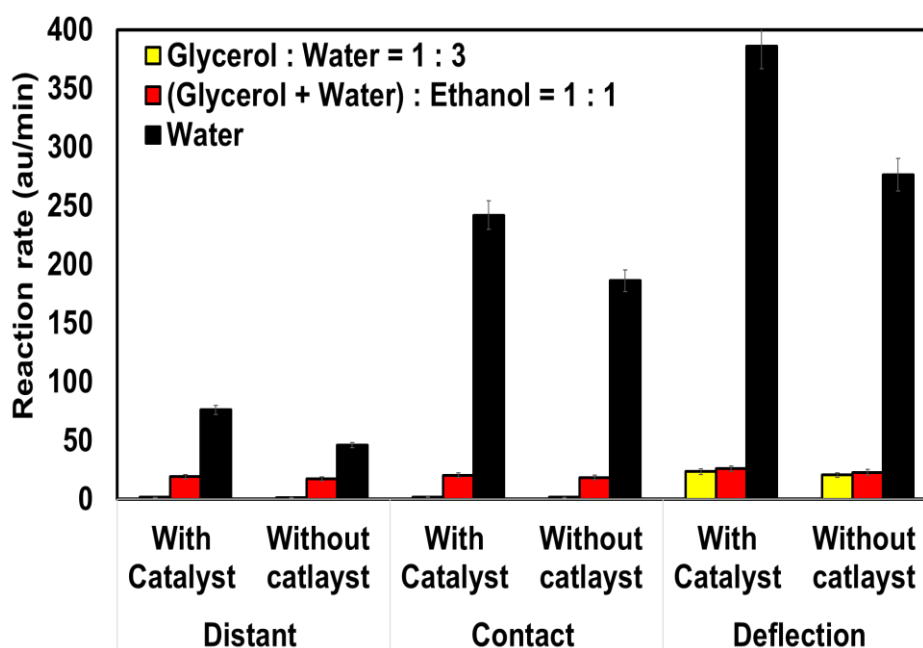


Fig. 14 Reaction rate of the synthesis reaction of NCQDs with and without  $Ni_{80}Cr_{20}$  catalysts various solvent liquids (pure water, glycerol + water, and glycerol + ethanol).

### 3.8. Evaporation control to prevent liquid phase media change

Evaporation is likely to happen when a high-velocity jet impinges on a liquid surface of large specific area. Evaporation of solvent might change reaction rate and product quality of the NCQDs nanomaterial, making necessary metering and control of evaporation. This may be facilitated by the fact that plasma commonly transfers heat to the surface of the liquid [9].

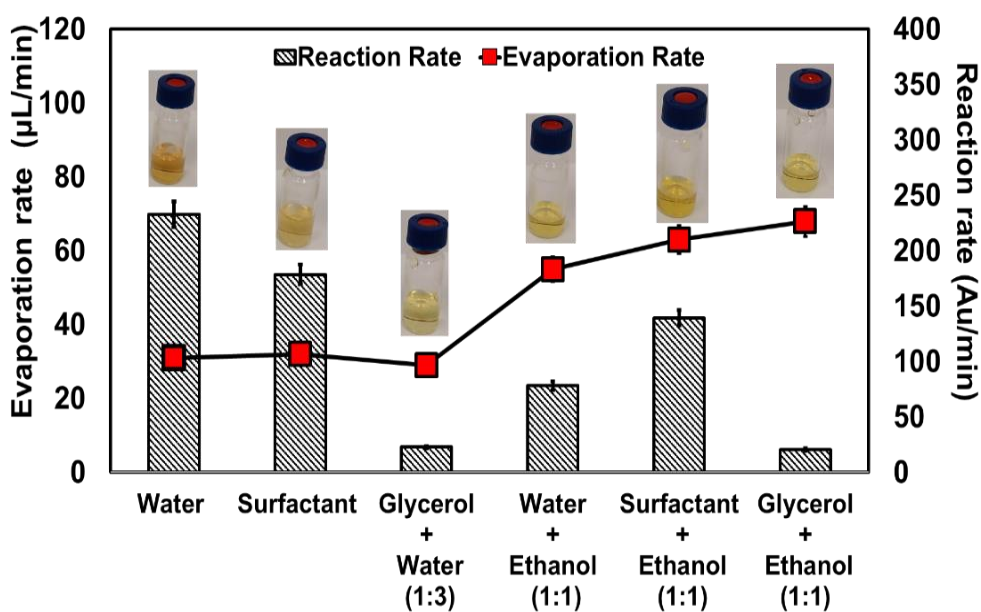
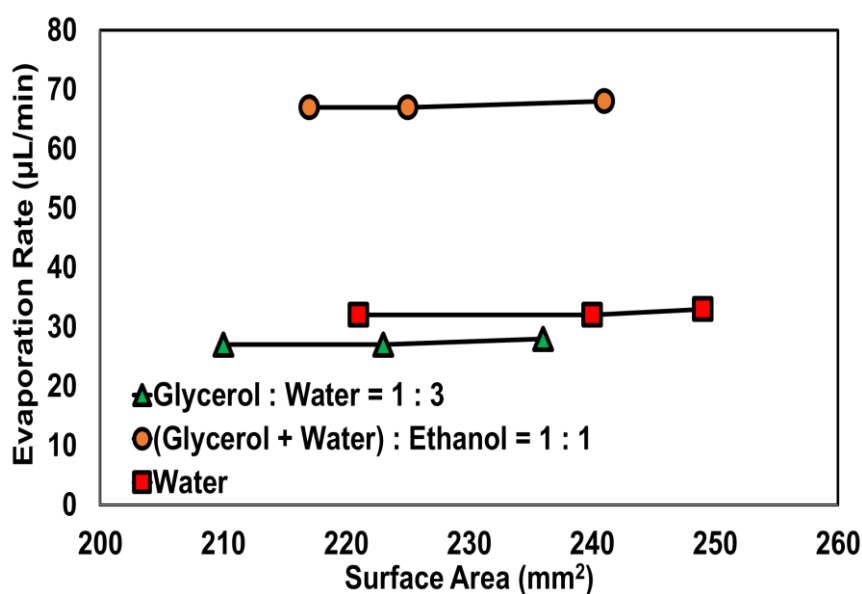


Fig. 15 Influence of solvents on evaporation and reaction rate in the synthesis of NCQDs operated at deflection mode.

The calculated evaporation and reaction rate were determined for the NCQDs synthesis in the deflection mode, when varying the physico-chemical parameters of the liquid reaction medium, Figure 15. The evaporation rate for pure water, surfactant, and glycerol : water (1:3) is relatively similar, in the vicinity of 30 ( $\mu\text{L}/\text{min}$ ). This changes when ethanol is added, a volatile solvent. The evaporation rate of water + ethanol, surfactant + ethanol, and glycerol + ethanol increased significantly, compared to reaction media without ethanol, Figure 15. The reaction rate decreased considerably, except for the case of glycerol + ethanol (20.49 au/min), which is almost invariant. The evaporated removal of ethanol might be one cause for the decline in reaction rate, adding to the other here reported causes, including the thickness of the inner liquid layer and the total and inner layer-related specific surface area.



**Fig. 16** *Evaporation rate as a function of the distance from the nozzle in the three hydrodynamic regimes of the plasma jet penetration in the liquid microvolume.*

Experiments demonstrate that the evaporation rate remains practically constant in all three hydrodynamic regimes within the investigated range, which is consistent with determination that the total surface area of the plasma crater only minorly varies for the regimes, Figure 16. The remaining difference might be due to that most evaporation takes place at the large specific surface of the inner aqueous layer, which is practically invariant to changes of the hydrodynamic regime and in the physico-chemical parameter; with one exception, Figure 9.

As expected, and seen in Figure 16, the addition of ethanol with a lower boiling point than water increases the evaporation rate. The addition of surfactant increases the total surface area. However, it does

not change the evaporation rate; which is consistent with above stated independence of the rate from the total surface area.

### 4. Conclusions

This study explored a new reaction engineering concept to generate 'in-process' a thin, almost flat solvent layer out of a bulk liquid through impingement of a high-velocity gas jet (plasma). This layer is as thin, or thinner, as typical microfluidic flows, used for chemical processing. Specifically, the study demonstrates that a fixed bed at the floor of the reaction vessel can aid in improving the profile shape of the thin layer and deciphers how this is controlled by generic changes of physico-chemical parameters of the reaction solution. The fixed bed may add catalytic function, which cannot be leveraged in the liquid layer only, but contact to the gas phase is possible as well; enabling 'plasma catalysis' for the study here.

The variation of the physico-chemical parameters allowed to decipher which mechanisms rule the reaction investigated, the formation of NCQDs quantum dots from a dissolved precursor. This applies, in more general terms, also to a monomolecular reaction in a liquid phase that is non-thermally activated. It turned out that the plasma-liquid system is controlled by viscosity of the reaction solvent, which confirms diffusivity limitation as governing mass transfer mechanism. Polarity, density, or surface tension variation has no impact on the reaction rate; unless being combined with a viscosity change. Water, with lowest viscosity, as reaction medium proved to have the highest reaction rate for the NCQDs synthesis. Solvent admixtures, including ethanol, that keep high viscosity but change other physico-chemical parameters (polarity, surface tension), reduce the reaction rate in aqueous media.

The total surface area of the crater and the specific surface area of the thinned ('inner') solvent layer have no impact on the NCQDs reaction rate, at least within the possible range of variation in this study via the diversity of crater shapes created. This indicates that gaseous excited reaction species are in excess, and the gas-liquid interfacial transition is not a limiting factor but the diffusion of the precursors toward the interface. That also demonstrates that the reaction happens at the surface and does not penetrate the liquid; leaving diffusion in the liquid as a limiting factor.

Energy-wise, only 1 W is consumed for the plasma, although 56 W is needed for gas pumping at a very high gas flow rate of 2 L h<sup>-1</sup>, totalling 57 W. Plasma generation of an energy-optimised laboratory DBD reactor takes 16 W and about 6 W for gas pumping; totalling in 22 W. Pumping energy of a microreactor consumes 200 W.

Evaporation is an unavoidable consequence of applying a high-velocity jet to a solvent or solvent mixture. It is undesired as it transiently changes the reaction medium and exposes volatile, potentially toxic



organic matter to the environment. Evaporation does not depend on the surface area of the entire crater, which demonstrates that evaporation happens only in the narrow area near the jet, which is almost constant under any experimental variation. As expected, evaporation depends on the boiling point of the solvent. Low-boiling solvents should be avoided, even as admixtures to a main solvent.

### Outlook

Understanding the fundamentals reported in this study opens paths for follow-up studies. The catalytic function needs to be corroborated and elucidated about the mechanism and how a catalyst needs to be designed to be optimal. For a broader and potentially larger impact of the new reactor engineering concept, tests with a very fast liquid reaction might exhibit a surface area dependence, impacting the interfacial transition of the excited species from the plasma phase. The surface area has been detailed in this study, and the way of changing and controlling it was deciphered. The new concept needs to be tested with reactions that do not impact polarity changes and might need to be stimulated in reaction rate by viscosity and density changes. Then the multitude of possible variations of surface profiles and hydrodynamics demonstrated in this study can be utilised for a broader application in synthetic chemistry, possibly even beyond plasma-chemical processing.

### Acknowledgements

Mr. Hue Quoc Pho received the divisional E.C.M.S. and full-fee scholarships from the University of Adelaide, Australia. The authors acknowledge support from the ERC Grant Surface-Confined fast-modulated Plasma for process and Energy intensification (SCOPE) from the European Commission with grant number 810182.

### References

- [1] Q.H. Pho, L. Lin, E.V. Rebrov, M. Mohsen Sarafraz, T.T. Tran, N.N. Tran, D. Losic, V. Hessel, Process intensification for gram-scale synthesis of N-doped carbon quantum dots immersing a microplasma jet in a gas-liquid reactor, *Chemical Engineering Journal* 452 (2023) 139164.
- [2] Q.H. Pho, H.Q. Tran, C.P. Zhuang, V.D.L. Nguyen, N.N. Tran, T.T. Tran, E.V. Rebrov, D. Losic, Z. Machala, V. Hessel, Deciphering Plasma-Catalysis in Triphasic Microplasma for N-doped Carbon Quantum Dots from Vitamin B9 via Optical Emission Spectroscopy Unpublished (2023).

- [3] A. Bokhari, S. Yusup, S. Asif, L.F. Chuah, L.Z.Y. Michelle, Chapter 3 - Process intensification for the production of canola-based methyl ester via ultrasonic batch reactor: optimization and kinetic study, in: L. Singh, A. Yousuf, D.M. Mahapatra (Eds.) *Bioreactors*, Elsevier 2020, pp. 27-42.
- [4] E. Nagy, *Basic equations of mass transport through a membrane layer*, Elsevier 2018.
- [5] F. Botes, L. Lorenzen, J. Van Deventer, The development of high intensity gas-liquid jet reactors, *Chemical Engineering Communications* 170 (1998) 217-244.
- [6] L. Chandana, P. Manoj Kumar Reddy, C. Subrahmanyam, Atmospheric pressure non-thermal plasma jet for the degradation of methylene blue in aqueous medium, *Chemical Engineering Journal* 282 (2015) 116-122.
- [7] A. Ananth, S. Dharaneedharan, H.-J. Seo, M.-S. Heo, J.-H. Boo, Soft jet plasma-assisted synthesis of Zinc oxide nanomaterials: Morphology controls and antibacterial activity of ZnO, *Chemical Engineering Journal* 322 (2017) 742-751.
- [8] F. Rezaei, P. Vanraes, A. Nikiforov, R. Morent, N. De Geyter, Applications of plasma-liquid systems: A review, *Materials* 12 (2019) 2751.
- [9] P.J. Bruggeman, M.J. Kushner, B.R. Locke, J.G.E. Gardeniers, W.G. Graham, D.B. Graves, R.C.H.M. Hofman-Caris, D. Maric, J.P. Reid, E. Ceriani, D. Fernandez Rivas, J.E. Foster, S.C. Garrick, Y. Gorbanev, S. Hamaguchi, F. Iza, H. Jablonowski, E. Klimova, J. Kolb, F. Krcma, P. Lukes, Z. Machala, I. Marinov, D. Mariotti, S. Mededovic Thagard, D. Minakata, E.C. Neyts, J. Pawlat, Z.L. Petrovic, R. Pflieger, S. Reuter, D.C. Schram, S. Schröter, M. Shiraiwa, B. Tarabová, P.A. Tsai, J.R.R. Verlet, T. von Woedtke, K.R. Wilson, K. Yasui, G. Zvereva, Plasma-liquid interactions: a review and roadmap, *Plasma Sources Science and Technology* 25 (2016) 053002.
- [10] S. Reuter, T. Von Woedtke, K.-D. Weltmann, The kINPen—A review on physics and chemistry of the atmospheric pressure plasma jet and its applications, *Journal of Physics D: Applied Physics* 51 (2018) 233001.
- [11] S. Bekeschus, A. Schmidt, K.-D. Weltmann, T. von Woedtke, The plasma jet kINPen – A powerful tool for wound healing, *Clinical Plasma Medicine* 4 (2016) 19-28.
- [12] A.L. Garner, T.A. Mehlhorn, A review of cold atmospheric pressure plasmas for trauma and acute care, *Frontiers in Physics* 9 (2021) 774.

- [13] O. Assadian, K.J. Ousey, G. Daeschlein, A. Kramer, C. Parker, J. Tanner, D.J. Leaper, Effects and safety of atmospheric low-temperature plasma on bacterial reduction in chronic wounds and wound size reduction: A systematic review and meta-analysis, *International Wound Journal* 16 (2019) 103-111.
- [14] Z. He, S. Liu, C. Zhang, L. Fan, J. Zhang, Q. Chen, Y. Sun, L. He, Z. Wang, K. Zhang, Coal based carbon dots: Recent advances in synthesis, properties, and applications, *Nano Select* 2 (2021) 1589-1604.
- [15] M. Behi, L. Gholami, S. Naficy, S. Palomba, F. Dehghani, Carbon dots: a novel platform for biomedical applications, *Nanoscale Advances* 4 (2022) 353-376.
- [16] W. Liang, C.E. Bunker, Y.-P. Sun, Carbon dots: zero-dimensional carbon allotrope with unique photoinduced redox characteristics, *Acs Omega* 5 (2020) 965-971.
- [17] J. Liu, R. Li, B. Yang, Carbon Dots: A New Type of Carbon-Based Nanomaterial with Wide Applications, *ACS Central Science* 6 (2020) 2179-2195.
- [18] Q.H. Pho, D. Losic, K. Ostrikov, N.N. Tran, V. Hessel, Perspectives on plasma-assisted synthesis of N-doped nanoparticles as nanopesticides for pest control in crops, *Reaction Chemistry & Engineering* 5 (2020) 1374-1396.
- [19] Y. Li, X. Xu, Y. Wu, J. Zhuang, X. Zhang, H. Zhang, B. Lei, C. Hu, Y. Liu, A review on the effects of carbon dots in plant systems, *Materials Chemistry Frontiers* 4 (2020) 437-448.
- [20] N.-A. Tran, N.T. Hien, N.M. Hoang, H.-L.T. Dang, D.Q. Huy, T. Van Quy, N.T. Hanh, N.H. Vu, V.-D. Dao, Carbon dots in environmental treatment and protection applications, *Desalination* 548 (2023) 116285.
- [21] C. Long, Z. Jiang, J. Shangguan, T. Qing, P. Zhang, B. Feng, Applications of carbon dots in environmental pollution control: A review, *Chemical Engineering Journal* 406 (2021) 126848.
- [22] P. Lesani, A.H. Mohamad Hadi, Z. Lu, S. Palomba, E.J. New, H. Zreiqat, Design principles and biological applications of red-emissive two-photon carbon dots, *Communications Materials* 2 (2021) 108.
- [23] J. Wang, J. Qiu, A review of carbon dots in biological applications, *Journal of materials science* 51 (2016) 4728-4738.
- [24] S.K. Kailasa, J.R. Koduru, Perspectives of magnetic nature carbon dots in analytical chemistry: From separation to detection and bioimaging, *Trends in Environmental Analytical Chemistry* 33 (2022) e00153.

- [25] W. Zhang, H. Zhong, P. Zhao, A. Shen, H. Li, X. Liu, Carbon quantum dot fluorescent probes for food safety detection: Progress, opportunities and challenges, *Food Control* 133 (2022) 108591.
- [26] L. Zhao, M. Zhang, A.S. Mujumdar, H. Wang, Application of carbon dots in food preservation: a critical review for packaging enhancers and food preservatives, *Critical Reviews in Food Science and Nutrition* (2022) 1-19.
- [27] A.S. Rasal, S. Yadav, A. Yadav, A.A. Kashale, S.T. Manjunatha, A. Altaee, J.-Y. Chang, Carbon quantum dots for energy applications: a review, *ACS Applied Nano Materials* 4 (2021) 6515-6541.
- [28] Z. Jiang, L. Guan, X. Xu, E. Wang, C. Wang, Applications of carbon dots in electrochemical energy storage, *ACS Applied Electronic Materials* 4 (2022) 5144-5164.
- [29] Y. Liu, S. Roy, S. Sarkar, J. Xu, Y. Zhao, J. Zhang, A review of carbon dots and their composite materials for electrochemical energy technologies, *Carbon Energy* 3 (2021) 795-826.
- [30] L. Đorđević, F. Arcudi, M. Cacioppo, M. Prato, A multifunctional chemical toolbox to engineer carbon dots for biomedical and energy applications, *Nature Nanotechnology* 17 (2022) 112-130.
- [31] C.Y. Chung, Y.J. Chen, C.H. Kang, H.Y. Lin, C.C. Huang, P.H. Hsu, H.J. Lin, Toxic or Not Toxic, That Is the Carbon Quantum Dot's Question: A Comprehensive Evaluation with Zebrafish Embryo, Eleutheroembryo, and Adult Models, *Polymers* 13 (2021).
- [32] Y. Zhai, Z. Zhu, C. Zhu, J. Ren, E. Wang, S. Dong, Multifunctional water-soluble luminescent carbon dots for imaging and Hg<sup>2+</sup> sensing, *Journal of Materials Chemistry B* 2 (2014) 6995-6999.
- [33] Y. Sun, X. Wang, C. Wang, D. Tong, Q. Wu, K. Jiang, Y. Jiang, C. Wang, M. Yang, Red emitting and highly stable carbon dots with dual response to pH values and ferric ions, *Microchimica Acta* 185 (2018) 83.
- [34] S. Pandiyan, L. Arumugam, S.P. Srirengan, R. Pitchan, P. Sevugan, K. Kannan, G. Pitchan, T.A. Hegde, V. Gandhirajan, Biocompatible Carbon Quantum Dots Derived from Sugarcane Industrial Wastes for Effective Nonlinear Optical Behavior and Antimicrobial Activity Applications, *ACS Omega* 5 (2020) 30363-30372.
- [35] S. Lu, B. Yang, Carbon dots are shining in the world, *SmartMat* 3 (2022) 207-207.

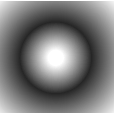
- [36] X. Qin, C. Fu, J. Zhang, W. Shao, X. Qin, Y. Gui, L. Wang, H. Guo, F. Chen, L. Jiang, Direct preparation of solid carbon dots by pyrolysis of collagen waste and their applications in fluorescent sensing and imaging, *Frontiers in Chemistry* 10 (2022).
- [37] Y. Xian, K. Li, Hydrothermal Synthesis of High-Yield Red Fluorescent Carbon Dots with Ultra-Narrow Emission by Controlled O/N Elements, *Advanced Materials* 34 (2022) 2201031.
- [38] D. Zhang, D. Chao, C. Yu, Q. Zhu, S. Zhou, L. Tian, L. Zhou, One-Step Green Solvothermal Synthesis of Full-Color Carbon Quantum Dots Based on a Doping Strategy, *The Journal of Physical Chemistry Letters* 12 (2021) 8939-8946.
- [39] M.P. Romero, F. Alves, M.D. Stringasci, H.H. Buzzá, H. Ciol, N.M. Inada, V.S. Bagnato, One-pot microwave-assisted synthesis of carbon dots and in vivo and in vitro antimicrobial photodynamic applications, *Frontiers in Microbiology* 12 (2021) 662149.
- [40] Y. Gang, E. Sarnello, J. Pellessier, S. Fang, M. Suarez, F. Pan, Z. Du, P. Zhang, L. Fang, Y. Liu, T. Li, H.-C. Zhou, Y.H. Hu, Y. Li, One-Step Chemical Vapor Deposition Synthesis of Hierarchical Ni and N Co-Doped Carbon Nanosheet/Nanotube Hybrids for Efficient Electrochemical CO<sub>2</sub> Reduction at Commercially Viable Current Densities, *ACS Catalysis* 11 (2021) 10333-10344.
- [41] Q. An, Q. Lin, X. Huang, R. Zhou, X. Guo, W. Xu, S. Wang, D. Xu, H.-T. Chang, Electrochemical synthesis of carbon dots with a Stokes shift of 309 nm for sensing of Fe<sup>3+</sup> and ascorbic acid, *Dyes and Pigments* 185 (2021) 108878.
- [42] C. Russo, B. Apicella, A. La Rocca, M. Sirignano, Fluorescent carbon dots synthesis in premixed flames: Influence of the equivalence ratio, *Carbon* 201 (2023) 659-666.
- [43] J. Zhang, S.-H. Yu, Carbon dots: large-scale synthesis, sensing and bioimaging, *Materials Today* 19 (2016) 382-393.
- [44] Q.H. Pho, M. Escriba-Gelonch, D. Losic, E.V. Rebrov, N.N. Tran, V. Hessel, Survey of Synthesis Processes for N-Doped Carbon Dots Assessed by Green Chemistry and Circular and EcoScale Metrics, *ACS Sustainable Chemistry & Engineering* 9 (2021) 4755-4770.
- [45] P. Bruggeman, M.J. Kushner, B.R. Locke, J.G. Gardeniers, W. Graham, D.B. Graves, R. Hofman-Caris, D. Maric, J.P. Reid, E. Ceriani, Plasma-liquid interactions: a review and roadmap, *Plasma sources science and technology* 25 (2016) 053002.

- [46] R. Botton, D. Cosserat, S. Poncin, G. Wild, A simple gas-liquid mass transfer jet system, 8th World Congress of Chemical Engineering, 2009, pp. CDrom du congrès.
- [47] S.R. McNeill, M.A. Sutton, Z. Miao, J. Ma, Measurement of surface profile using digital image correlation, *Experimental Mechanics* 37 (1997) 13-20.
- [48] F. Yan, Z. Sun, H. Zhang, X. Sun, Y. Jiang, Z. Bai, The fluorescence mechanism of carbon dots, and methods for tuning their emission color: a review, *Microchimica Acta* 186 (2019) 583.
- [49] L. Shui, J.C. Eijkel, A. Van den Berg, Multiphase flow in microfluidic systems—Control and applications of droplets and interfaces, *Advances in colloid and interface science* 133 (2007) 35-49.
- [50] A. Hendrawan, A. Cilacap, Calculation of power pumps on otec power plant ocean (ocean thermal energy conversion), ICoSASTE 201 9) Kupang, May 14-15, 201 9 The 1 International Conference on Science, Applied Science, Teaching and Education 2019, 2019, pp. 1-13.
- [51] B. Liu, W. Li, Y. Chang, W. Dong, L. Ni, Extraction of berberine from rhizome of *Coptis chinensis* Franch using supercritical fluid extraction, *Journal of Pharmaceutical and Biomedical Analysis* 41 (2006) 1056-1060.
- [52] K. Sato, A. Hibara, M. Tokeshi, H. Hisamoto, T. Kitamori, Microchip-based chemical and biochemical analysis systems, *Advanced Drug Delivery Reviews* 55 (2003) 379-391.
- [53] I. Avramov, Relationship between diffusion, self-diffusion and viscosity, *Journal of Non-Crystalline Solids* 355 (2009) 745-747.
- [54] H. Kyushiki, A. Ikai, The effect of solvent viscosity on the rate-determining step of fatty acid synthetase, *Proteins* 8 (1990) 287-293.
- [55] A.F. Olea, J.K. Thomas, Rate constants for reactions in viscous media: correlation between the viscosity of the solvent and the rate constant of the diffusion-controlled reactions, *Journal of the American Chemical Society* 110 (1988) 4494-4502.

**BLANK PAGE**

# Chapter 8

## Conclusions & Perspectives



---

**I**n this chapter, the main findings, challenges, and future direction of this thesis PhD are summarised. This chapter consists of the summary of the conducted experiments, contributions of each chapter, and research conclusion carried out throughout this project study. Finally, perspectives and recommendations for the future direction of this work are also described.

---



### 1. Conclusions

This thesis contributes to developing a new kind of microplasma to address the challenges associated with the large-scale production of multifunctional advanced nanomaterials for selected emerging applications (nanofertilisers/nanopesticides, environmental treatment, and theranostic medicine) in a sustainable manner (green, eco-friendly, energy-efficient production). This comprehensive study aims to address specific challenges associated with the large-scale synthesis of NCQDs, which will have an enormous impact on agriculture, the environment, and the healthcare system. In essence, this thesis is devoted to the discovery and development of a microplasma jet (kINPen®IND)-based reactor to produce high-quality N-doped carbon quantum dots with outstanding properties (water-soluble, intense fluorescence, ultrasmall size, crystallinity, etc.) from a green chemical (Vitamin B9). Then, an attempt to improve mass production efficiency by process design engineering and the support of catalysts, as well as to understand the synthesis reaction mechanism, has been made in this thesis. Four main concepts can be summarized based on the research outcomes in this thesis:

**Chapter 3** focuses on a deep understanding of available six large-scale synthesis methodologies of N-doped carbon dots (NCQDs) in the up-to-date literature review. Then, based on collected information from the literature review, a comprehensive assessment to compare the key components (greenness, sustainability, energy-efficiency, and cost) of these fabrication methodologies using green chemistry, circular and ecoScale metrics. Following are the main findings and contributions of this chapter (**Aim 2**):

- Thermal synthesis method (scenario 3) of NCDs using citric acid with monoethanolamine, show the most promise when all assessments are considered. Scenario 3 is circular, with the highest material circularity indicator (MCI) of 0.971 and the second-best EcoScale index of 56%.
- Thermal synthesis method (scenario 2), using oleic acid and sucrose for NCDs synthesis, scores best at 60%.
- The assessment of the six synthesis process methodologies for N-doped carbon dots nanoparticles determines that hydrothermal (scenario 1), thermal (scenario 3), and microwave (scenario 4) score best in terms of green metrics, while thermal (scenarios 2 & 3), and thermal plasma (scenario 5) do likewise with circular metrics. Finally, concerning good manufacturing criteria, thermal (scenarios 2 & 3) and microwave (scenario 4) shows the best performance. NCDs produced from hydrothermal (scenario 1), microwave (scenario 4), and thermal methods (scenario 2) need a purification process for good sustainability performance.

- Considering all metrics, scenario 3 (thermal method using citric acid with MEA) ranks best, followed by scenario 4 (microwave with glucose). Interesting to note that thermal plasma (scenario 5) shows good indices despite the high-energy consumption. The latter is overcompensated by the fact that scenario 5 (as well as scenario 3) does use neither water nor solvent, which reduces waste generation. Therefore, any improvement in energy consumption for the thermal plasma would let it jump up to even the best scenario. This also gives hope for future use of nonthermal plasma and its miniaturized version (scenario 6), also known as an energy-consuming technology, yet with considerable improvements over the years. It needs fewer operating processes than conventional methods and profits from process simplicity. Yet this is not paid off so far in terms of green chemistry and circularity.
- “Utility” is a strong point to enhance circularity in the Ellen MacArthur definition. The plasma-prepared nanomaterials are rich in functional groups such as  $-\text{NH}_2$ ,  $-\text{COOH}$ ,  $-\text{CHO}$ , etc., without requiring chemicals for surface modification. Those surface groups are key to the NCD functionality, *i.e.* their photoluminescent properties.
- Based on the information provided by the manufacturer, the power consumption of this device is 50 W. It was calculated that about 1 g of NCQDs per day (24 hours). To produce 1 gram of NCQDs, this device will consume 1200 watts of energy per day. Based on this calculation, non-thermal plasma is considered superior in terms of "gram-scale synthesis" in relation to plasma power consumption. The power consumption of a plasma system is an important factor to consider when evaluating its efficiency and cost-effectiveness for gram-scale synthesis. Generally, a plasma system that can produce a high yield of material with a low power consumption is considered more efficient than one that requires a higher power input for the same amount of material produced. Therefore, when evaluating the efficiency of a plasma system for gram-scale synthesis, it's important to consider not only the productivity (in grams per second or gram/s) but also the power consumption (in watts or joules). A system that can produce a high yield of material while consuming relatively little energy (*i.e.*, a high gram/s/Watt or gram/Joule ratio) is generally considered more efficient than one that consumes more energy for the same amount of material produced.

**Chapter 4** focuses on the improvement of the mass efficiency of the microplasma jet-based synthesis process, which was revealed after the comprehensive assessment from Chapter 3. The aim of this chapter is to attempt to reach the gram-scale production of N-doped carbon dots by adjusting the distance of the tip of the microplasma jet to the water surface in three steps, named distant, contact, and deflection modes.

As a further variation, the liquid volume is either stirred or unstirred and may contain glass beads or metal flakes. In this way, the mass transfer, hydrodynamics, and the electrical field are influenced and create the specific gas–liquid interface, possibly including plasma-catalytic effects. Following are the main findings and contributions of this chapter (**Aim 3**):

- The closer it came, the more the plasma was deformed and spread out into the whole gaseous reaction volume. In the contact and deflection mode, the jet penetrated the liquid volume down to the reaction well floor.
- Stirred microwell operation delivers higher photoluminescence than unstirred one. The addition of glass beads results in higher photoluminescence, demonstrating the impulse transfer-based mass transfer improvement than the unstirred mode but cannot reach the quality of the stirred plasma operation.
- Adding metal flakes is superior to all modes of operation. This cannot be alone because of better mass transfer and hydrodynamics but may be due to changing the electrical field and possibly plasma-catalytic effects.
- A thermofluidic analysis confirms a uniform temperature profile and a positive temperature effect on mass transfer. In this way, the research demonstrated that we achieved process intensification.
- The photoluminescence intensity's intended performance for the foreseen applications of the nanomaterial was maximised. In addition, we could reach a productivity of 1 g per day. This is much more than many reported plasma-based and other process-based nanomaterial syntheses in literature and is even quoted to be on the way to production (as nanomaterials most often are only needed in minute volumes).

**Chapter 5** focuses on developing a new conceptual strategy to rationally design and synthesise the desirable for three main applications (nanopesticides, water purification, and theranostic treatment). One of the critical problems of CD in these applications is enhancing the high-quality intrinsic properties of CD, including water solubility, stability, and fluorescence intensity. Therefore, this conceptual design approach is proposed to address these problems and achieve these desired properties, targeting to create CD with the required modification of the CD's bulk/size, surface, and morphology. Following are the main findings and contributions of this chapter (**Aim 4**):

- Three molecular targets guiding the rational designs have been achieved in a proof-of-principle fashion. The NCQD were monodispersed with a mean particle size of 3.13 nm. The core structure of NCQD was in the form of a crystalline. It consisted of multilayered graphitic- and pyrrolic-nitrogen-defected graphene sheets, while their surface was decorated by  $-\text{NH}_2$ ,  $-\text{OH}$ , and  $-\text{COOH}$  functional groups. The resulting NCQD had an intensely blue fluorescence performance with a QY of 35%, the highest among other plasma synthesis approaches and the best of all methods applied.
- NCQD showed the most intense fluorescence in pH values of 6–8. By performing the strongest fluorescence in water, the NCQD was considered hydrophilic, in line with the presence of protic and polar surface groups. DLVO theory predicts that at a potential of  $\pm 40$  mV, NCQD may have the most stable colloidal behaviour in water.

**Chapter 6** investigates the relationship between the microplasma multiphase design and the plasma-catalytic effect. To do this, the study employs optical emission spectroscopy (OES) to examine how a plasma-heterogeneous catalyst in a multiphase reaction impacts the generation of NCQD from Vitamin B9. The focus is on understanding and improving multiphase hydrodynamics and reactions by using a plasma jet to create a specific surface profile that penetrates deep into the liquid volume. Following are the main findings and contributions of this chapter (**Aim 5**):

- The gas flow of Ar at 2 sccm at “deflection” mode enhanced the intensity of positively charged species.
- $\text{Ni}_{80}\text{Cr}_{20}$  exhibited a better catalytic activity based on OES analysis and electric potential comparison.
- The thermal imaging results also indicated that the reaction temperature at the plasma-liquid-catalyst interface is lower than 25 °C. Heat and mass transfer processes play a key role in controlling the temperature of the reaction via water evaporation.
- The plasma jet in the deflection mode is stopped at the metal ( $\text{Ni}_{80}\text{Cr}_{20}$ ) flakes interface surrounded by a liquid, giving rise to a different surface profile than water alone.
- The mechanism of plasma-liquid-catalysts synthesis of N-doped quantum dots was proposed with seven main steps.

**Chapter 7** aims to improve reactivity in a plasma-activated three-phase catalyst system using bespoke transient hydrodynamics. Existing three-phase plasma systems are poorly designed, understood, and not commercially available. The study evaluated N-doped carbon quantum dots as fertilizers and wastewater

treatment using a commercial plasma system generating a plasma microjet. The plasma can penetrate the catalyst bed via the stagnant thin liquid film and polarize the plasma-liquid interface, resulting in an increased reaction rate by reducing the solvent's viscosity and increasing liquid component diffusivity towards the catalyst bed. Following are the main findings and contributions of this chapter (**Aim 6**):

- N-doped carbon quantum dots were used as a model reaction for fertilizer and wastewater treatment applications.
- A commercial plasma system generating a plasma microjet was used to create a hydrodynamic regime where plasma can penetrate the catalyst bed.
- The reaction rate is enlarged by increasing liquid component diffusivity and interfacial area below the crater.
- The plasma process is energy-efficient and consumes lower energy than microfluidic processing but requires consideration of volatile additive evaporation.
- Reaction kinetics are critical for cost and environmental profile of processes derived from the reactions.

### 2. Perspectives

This research study marked an exciting journey with the novel discovery underpinning the mastery of nitrogen fixation microplasma synthesis technology for multifunctional nanoparticles towards selected applications that open many new frontiers requiring further exploration. For future direction, several key aspects highlighted as the following are recommended to fully unlock the potential of nitrogen fixation microplasma synthesis technology and N-doped carbon quantum dots:

#### 1) **Scaling up the nitrogen fixation microplasma synthesis process of N-doped carbon quantum dots.**

Scaling up the microplasma synthesis process of N-doped carbon quantum dots (NCQDs) refers to increasing the production of these quantum dots using the microplasma synthesis method. This can be achieved by increasing the size of the reactor, increasing the flow rate of the precursor solution, or by running the process in parallel reactors. One of the main challenges in scaling up the microplasma synthesis process is maintaining the quality of the NCQDs produced. When scaling up the process, it is important to ensure that the reaction conditions, such as the plasma power, the precursor concentration, and the reaction time, are maintained at optimal levels. Another approach to scaling up the microplasma synthesis process is to develop new reactor designs that can handle larger quantities of precursor solution and generate a more uniform microplasma. This could include using continuous flow reactors (microfluidic

microplasma), which can handle a larger volume of solution than batch reactors, and parallel reactors (an array of microplasma jets), which can produce a larger quantity of NCQDs in a shorter period.

The microfluidic microplasma synthesis of N-doped carbon quantum dots (NCQDs) is a method for producing NCQDs that utilizes a microfluidic device to generate a microplasma within a liquid solution containing the precursor materials for the NCQDs. The microfluidic device consists of two main components: a microchannel and an electrode. The microchannel is used to flow the precursor solution through, while the electrode is used to generate the microplasma. The electrode can be made of various materials such as stainless steel, gold, or carbon. The microplasma is generated by applying a high-voltage electric field across the microchannel and the electrode, which causes the precursor solution to become ionized and form a plasma. The microfluidic microplasma synthesis method has several advantages over other methods for producing NCQDs. For example, the small scale of the microfluidic device allows for precise control of the reaction conditions, such as the flow rate of the precursor solution and the plasma power. This enables the production of NCQDs with high reproducibility and uniformity. The microfluidic microplasma synthesis method can produce NCQDs with a high nitrogen content, which is important for many applications, such as bio-imaging and catalysis. Another advantage of the microfluidic microplasma synthesis method is that it is a green and eco-friendly method, as it consumes less energy, and generates less waste and pollution than other methods. It is worth mentioning that, the microfluidic microplasma synthesis method is still an active area of research, and further optimization of the reaction conditions and the design of the microfluidic device are needed to improve the yield and quality of the NCQDs produced.

An array of microplasma jets allows for the simultaneous synthesis of multiple NCQDs, which can increase the overall yield and productivity of the synthesis process. Additionally, the small scale of the microplasma jets allows for precise control of the reaction conditions, such as the flow rate of the precursor solution and the plasma power, which can lead to the production of NCQDs with high reproducibility and uniformity. Another advantage of using an array of microplasma jets is that it allows for a low-power plasma source, which reduces energy consumption and the cost of the synthesis process. Microplasma jet methods have been widely used to synthesise various materials. However, it is still an active area of research in the field of N-doped carbon quantum dots, and further optimization of the reaction conditions and the design of the microplasma jets are needed to improve the yield and quality of the NCQDs produced. It is worth mentioning that the microplasma jet method is a greener and eco-friendly method, as it consumes less energy and generates less waste and pollution than other methods.

Additionally, using advanced process control techniques such as computer-controlled systems and implementing quality control methods such as statistical process control (SPC) can help maintain the

quality of the NCQDs produced while scaling up the process. Overall, scaling up the microplasma synthesis process of NCQDs is an active area of research, with the goal of making this technology more accessible for various applications by producing NCQDs in large quantities at a lower cost.

### **2) Optimizing purifying process for N-doped carbon quantum dots.**

In this thesis, the results indicated that purifying N-doped carbon quantum dots and recycling the unreacted reactants improve the sustainability of the overall production process. This study has paved the way for large-scale purification and recycling research to enhance the quality of NCQDs products. Several methods can be used to purify N-doped carbon quantum dots (NCQDs), depending on the desired purity level and the specific application of the NCQDs. One common method for purifying NCQDs is size-exclusion chromatography (SEC), which is based on the principle of separating particles based on their size. SEC can be used to separate NCQDs from impurities such as unreacted precursors, by-products, and other contaminants. Another method that can be used for purifying NCQDs is centrifugation. This method separates NCQDs from impurities based on their density. The NCQDs are centrifuged at high speed, and the impurities are separated from the NCQDs due to their different densities. Other methods that can be used to purify NCQDs include: Dialysis, which is a method that separates small molecules from large ones by passing the solution through a semi-permeable membrane. Ultracentrifugation is a method that separates particles based on their size, shape, and density by centrifuging the solution at very high speeds. Precipitation is a method that separates dissolved substances from a solution by adding a reagent that causes the substance to form a solid precipitate. Additionally, advanced purification techniques such as high-performance liquid chromatography (HPLC) and solid-phase extraction (SPE) can purify NCQDs to a very high purity level. It is important to note that the purification process of NCQDs may vary depending on the synthesis method and the impurities present in the initial sample. Therefore, optimising the purification methods for each specific synthesis method is important.

### **3) Using the rationally designed NCQDs from microplasma jet-based synthesis in crop control, environmental treatment, and theranostic medicine**

The outcome of this study finishing to demonstrate the concept of using a microplasma jet-based reactor for generating high-quality NCQDs. At the early stage, these as-prepared NCDs are rationally designed with purposes for agriculture, environmental treatment, and theranostic medicine, which opens new doors for generating desired and on-purpose NCQDs for specific applications.

Using rationally designed N-doped carbon quantum dots (NCQDs) from microplasma jet-based synthesis in crop control, environmental treatment, and theranostic medicine is an emerging area of research. In crop control, NCQDs have been shown to have the potential as a photosensitizer for photodynamic therapy (PDT) in controlling plant pathogens. In addition, NCQDs have also been used to improve the efficiency of fertilizers in crop growth by acting as a catalyst for nitrogen fixation. In environmental treatment, NCQDs have been shown to have potential for use in the removal of heavy metals and pollutants from water bodies and in the treatment of wastewater. Additionally, NCQDs have also been used as catalysts for the degradation of pollutants in the air. In theranostic medicine, NCQDs has been used as a contrast agent for imaging in cancer diagnosis and as a drug delivery system for cancer therapy. They have also been used as a therapeutic agent for the treatment of various diseases, such as inflammation and infections. Overall, rationally designed NCQDs from microplasma jet-based synthesis have shown great potential in various fields such as crop control, environmental treatment, and theranostic medicine. However, more research is needed to fully understand their potential applications and to develop appropriate methods for their use in these fields.

#### **4) Investigating the safety and environmental risk of developed N-doped carbon quantum dots**

After demonstrating the potential of these NCQDs in crop control, environmental treatment, and theranostic medicine. A study on a comprehensive assessment of the safety and environmental risk of NCQDs also should be accomplished in the future. The safety and environmental risks of developed N-doped carbon quantum dots (NCQDs) are currently an active area of research, as there is limited information available on these materials' potential hazards and effects. Regarding safety, NCQDs are considered low-toxicity materials, as they are made from carbon and nitrogen atoms, which are abundant in nature. However, some studies have shown that NCQDs may cause some toxicity to cells and organisms, especially when they form nanoparticles. Therefore, it is important to use appropriate protective measures when handling NCQDs, such as wearing gloves and masks and avoiding inhalation and ingestion of the materials. Regarding environmental risks, NCQDs are considered relatively benign materials, as they are not persistent in the environment and do not bioaccumulate. However, some studies have shown that NCQDs can impact aquatic organisms when released into water bodies. Therefore, it is important to implement appropriate measures to prevent the release of NCQDs into the environment.